Delft University of Technology
Faculty of Electrical Engineering, Mathematics and Computer Science
Delft Institute of Applied Mathematics

Arbitrage-free approaches for pricing interest rate derivatives under the SABR model

A thesis submitted to the
Delft Institute of Applied Mathematics
in partial fulfillment of the requirements

for the degree

MASTER OF SCIENCE
in
APPLIED MATHEMATICS

by

Maximiliaan Richard de Groot
Delft, the Netherlands
September, 2015

MSc THESIS APPLIED MATHEMATICS

"Arbitrage-free approaches for pricing interest rate derivatives under the SABR model"

Maximiliaan Richard de Groot

Delft University of Technology

Daily supervisors

Ir. B. Hoorens
Dr. V. Malafaia

Responsible professor

Prof.dr.ir. C.W. Oosterlee

Other thesis committee member

Dr. C. Kraaikamp

September, 2015

Delft, the Netherlands

Acknowledgements

This thesis has been submitted for the degree Master of Science in Applied Mathematics at Delft University of Technology. The responsible professor of this thesis was Kees Oosterlee, professor at the Numerical Analysis group of Delft Institute of Applied Mathematics. Research for this thesis took place during an internship at ING Bank, FI/FM Quantitative Analytics Credit and Trading Risk, under the supervision of Bart Hoorens and Veronica Malafaia.

I would like to thank my supervisors Kees Oosterlee, Bart Hoorens and Veronica Malafaia for their assistance during the writing of this thesis. Furthermore, I would like to thank all my colleagues of the QA team for the wonderful time. Finally, I would like to thank C. de Mooij and F. Abcouwer for their feedback on my draft versions of the thesis.

Maximiliaan R. de Groot Delft, September 2015

Abstract

This thesis is about pricing swaptions under the SABR model or a variant thereof. In the interest market a stochastic local volatility is often used by practitioners to describe the volatility curve in the strike dimension of swaptions. It is a fast approach to inter- and extrapolate market quotes. It is however well-known that this approach is not arbitrage-free. This led to the investigation of approaches that are arbitrage-free. Several approaches have been proposed in the literature to resolve the arbitrage. Computationally rapid approaches that are arbitrage-free are desired as an alternative for Hagan's formulas. These approaches can be used to describe the volatility curve in the strike dimension. The focus will be on an approach that is analytically exact under the SABR model, an approach that reduces the dimensionality in the dynamics of the SABR process and the stochastic collocation method (SCM). The SCM will be used to remove the arbitrage in the stochastic local volatility approach. All approaches will be calibrated to swaption volatility curves and the impact on the inter- and extrapolation of the market quotes is investigated. This is done by investigating the extrapolation of the volatilities, the sensitivities and pricing constant maturity swap (CMS) derivatives using a convexity adjustment method dependent on the complete volatility curve.

Keywords: SABR, volatility, swap, swaption, constant maturity swap, arbitrage, stochastic collocation method, convexity adjustment.

Glossary

LIBOR	London interbank offered rate.
EURIBOR	Euro interbank offered rate.
bp	Basis point, a unit equal to 1/100th of 1%.
$D(t,T)$	The zero-coupon bond price, contracted at time t with maturity T.
Swap	An agreement where two parties exchange a floating rate to a fixed rate.
Swap rate	The value of the fixed rate that gives the swap zero value as seen from today.
Swaption	An option to enter in a swap at a future time. In a receiver swaption the holder of the option agrees to pay the floating rate in the underlying swap, in a payer swaption the holder of the option agrees to pay the fixed rate in the underlying swap.
CMS	Constant maturity swap.
Call option	An option to buy a financial quantity for a fixed price at a prescribed time in the future.
Option price	the price of the corresponding option, i.e. call price is the price of a call option.
At-the-money	An option where the strike is equal to the forward is called at-the-money. A swaption is at-the- money if the strike is equal to the swap rate of the underlying swap.
A	Annuity.
PDE	Partial differential equation.
$\mathbb{Q}$	Risk-neutral measure.
$\mathbb{Q}^A$	Annuity measure.
$\mathbb{Q}^T$	T-forward measure.
f	Probability density function.
F	Cumulative density function.
$(x)^+$	A function, where $(x)^+ := \max(0,x) = x1_{\{x\geq 0\}}$, with $1_{\{\cdot\}}$ the indicator function. Not be confused with possible notations as x^+ (without parentheses).
Itô's Lemma	A lemma to switch between the dynamics of processes.
Fokker-Planck equation	A PDE to describe the probability density function of a process.
Bachelier's model	A model to value options, see Section 2.3.1.
Black's model	A model to value options, see Section 2.3.2.

Implied Bachelier volatility	The value of the volatility in Bachelier's model such that Bachelier's model gives the market option price.
Implied Black volatility	The value of the volatility in Black's model such that Black's model gives the market price.
CEV process	Constant elasticity of variance process, see Section 2.4.1.
SABR	An abbreviation of Stochastic Alpha Beta Rho.
α, β, ρ, ν	The model parameters in the SABR model, where α is the volatility, β is the skewness parameter, ρ is the correlation between the Brownian motions described in the SABR model and ν is the volatility of the volatility.
$\text{Norm}(\mu, \sigma^2)$	A normal distribution with mean μ and standard deviation σ.
$\text{Gam}(\alpha_\Gamma, \beta_\Gamma)$.	A gamma distribution with shape parameter α_Γ and rate parameter β_Γ.
Hagan's formulas	The approximations of Hagan et al. to describe the implied Black and Bachelier volatilities under the SABR model, see Section 2.5.
Hagan's AF SABR model	A model derived by a reduction of dimensionality in the dynamics of the SABR model by Hagan et al, see Section 3.1.
Uncorrelated Antonov	An approach to price call options under the SABR model for the uncorrelated case, see Section 3.2.
SCM	Stochastic collocation method, see Chapter 4.

Contents

Chapter 1

Introduction

This thesis investigates different arbitrage-free approaches for pricing interest rate derivatives under the SABR model, focusing on the impact on the prices and vega sensitivities. To formulate the research question, an introduction on financial products is given.

A financial derivative is a security whose price depends on a certain underlying asset. This underlying asset can be for instance a stock, the oil price, a bond price or an interest rate. One of the most common derivatives are options. For example, a call option on a share, gives the holder the right but not the obligation to buy the share on a predefined time in the future, for a predefined price.

In the *Over-The-Counter* (OTC) market derivatives are traded directly between two counterparties instead of via an exchange. The trade can be fully customized to the needs of the counterparties. Table 1.1 summarizes the notional amounts outstanding of the OTC derivates. The interest rate derivatives market is the largest, with approximately 81% of the total notional.

	Forwards and swaps	**Options**
Foreign exchange	61,331	13,451
Interest rate	513,848	49,442
Equity	2,433	4,508
Commodities	1,474	732
Credit default swaps	19,462	-
Unallocated	22,274	2,535
All contract	620,823	70,668

Table 1.1: Notional amounts of outstanding OTC derivatives in billions of US dollars, end-June 2014 [10].

An example of an interest rate derivative is a swap. When two parties enter into a swap, one party exchanges a fixed rate to a floating rate with the other party. The fixed and floating rates are exchanged at a predefined set of dates. The floating rate is usually based on a reference rate, like LIBOR or EURIBOR. LIBOR is the London interbank offered rate and EURIBOR is the euro interbank offered rate. These are the average interest rates estimated by a panel of banks in London and in the Eurozone respectively, at which banks would charge other banks for unsecured borrowing. The time-length of the swap is called the swap tenor. A vanilla swap is frequently traded within the interest rate derivative market, and considered as one of the most liquid interest rate products.

Another commonly traded interest rate product within the interest derivatives market is a swaption. The holder of this option has the right to enter into a swap at a predefined future time. The date when this decision has to be made is called the option maturity. Prices of swaptions are quoted for different sets of fixed rates, option maturities and swap tenors.

These market quotes are however only given for a limited set of fixed rates, option maturities and swap tenors. Outside these points one has to inter- and extrapolate the market quotes. It is important to inter- and extrapolate market quotes in an arbitrage-free way. An arbitrage opportunity is an opportunity where one has the possibility of making a profit and is certain to make no loss, without initial costs. An adequate market risk management is based on the fair prices and sensitivities and therefore requires arbitrage-free approaches.

More complex derivatives can depend on the the inter- and extrapolation of the market quotes. In the interest rate market, constant maturity swaps (CMS) derivatives depend on the inter- and extrapolation of the market quotes. These have to be fairly prices as with with the swaptions for adequate risk management.

The SABR model or a variant of the SABR model [29] is widely used in the interest rate market for inter- and extrapolating swaption prices in the strike (fixed rate) dimension. The approach by Hagan et al. [29], the so-called Hagan's formulas, is one of these variants and is considered the market standard in the interest rate market. This approach is very fast in practice to inter- and extrapolate market quotes. It is however well-known that this approach is not arbitrage-free [30].

The goal of this thesis is to find an arbitrage-free approach for pricing swaptions under the SABR model or a variant of the SABR model. This approach must be fast, accurate and competitive against recently proposed approaches. After such an approach is found, the impact on the inter- and extrapolation of market quotes is investigated. The research question is:

What is the impact of an arbitrage-free approach on the inter- and extrapolation of market quotes compared to Hagan's formulas?

To answer this research question, the thesis is structured as follows. Chapter 2 starts with the mathematical fundamentals and a price derivation for a swap and a swaption. Bachelier's model and Black's model will be presented and it is discussed how they are related to market quotes. The SABR model will be presented by a constant elasticity of variance (CEV) process. Finally in this chapter, Hagan's formulas are presented, along with its benefits and drawbacks. Hagan's formulas will be used as a benchmark with which the other approaches will be compared, since it is one of the market standards approaches.

Chapter 3 - 6 are the core of the thesis. Chapter 3 discusses in more detail two recently proposed approaches that are arbitrage-free and computationally rapid such that these can inter- and extrapolate market quotes in practice. These two approaches are the approaches by Hagan et al. [30] and Antonov et al. [3], which are referred to as Hagan's AF SABR and uncorrelated Antonov. The first approach is a reduction of dimensionality in the dynamics of the SABR model, creating a new model. The latter one gives an analytically exact solution for a swaption under a special case in the dynamics the SABR model, the uncorrelated case.

For Hagan's AF SABR a PDE has to be solved. In this thesis the approach by Le Floch et al. [15] is followed to ensure a sufficiently efficient implementation and an alternative integration technique is proposed for more stability. With uncorrelated Antonov, more insight into of the

SABR model is created. The stability of the approach is investigated and it is shown when this approach is less stable.

The stochastic collocation method (SCM) introduced by Grzelak et al. [25, 26] is presented in Chapter 4. It is an approach in which an expensive random variable is mapped to a simpler random variable. The mapping will be used to remove the arbitrage in Hagan's formulas. In this chapter, different interpolation techniques are considered to approximate the mapping accurately. In the approach by Grzelak et al, a normal distribution is considered for the simpler random variable in the mapping, where in this chapter it is compared to a gamma distribution. It is discussed when a gamma distribution can give more accurate results. A direct approach of Grzelak et al. does not directly guarantee that the approach is completely arbitrage-free. Therefore, the approach is extended such that it removes the arbitrage completely, whereas the other two approaches provide this a priori. It is thus an approach that gives a posteriori an arbitrage-free approach.

Chapter 5 and 6 compare the approaches. Chapter 5 compares the approaches by inter- and extrapolating the market quotes. The impact on prices and sensititivies of swaptions are investigated. In this chapter it will be shown how one can stabilize the approach of Hagan et al. [3] during calibration for daily use and it its investigated if the uncorrelated case of the SABR model can fit the market quotes accurately.

Chapter 6 compares the approaches by pricing CMS derivatives. The prices of CMS derivatives depend on the entire inter- and extrapolation of the market quotes and the impact of the approaches can therefore be measured by comparing the prices of these derivatives. To do so, CMS swaplets, floorlets and caplets are priced by a convexity adjustment method.

Chapter 7 concludes after summarizing the main results and describes possible future research.

Chapter 2

The SABR model and Hagan's formulas

This chapter gives basic definitions of stochastic processes. These are important to understand since they are the mathematical backbone for the pricing framework and used throughout the thesis. The pricing framework for derivatives is introduced and it is shown how to price a swap and swaption. For the latter one, it is desired to price in an arbitrage-free way in the inter- and extrapolation of market prices. To explain how market prices are quoted, Bachelier's and Black's model are introduced and are linked to the market quotes. To inter- and extrapolate market quotes, it is chosen to use the SABR model or a variant of the SABR model. The SABR model is widely used in the interest rate market due to the approximation formulas of Hagan et al. [29], i.e. Hagan's formulas. Hagan's formulas have a drawback, namely that they can generate arbitrage. It is shown in which manner they generate arbitrage. This give rise to alternative approaches, which are guaranteed to be arbitrage-free which will be investigated in later chapters. Finally, this chapter ends with a summary.

2.1 Mathematical preliminaries

Mathematical definitions, lemmas and theorems are introduced that are used as the basis of in the pricing framework of derivatives. First, the definition of a martingale, stopping time and theorem of a stopped martingale process will be given. The background is based on Steele [38] and Jeanblanc [13].

Definition 2.1 (Martingale)**.** A stochastic process $X_t : [0,T] \times \Omega \to \mathbb{R}$ is a martingale with respect to a filtration $\mathcal{F}_t$ and a probability measure $\mathbb{P}$ if

- $\mathcal{F}_t$ is a filtration of the underlying probability space $(\Omega, \mathcal{F}, \mathbb{P})$.
- X_t is adapted to the filtration $\mathcal{F}_t$.
- $\mathbb{E}\left[|X_t|\right] < \infty$ for each t.
- $\mathbb{E}\left[X_t | \mathcal{F}_s\right] = X_s$ for each $s \leq t$ and $\mathcal{F}_s \subset \mathcal{F}$.

Definition 2.2 (Stopping time)**.** A stochastic process $\mathcal{S}_t : [0,T] \times \Omega :\to \mathbb{R} \cup \{+\infty\}$ with respect to the filtration $\mathcal{F}_t$ is called a stopping time if

$$\{\omega : \mathcal{S}_t(\omega) \leq t\} \in \mathcal{F}_t \text{ for all } t \geq 0.$$

Theorem 2.3 (Stopped Martingale Theorem)**.** *Let $\mathcal{S}_t$ denote a stopping time and X_t be a martingale. Then the process $X_{t\wedge\mathcal{S}_t}$ is also a martingale, where $t \wedge \mathcal{S}_t = \min\{t, \mathcal{S}_t\}$.*

Proof. A proof can be found in Steele [38]. □

If a process $\{X_t\}_{t\geq 0}$ is stopped, for example at zero with $X_0 > 0$, it accumulates mass in its probability density function at zero. If there are no other points where the process is stopped, the probability density function can be written as

$$f_X(t,x) = \begin{cases} f(t,x), & \text{for } x > 0, \\ \mathcal{P}_0(t)\delta(x), & \text{for } x \leq 0, \end{cases}$$

where $f(t,x)$ is the probability density function for $x > 0$, δ is the Dirac function and $\mathcal{P}_0$ is the point mass at zero. The point mass at zero can be computed by $\mathcal{P}_0(t) = 1 - \int_0^\infty f(t,x)\,\mathrm{d}x$. This convention will be used in the thesis. Furthermore, a stopped process can be seen as absorption at some point (in the above case, absorption at zero is assumed).

The definition of a Brownian motion is presented to introduce Itô's Lemma and the Fokker-Planck equation.

Definition 2.4 (Brownian Motion)**.** A stochastic process W_t for $t \in [0,\infty)$ is called a Brownian motion if:

- $W_0 = 0$ and $W_t \sim \mathrm{Norm}(0,t)$ for $t > 0$.
- It has stationary, independent increments.
- It is continuous with probability one.

Lemma 2.5 (Itô's Lemma)**.** *Suppose X_t follows an Itô process:*

$$\mathrm{d}X_t = \mu(t,X_t)\,\mathrm{d}t + \sigma(t,X_t)\,\mathrm{d}W_t, \text{ with } X_0 = x_0,$$

i.e.

$$X_t = X_0 + \int_0^t \mu(s,X_s)\,\mathrm{d}s + \int_0^t \sigma(s,X_s)\,\mathrm{d}W_s,$$

with $\mu(t,X_t)$ being the drift term and $\sigma(t,X_t)$ the diffusion term. Let $g(t,X_t)$ be a function with continuous derivatives (up to second order). Then $Y_t := g(t,X_t)$ follows an Itô process with the same Brownian motion W_t:

$$\mathrm{d}Y_t = \left(\frac{\partial g}{\partial x}\mu + \frac{\partial g}{\partial t} + \frac{1}{2}\frac{\partial^2 g}{\partial x^2}\sigma^2\right)\mathrm{d}t + \frac{\partial g}{\partial x}\sigma\,\mathrm{d}W_t.$$

Proof. A proof can be found in Steele [38]. □

Lemma 2.6 (Fokker-Planck Equation)**.** *If X_t follows the Itô process:*

$$\mathrm{d}X_t = \mu\left(X_t,t\right)\mathrm{d}t + \sigma\left(X_t,t\right)\mathrm{d}W_t,$$

the probability density $f(x,t)$ of X_t satisfies the Fokker-Planck equation

$$\frac{\partial f(x,t)}{\partial t} = -\frac{\partial}{\partial x}\left(\mu(x,t)f\right) + \frac{1}{2}\frac{\partial^2}{\partial x^2}\left(\sigma^2(x,t)f(x,t)\right)$$

Proof. A proof can be found in Jeanblanc [13]. □

Lemma 2.7. *Let X_t be an Itô process with drift term μ and diffusion term σ such that $\mu(t,x) \equiv 0$ and $\int_{-\infty}^{+\infty} \sigma^2(t,x)\,\mathrm{d}x$ for $t \geq 0$. Then the process X_t is a martingale.*

Proof. A proof can be found in Steele [38]. □

In the financial modeling, financial quantities are often described by an Itô process, also known as a stochastic differential equation (SDE). Itô's lemma shows how to switch between processes. With a well chosen transformation, a simpler SDE can be derived and in some cases an analytically expression can be derived for the solution of the SDE. If the drift term in the SDE is set equal to zero, the process becomes a martingale. The measure under which a financial quantity is described, is often chosen such that the financial quantity is a martingale and it is therefore easier to model (the drift term does not have to be described). The Fokker-Planck equation can give more insight to the process by giving the PDE for the probability density function. Solving this PDE gives the distribution of the process. This gives the mathematical background needed for pricing options.

2.2 Pricing preliminaries

The basic financial quantities are defined in this section that are required for pricing swaptions. The background is based on Andersen et al. [33]. Unless stated otherwise, time is denoted in years.[1]

Definition 2.8 (Basic Financial Quantities)**.**

- A *zero-coupon bond* is a financial product that delivers 1 unit of currency at maturity T. $D(t,T)$ denotes the price of a zero-coupon bond at time $t \leq T$.

- It can be shown that the fair *forward price* of a zero coupon bond that starts at time T and matures at time $T+\tau$, at time $t \leq T$ is equal to:

$$D(t,T,T+\tau) := \frac{D(t,T+\tau)}{D(t,T)}.$$

- The *simple compounded forward rate* $L(t,T,T+\tau)$ is defined as:

$$L(t,T,T+\tau) := \frac{1}{\tau}\left(\frac{1}{D(t,T,T+\tau)} - 1\right), \tag{2.1}$$

  which originates from the relation

$$D(t,T,T+\tau) = \frac{1}{1+\tau L(t,T,T+\tau)}.$$

[1] In general, financial contracts are specified in dates, but for convenience year fractions are used. Year fractions can be obtained by a particular day counting rule. For more details on this subject, see Andersen et al.[33].

- The *instantaneous* forward rate is defined as:

$$h(t,T) := \frac{\partial \ln\left(D(t,T)\right)}{\partial T},$$

  which originates from the relation

$$D(t,T,T+\tau) = \exp\left(-\int_T^{T+\tau} h(t,u)\,\mathrm{d}u\right).$$

- The *short rate* is given by

$$r(t) := h(t,t).$$

- A *tenor structure* is a set of predefined dates

$$0 \leq T_0 < T_1 < \ldots < T_M,$$

  where for each interval $\tau_n := T_{n+1} - T_n$ for $0 \leq n \leq M-1$. If $M = 1$, it is called a *tenor*.

- Let $k, M \in \mathbb{N}$ such that $0 \leq k < M$ and a tenor structure be given as above. The *annuity factor* $A_{k,M}$ is defined as:

$$A_{k,M}(t) = \sum_{n=k}^{M-1} D(t,T_{n+1})\tau_n.$$

With the basic financial quantities, mathematical theorems for pricing interest rate derivatives can be presented.

2.2.1 Mathematical fundaments in pricing interest rate derivatives

Arbitrage is an important concept in pricing and will play an important role in this thesis. It is defined as follows:

Definition 2.9 (Arbitrage)**.** An arbitrage opportunity occurs when there exists a self-financing strategy which has value m such that $m(0) = 0$ and, for some $t \in [0,T]$,

$$m(t) \geq 0 \text{ with probability one, and } \mathbb{P}(m(t) > 0) > 0.$$

Thus, an arbitrage opportunity is an opportunity where one can trade in a product or a set of products with no initial costs. This can involve buying and selling products. At the end of the life-time of the products, one has or had the possibility of making a profit, but no possibility of making a loss. The main concept in the arbitrage opportunity is the possibility of a profit and the certainty of no loss. One can make money out of no money.

A numeraire is defined to introduce the equivalent martingale measure theorem.

Definition 2.10 (Numeraire)**.** A numeraire is a continuously tradeable asset which is strictly positive and pays no dividends.

Definition 2.11 (Equivalent Martingale Measure)**.** Let

$$X(t) := (X_1(t), \ldots, X_M(t)),$$

be a random variable under a measure $\mathbb{P}$. Let $\mathcal{N}(t)$ denote a numeraire, and define the normalized asset process

$$X^{\mathcal{N}}(t) := \left(\frac{X_1(t)}{\mathcal{N}(t)}, \ldots, \frac{X_M(t)}{\mathcal{N}(t)} \right)^{\mathrm{T}}.$$

Then the measure $\mathbb{Q}^{\mathcal{N}}$ is an equivalent martingale measure induced by $\mathcal{N}$ with respect to $\mathbb{P}$, if $\mathbb{Q}^{\mathcal{N}}$ is equivalent to the measure $\mathbb{P}$ and $X^{\mathcal{N}}(t)$ is a martingale with respect to $\mathbb{Q}^{\mathcal{N}}$.

A numeraire can be seen as a reference asset that is chosen to normalize all other asset prices with respect to it. A widely used measure in finance is the risk-neutral measure $\mathbb{Q}$. It is the measure defined by the continuously compounded money market account $B(t) := e^{\int_0^t r(u)\,\mathrm{d}u}$, where $r(u)$ is the short rate. If there exist the risk-neutral measure, it has been proven that there is no arbitrage [33]. Let $V(t)$ be the price of a derivative at time t, then the process $\frac{V(t)}{B(t)}$ is a martingale under the risk-neutral measure [33]. This leads to the pricing formula:

$$V(t) = B(t)\mathbb{E}^{\mathbb{Q}}\left[\frac{V(T)}{B(T)} \middle| \mathcal{F}_t \right].$$

For pricing it is sometimes more convenient to switch to another measure induced by a different numeraire. Switching to a different measure is usually done such that the process to be modeled is a martingale under this measure. Modeling a martingale is more convenient when the process is described by a SDE, since the drift term in the SDE does not have to be modeled. Switching between measures can be done with the Change of Numeraire theorem.

Theorem 2.12 (Change Of Numeraire)**.** *Consider two numeraires $\mathcal{N}(t)$ and $\tilde{\mathcal{N}}(t)$, inducing equivalent martingale measures $\mathbb{Q}^{\mathcal{N}}$ and $\mathbb{Q}^{\tilde{\mathcal{N}}}$, respectively. If the market is complete, then the density of the Radon-Nikodym derivative relating the two measures is uniquely given by*

$$Z(t) = \mathbb{E}^{\mathbb{Q}^{\mathcal{N}}}\left[\frac{\mathrm{d}\mathbb{Q}^{\tilde{\mathcal{N}}}}{\mathrm{d}\mathbb{Q}^{\mathcal{N}}} \middle| \mathcal{F}_t \right] = \frac{\tilde{\mathcal{N}}(t)\mathcal{N}(0)}{\mathcal{N}(t)\tilde{\mathcal{N}}(0)}.$$

Proof. A proof can be found in Andersen et al. [33]. □

Two other measures that are relevant for swaption pricing are the annuity measure and the T-forward measure.

Definition 2.13 (Annuity And T-forward Measures)**.**

- The *annuity measure* $\mathbb{Q}^A$ is the measure induced by taking the annuity $A_{k,M}$ as the numeraire.
- The *T-forward measure* $\mathbb{Q}^T$ is the measure induced by taking the zero coupon bond price $D(t,T)$ as the numeraire.

With these definitions and theorems swaps and swaptions can be priced.

2.2.2 Interest rate derivatives and pricing formulas

Interest rate derivatives and their pricing formulas are introduced in this section. First, a swap is introduced. It is a product where two parties exchange rates. The swap is defined to introduce a swaption, which is an option on a swap. It is a product used to inter- and extrapolate market quotes.

Definition 2.14 (Swap)**.** Let a tenor structure $0 \leq T_0 < T_1 < \ldots < T_M$, $\tau_n := T_{n+1} - T_n$ for $0 \leq n \leq M-1$, the corresponding annuity, a fixed rate K and a floating rate L be given. One party pays simple compounded interest based on the fixed rate K in return for simple interest payments based on the floating rate fixing on date T_n, for each period $[T_n, T_{n+1}]$, $n = 0, \ldots, M-1$. The payments are exchanged at the end of each period, i.e. T_{n+1}. The payments are assumed to have the same tenor structure, day count convention and business day convention. The payments based on the fixed rate are called the fixed leg and the payments based on the floating rate are called the floating leg. The net cash flow from perspective of the fixed rate payer is at time T_{n+1}:

$$N\tau_n(L(T_n, T_n, T_{n+1}) - K).$$

The value of a swap is a summation of these payments discounted by zero-coupon bonds to get the present value. It can be shown that the value of a swap at $T_{k-1} \leq t \leq T_k$ is:

$$\begin{aligned} V_{\text{swap}}(t) &= N \sum_{n=k}^{M-1} \tau_n D(t, T_{n+1})(L(t, T_n, T_{n+1}) - K) \\ &= N A_{k,M}(t) \left(\frac{\sum_{n=k}^{M-1} \tau_n D(t, T_{n+1}) L(t, T_n, T_{n+1})}{A_{k,M}(t)} - K \right), \end{aligned}$$

where $A_{k,M}$ is the annuity, N is the notional, i.e. the amount of money on which interest rate is payed for.

If $M = 1$, the swap reduces to a Forward Rate Agreement (FRA), with the slight difference that the payment is done at time T_1 for a swap and is done at time T_0 for the FRA. A useful quantity for the swap is the swap rate. This is the quantity that will be modeled in this thesis under the annuity measure.

Definition 2.15 (Forward Swap Rate)**.** The forward swap rate $S_{k,M}(t)$ is defined as the fixed rate that gives the swap the value zero as seen from time t. From the pricing formula of a swap, it follows that:

$$S_{k,M}(t) := \frac{\sum_{n=k}^{M-1} \tau_n D(t, T_{n+1}) L(t, T_n, T_{n+1})}{A_{k,M}(t)}, \ t \leq T_k. \tag{2.2}$$

It follows from the equivalent martingale measure that the swap rate $S_{k,m}(t)$ is a martingale under the annuity measure $A_{k,m}$. The annuity measure is therefore also known as the swap measure.

Definition 2.16 (Swaption)**.** A swaption gives the holder the right, but not the obligation, to enter into a swap at a pre-defined future time T. Time T is called the option maturity, often referred to as the exercise time.

The length of the underlying tenor structure of a swap is often referred to as the swap tenor. A xYzY swaption is shorthanded for a swaption with maturity $T = x$ years, where the underlying swap has a swap tenor of y years. Assuming that the underlying swap starts on the expiry date T_0, the value of a swaption at maturity T_0, is given by

$$V_{\text{swaption}}(T_0) = (V_{\text{swap}}(T_0))^+,$$

where $(x)^+ = \max(x, 0)$. It is chosen to use the annuity measure as the measure to price a swaption. This ensures that the swap rate can be modeled by a martingale. This gives the value of a swaption at time $t \leq T_0$:

$$\begin{aligned} V_{\text{swaption}}(t) &= A_{0,M}(t) N \mathbb{E}^A \left[A_{0,M}(T_0) \left(\frac{S_{0,M}(T_0) - K}{A_{0,M}(T_0)} \right)^+ \middle| \mathcal{F}_t \right] \\ &= A_{0,M}(t) N \mathbb{E}^A \left[(S_{0,M}(T_0) - K)^+ \middle| \mathcal{F}_t \right]. \end{aligned}$$

All the above is derived for a payer-swaption, where the holder has the option to enter into a swap where he receives the floating rate in exchange for paying fixed rate. It can be observed that the value of a swaption is the price of a call option on the swap rate under the annuity measure. The same can be derived for a receiver-swaption, where the holder has the option to enter into a swap where he receives the fixed rate in exchange for paying the floating rate. In this case the value of a swaption is the price of a put option on the swap rate under the annuity measure. The prices of a call (C) and put (P) options will be denoted by:

$$\mathrm{C}(t, T, K) = A(t) N \mathbb{E}^A \left[(S(T) - K)^+ \middle| \mathcal{S}_t \right], \tag{2.3}$$

$$\mathrm{P}(t, T, K) = A(t) N \mathbb{E}^A \left[(K - S(T))^+ \middle| \mathcal{S}_t \right], \tag{2.4}$$

where for convenience the swap rate is written by $S(t) := S_{0,M}(t)$. In the special case $K = S(t)$, the swaption is called an at-the-money swaption. The prices of a call and put option will be referred to as call and put prices respectively. For some fixed strikes, option maturities and swap tenors, the prices of swaptions are quoted in the market. This is explained in the next section.

2.3 Market quotes

Under the annuity measure the swap rate is a martingale. It is however not known what the dynamics of the swap rate are under the annuity is. Therefore, a model is needed to describe the dynamics of the swap rate. Bachelier's model and Black's model will be introduced, which are well-known models in financial modeling. These two models will give insight on how market quotes are given, for which the implied volatility curve is introduced.

2.3.1 Bachelier's model

Under Bachelier's model it is assumed that a financial quantity follows the SDE:

$$\mathrm{d}S_t = \mu \, \mathrm{d}t + \sigma \, \mathrm{d}W_t, \quad S(0) = S_0 > 0,$$

where W_t is a Brownian motion under a measure $\mathbb{P}$. The parameters μ and σ are called the drift and volatility parameter respectively.

Usually, one switches to an equivalent measure $\mathbb{Q}^*$ such that the underlying process is a martingale. For the swap rate, this equivalent measure is the annuity measure. The underlying process satisfies the following SDE under this equivalent measure:

$$\mathrm{d}S_t = \sigma \,\mathrm{d}W_t, \quad S(0) = S_0 > 0,$$

where W_t is the standard Brownian motion under $\mathbb{Q}^*$, and $\sigma \in \mathbb{R}_{\geq 0}$. This gives the well-known solution:

$$S(t) = S_0 + \sigma W_t.$$

The call and put price under Bachelier's model are given by Lemma 2.17:

Lemma 2.17 (Bachelier's Call and Put Price)**.** *The price of a call option (C) and put option (P) with maturity T under Bachelier's model for strike K at time t is:*

$$\mathrm{C}_{\mathrm{Bachelier}}(t, T, K, \sigma) = (S(t) - K)F_{\mathcal{N}}(-d) + \sigma\sqrt{T-t}f_{\mathcal{N}}(d), \tag{2.5}$$

$$\mathrm{P}_{\mathrm{Bachelier}}(t, T, K, \sigma) = (K - S(t))F_{\mathcal{N}}(-d) + \sigma\sqrt{T-t}f_{\mathcal{N}}(d), \tag{2.6}$$

with

$$d = \frac{K - S(t)}{\sigma\sqrt{T-t}},$$

and where $f_{\mathcal{N}}(\cdot)$ is the probability density function and $F_{\mathcal{N}}(\cdot)$ is the cumulative density function of the standard normal distribution. These formulas will be referred to as Bachelier's formulas.

Proof. A proof can be found in Iwasawa [22]. □

2.3.2 Black's model

Under Black's model it is assumed that a financial quantity is log-normally distributed at option time T and can be written as

$$S(T) = S_0 \exp\left(-\frac{\sigma^2}{2}T + \sigma W_T\right),$$

at option date T. W_T is a Brownian motion under a measure $\mathbb{Q}^*$. For the swap rate, $\mathbb{Q}^*$ is the annuity measure. S_0 is extracted from forward contracts. For the swap rate, the forward rate agreements imply rates by the market quotes such that the swap rate can be computed. This model originates from the Black and Scholes model, where it is assumed that a financial quantity follows the SDE:

$$\mathrm{d}S_t = \mu S_t \,\mathrm{d}t + \sigma S_t \,\mathrm{d}W_t, \quad S(0) = S_0 > 0.$$

The parameter μ is set equal to zero such that S_t is a martingale in Black's model under the appropriate measure, which is the annuity measure for the swap rate. For Black's model the call and put price can be derived analytically and are given in Lemma 2.18.

Lemma 2.18 (Black's Call and Put Price)**.** *The price of a call option (C) and put option (P) with option date T under Black's model for strike K at time t is:*

$$\mathrm{C}_{\mathrm{Black}}(t, T, K, \sigma) = S(t)F_{\mathcal{N}}(d_1) - KF_{\mathcal{N}}(d_2), \tag{2.7}$$

$$\mathrm{P}_{\mathrm{Black}}(t, T, K, \sigma) = KF_{\mathcal{N}}(-d_2) - S(t)F_{\mathcal{N}}(-d_1), \tag{2.8}$$

with

$$d_1 = \frac{\log\left(\frac{S(t)}{K}\right) + \frac{1}{2}\sigma^2(T-t)}{\sigma\sqrt{T-t}},\ d_2 = d_1 - \sigma\sqrt{T-t}.$$

These formulas will be referred to as Black's formulas.

Proof. A proof can be found in Shreve [37]. □

2.3.3 Implied volatility

Before the market crash of 1987 it was assumed that Black's model was a good approximation of the dynamics of the forward swap rate. Prices were quoted in terms of a constant Black volatility for all strikes, but the volatility differed for different maturities and tenors [19]. All other model parameters (S_0, t, T, K) could be observed from the market and therefore the prices of swaptions were known.

Market prices ceased being quoted with a constant Black volatility for all strikes after the market crash of 1987. Market prices are still quoted by Black volatilities, however the volatility differs for the strikes, i.e. each strike for which a market quote is provided has its own Black volatility. These volatilities are the *implied* Black volatilities, which means that these volatilities give the correct price given the wrong model. For example, let N be the notional of the underlying swap, $A(t)$ the annuity of the swap at time t, $S(t)$ the swap rate, T the option maturity of the swaption, K_i the corresponding fixed rate and σ_i^{market} be the volatility implied by the market. The price of a swaption at time t is given by

$$NA(t)C_{\text{Black}}(t, T, K_i, \sigma_i^{\text{market}}).$$

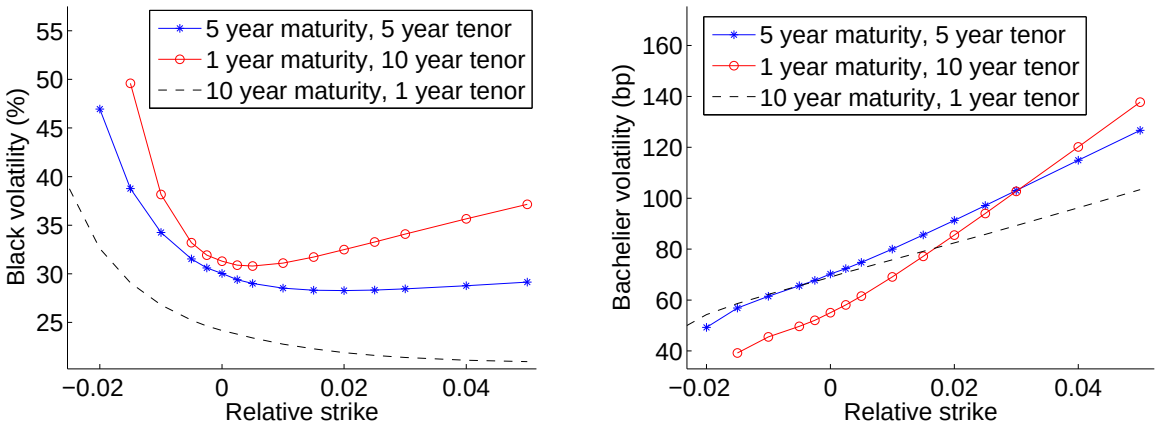

(a) Black's implied volatilities.

(b) Bachelier's implied volatilities.

Figure 2.1: Quotations for swaptions in implied volatilities plotted against relative strikes, i.e. the difference between the swap rate and the strike.

The implied volatilities vary in the strike, maturity and tenor direction. If the implied volatilities are described for one, two or all directions, it is called a volatility curve, surface or cube respectively. For convenience, the volatility curve described in the strike dimension will be referred to as the volatility curve.

Quotations can also be done in terms of implied Bachelier volatilities. For example, consider Figure 2.1a for the implied Black volatilities and Figure 2.1b for the implied Bachelier volatilities quoted on June 26th, 2014. Market quotes are plotted for $xYzY$ swaptions, where it is chosen to set approximately $x + y \equiv$ constant. Volatility curves are assumed to be more stable over time than option prices [19], which is the reason why quotations are done in volatilities. To determine the prices of swaptions outside the market quotes, a model is needed that can accurately describe the market quotes.

2.4 The SABR model

Bachelier's and Black's model can not replicate the volatility curve of the market quotes. Therefore, a more advanced model is needed which can capture the market volatility curve. In this thesis it is chosen to do so with the SABR model or a derivation of it. It is well-known that the SABR model can capture the market volatility curve accurately [29].

2.4.1 CEV process

The SABR model is presented by a constant elasticity of variance (CEV) process. Using the CEV process to model a financial quantity will be referred to as a CEV model. The CEV model is a special case of the SABR model and will give insight into the SABR model. The dynamics of a CEV process S_t is given by the SDE:

$$\mathrm{d}S_t = \sigma S_t^{\beta}\,\mathrm{d}W_t,$$

where it is chosen that $0 < \beta < 1$. The cases $\beta = 0$ and $\beta = 1$ relate to Bachelier's and Black's model respectively. For other cases, the process does not have a unique solution to the SDE.[2]

It is shown below how a CEV process relates to a Bessel process and how properties for a CEV process can be derived by a Bessel process. A brief introduction on Bessel processes can be found in Appendix A.1. Define $X_t := \frac{1}{\sigma(1-\beta)} S_t^{1-\beta}$. It follows by Itô's Lemma that:

$$\mathrm{d}X_t = \mathrm{d}W_t - \frac{\beta}{2(1-\beta)}\frac{1}{X_t}\,\mathrm{d}t.$$

Therefore, X is Bessel process of negative index $\frac{1}{2(1-\beta)}$, it hits zero in finite time for $0 \leq \beta < 1$. In the case $\frac{1}{2} \leq \beta < 1$ it corresponds to a Bessel process with dimension w with $0 \leq w < 2$ and the processes stops naturally at zero. Therefore, it has a point mass at zero. For $0 < \beta < \frac{1}{2}$ it corresponds to a Bessel process with negative dimension and a boundary condition has to be chosen when the process hits zero. If it is stopped at zero, the process stays a martingale by the stopped martingale theorem. The probability density function of a CEV process from S_0 to $S_t = y$ is given by [6]:

$$f_A(t,y) = \frac{1}{\sigma^2(1-\beta)}\frac{y^{1-2\beta}}{t}\left(\frac{y}{S_0}\right)^{-\frac{1}{2}} e^{-\frac{q^2+q_0^2}{2t}} I_{|\eta|}\left(\frac{qq_0}{t}\right). \tag{2.9}$$

The process can also be reflected at zero, but then the process does not stay a martingale. If the process is reflected for $0 \leq \beta < \frac{1}{2}$ at zero, the probability density is given by [6]:

$$f_R(t,y) = \frac{1}{\sigma^2(1-\beta)}\frac{y^{1-2\beta}}{t}\left(\frac{y}{S_0}\right)^{-\frac{1}{2}} e^{-\frac{q^2+q_0^2}{2t}} I_{\eta}\left(\frac{qq_0}{t}\right), \tag{2.10}$$

[2] See Shreve [37] for an existence and uniqueness theorem for SDEs.

where $\eta = \frac{-1}{2(1-\beta)}$, $q_0 = \frac{S_0^{1-\beta}}{\sigma(1-\beta)}$ and $q = \frac{y^{1-\beta}}{\sigma(1-\beta)}$. The probability density function describes the distribution of the process over time and option prices can be calculated as an integral by calculation the expectation $\mathbb{E}[V(S_T)|\mathcal{F}_t] = \int_{-\infty}^{+\infty} V(x)f(T,x)\,\mathrm{d}x$. Under the CEV process, an analytically expression for a call price can be derived [20]. The probability density function of a CEV process will be used as a fundamental in Chapter 3 and 4.

The cumulative density function of a CEV process for $\frac{1}{2} \leq \beta < 1$ and assuming absorption for $0 < \beta < \frac{1}{2}$ is given by [20]:

$$F(y) = 1 - F_{\chi^2(b,c(y))}(a), \tag{2.11}$$

with

$$a = \frac{S_0^{2(1-\beta)}}{(1-\beta)^2\sigma^2 T},\ b = \frac{1}{1-\beta},\ c(y) = \frac{y^{2(1-\beta)}}{(1-\beta)^2\sigma^2 T},$$

where $F_{\chi^2(b,c)}$ is the cumulative density function of the non-central chi-squared distribution with b degrees of freedom and the non-central parameter c.

2.4.2 An introduction to the SABR model

The SABR model is an extension of the CEV process, where the volatility of the model is chosen to be a stochastic process. The dynamics of a financial quantity S_t under the SABR model are given by:

$$\begin{cases} \mathrm{d}S_t = \alpha_t S_t^{\beta}\,\mathrm{d}W_t^1, & S(0) = S_0 > 0, \\ \mathrm{d}\alpha_t = \nu\alpha_t\,\mathrm{d}W_t^2, & \alpha(0) = \alpha > 0, \\ \mathrm{d}W_t^1\,\mathrm{d}W_t^2 = \rho\,\mathrm{d}t. \end{cases}$$

with $\nu > 0$, $0 \leq \beta \leq 1$ and $-1 \leq \rho \leq 1$. S_t is the value of the financial quantity at time t and α_t is its volatility.

SABR is an abbreviation for Stochastic Alpha Beta Rho, a name derived from the corresponding model parameters. The SABR model is an example of a stochastic volatility model, since the volatility α_t is modeled by a process driven by a Brownian motion W_t^2. If $\nu = 0$ it reduces to Black's model for $\beta = 1$, Bachelier's model for $\beta = 0$ and a CEV model for $0 < \beta < 1$.

As for the CEV process, the process has to be stopped for $0 < \beta < \frac{1}{2}$ in order to remain a martingale [18]. For $\frac{1}{2} \leq \beta < 1$, it has a natural absorption at zero and remains a martingale [18]. Only for $\beta = 0$, the SABR model allows the financial quantity to become negative.

By modeling the swap rate with the SABR model, prices for swaptions can be computed for a given set of parameters. With these prices, an implied volatility for Black's or Bachelier's model can be obtained for each strike. In general these implied volatilities will give not a constant volatility curve in the strike dimension, but it will vary like the market quotes. Furthermore, the four model parameters of the SABR model have the following impact on this implied volatility curve [29][3]:

- α controls the overall height of the curve.
- ν controls how much curvature the curve exhibits.
- β and ρ control the skewness of the curve.

[3]This impact should not be confused with Hagan's formulas. Hagan's formulas have a similar impact in the volatility curve as the SABR model.

The SABR model is often used in the interest rate market to construct a volatility curve implied by the model to fit the volatility curve of the market. The impact on the implied volatility curve of the model by the parameters make it an easy to understand model. It is known that this model can fit the market volatility curve accurately [29].

In general, no closed-form solutions for option prices are known under the SABR model. The exception is the special case of $\rho = 0$, for which a two-dimensional integral is derived by Antonov et al. [3]. For the general case, one could consider to apply the multivariate version of the Fokker-Planck equation to the SABR model. This gives the full SABR (S, α, t)-PDE for the probability density function f:

$$\frac{\partial f(t,S,\alpha)}{\partial t} = \frac{1}{2}\frac{\partial^2\left(\alpha^2 S^{2\beta} f(t,S,\alpha)\right)}{\partial S^2} + \frac{\partial^2\left(\rho\nu\sigma^2 S^{\beta} f(t,S,\alpha)\right)}{\partial S \partial \alpha} + \frac{1}{2}\frac{\partial^2\left(\nu^2\alpha^2 f(t,S,\alpha)\right)}{\partial \alpha^2}.$$

This is a two-dimensional PDE and therefore computationally expensive to solve numerically. It is however desired to have a fast approach such that it can be used in practice.

2.5 Hagan's Formulas

Hagan's formulas are introduced along with their benefits and drawbacks. These are approximations of the Black's and Bachelier's volatility implied by the SABR model, which is a stochastic *local* volatility model. The volatility is locally described, where the volatility is implied by a stochastic process. The benefit of describing the volatility curve directly is that it is directly linked to the market quotes.

These formulas are derived under the assumption that:

$$\alpha\sqrt{T} \ll 1,\ \nu\sqrt{T} \ll 1 \text{ and } \frac{|S_0 - K|}{\alpha\sqrt{T}} = \mathcal{O}(1). \tag{2.12}$$

These are not the exact implied Black and Bachelier volatility, but the unstated argument by Hagan et al. is that "*instead of treating these formulas as a reasonably accurate approximation to the SABR model, they should be treated as the exact solution to some other model which is well approximated by the SABR model*" [30][4].

2.5.1 Hagan's Black formula

Under the SABR model, the implied Black volatility can be approximated under the assumptions in Equation (2.12) by[5][29]:

$$\sigma_B = I_1 \cdot (1 + I_2 \cdot T), \tag{2.13}$$

[4]Hagan et al. argues that these formulas should not be considered as the SABR model, but a different model for which the dynamics of the underlying process are not known. Rather, these formulas will give a parameterization of the volatility curve. As discussed earlier, it is known that the market volatility curve stays approximately constant over time [19], and it therefore makes sense to describe the market volatility curve rather than a process.

[5]The functions I_1 and I_2 are only introduced for as dummy functions and should not be confused with the modified Bessel function. Similarly it holds for the functions z, χ and ζ. They should only be considered as dummy functions.

where

$$I_1 := I_1(\alpha,\beta,\rho,\nu,S_0,K) = \frac{\alpha z}{\chi(z)\left(S_0K\right)^{\frac{1-\beta}{2}}\left(1+\frac{(1-\beta)^2}{24}\log^2\left(\frac{S_0}{K}\right)+\frac{(1-\beta)^4}{1920}\log^4\left(\frac{S_0}{K}\right)\right)},$$

$$I_2 := I_2(\alpha,\beta,\rho,\nu,S_0,K) = \frac{(1-\beta)^2}{24}\frac{\alpha^2}{\left(S_0K\right)^{1-\beta}}+\frac{1}{4}\frac{\rho\beta\nu\alpha}{\left(S_0K\right)^{\frac{1-\beta}{2}}}+\frac{2-3\rho^2}{24}\nu^2,$$

$$z := z(\alpha,\beta,\nu) = \frac{\nu}{\alpha}\left(S_0K\right)^{\frac{1-\beta}{2}}\log\left(\frac{S_0}{K}\right),$$

$$\chi := \chi(z,\rho) = \log\left(\frac{\sqrt{1-2\rho z+z^2}+z-\rho}{1-\rho}\right).$$

This formula will be referred to as Hagan's Black formula.

2.5.2 Hagan's Bachelier formula

Under the SABR model, the implied Bachelier volatility can be approximated under the assumption in Equation (2.12) by[5][29]:

$$\sigma_N = I_1\cdot(1+I_2\cdot T), \tag{2.14}$$

where

$$I_1 := I_1(\alpha,\beta,\rho,\nu,S_0,K) = \frac{\alpha(1-\beta)(S_0-K)}{S_0^{1-\beta}-K^{1-\beta}}\frac{\zeta}{\chi(\zeta)},$$

$$I_2 := I_2(\alpha,\beta,\rho,\nu,S_0,K) = \frac{\beta(\beta-2)\alpha^2}{24}\left(S_0K\right)^{\beta-1}+\frac{\alpha\beta\rho\nu}{4}\left(S_0K\right)^{\frac{\beta-1}{2}}+\frac{2-3\rho^2}{24}\nu^2,$$

$$\zeta := \zeta(\alpha,\beta,\nu,S_0,K) = \frac{\nu\left(S_0-K\right)}{\alpha\left(S_0K\right)^{\frac{\beta}{2}}},$$

$$\chi := \chi(\zeta,\rho) = \log\left(\frac{\sqrt{1-2\rho\zeta+\zeta^2}+\zeta-\rho}{1-\rho}\right).$$

This formula will be referred to as Hagan's Bachelier formula. Hagan's Black and Bachelier formulas will be referred to as Hagan's formulas.

2.5.3 Benefits of Hagan's formulas

The implied volatilities derived by Hagan et al. are straightforward to implement compared to more sophisticated methods. This is one of the benefits of Hagan's formulas. It is also well-known by market practitioners that the implied volatility curve by Hagan's formulas can be fitted to the market accurately by choosing the SABR parameters α,β,ρ,ν such that the difference between the market quotes and the implied volatility curve by Hagan's formulas is minimal. As an example, a 30Y10Y swaption quoted on 26th of June 2014 is taken. The result is presented in Figure 2.2. This figure show that that Hagan's formulas can accurately capture the market volatility, even for a long maturity. The latter may seem contradictory against the derivation of the formulas, but this shows that these formulas seem usable for longer maturities too.

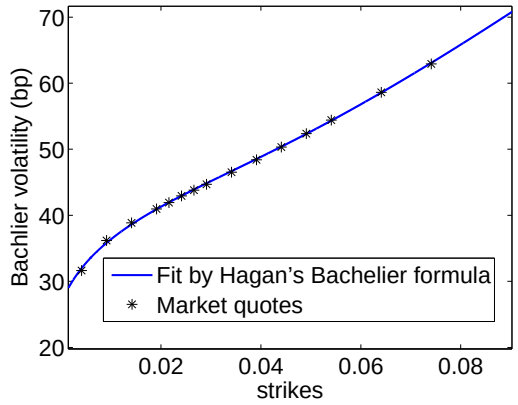

(a) Fit by Hagan's Bachelier formula.

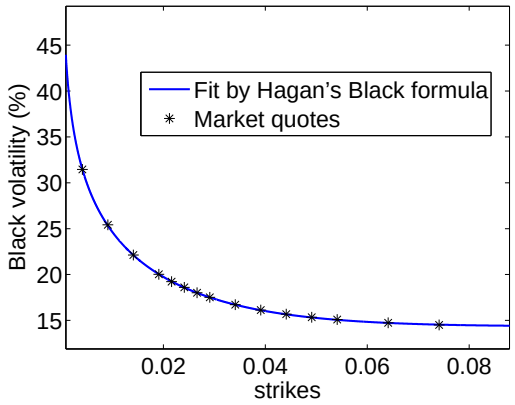

(b) Fit by Hagan's Black formula.

Figure 2.2: Fit with Hagan's formulas to volatility curve for a 30Y10Y swaption in the euro market. The calibrated parameters are given by Table 2.1.

General parameters		Hagan's Black formula				Hagan's Bachelier formula			
T	S_0	α	β	ρ	ν	α	β	ρ	ν
30	0.02407	0.0411	0.5960	-0.3538	0.1309	0.0662	0.7117	-0.4788	0.1309

Table 2.1: Calibrated SABR parameters for Hagan's formulas in Figure 2.2.

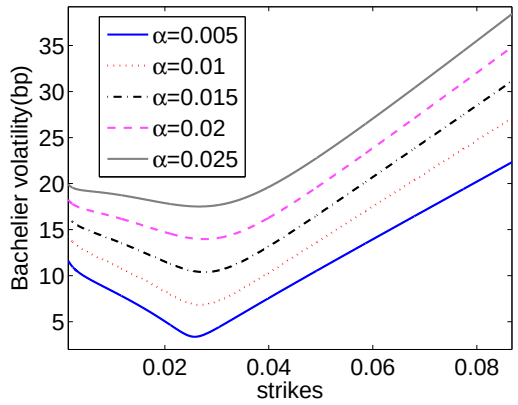

(a) Different values of α in Hagan's Bachelier formula.

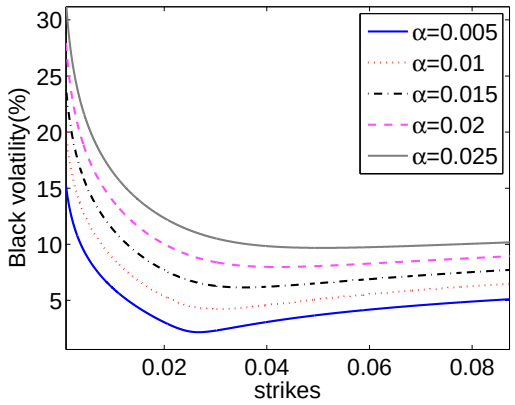

(b) Different values of α in Hagan's Black formula.

Figure 2.3: Hagan's implied volatility for Bachelier's and Black's model for different values of the parameters. Fixed parameters are given by Table 2.1.

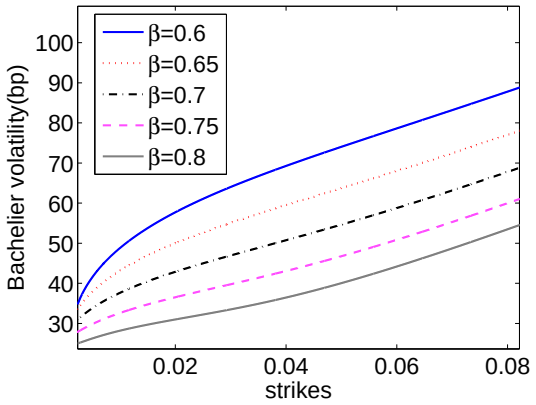

(a) Different values of β in Hagan's Bachelier formula.

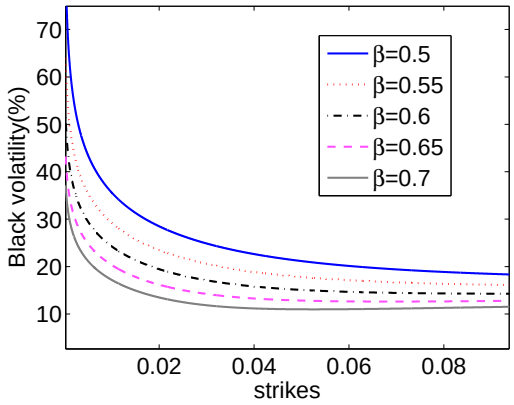

(b) Different values of β in Hagan's Black formula.

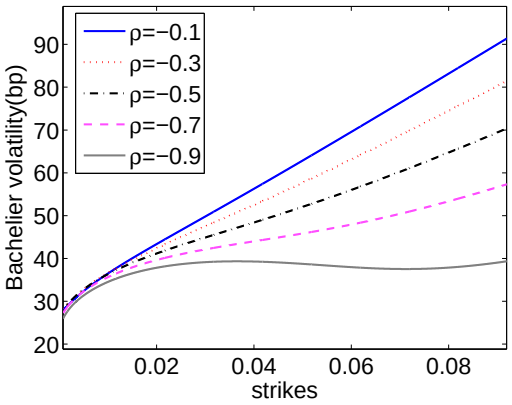

(c) Different values of ρ in Hagan's Bachelier formula.

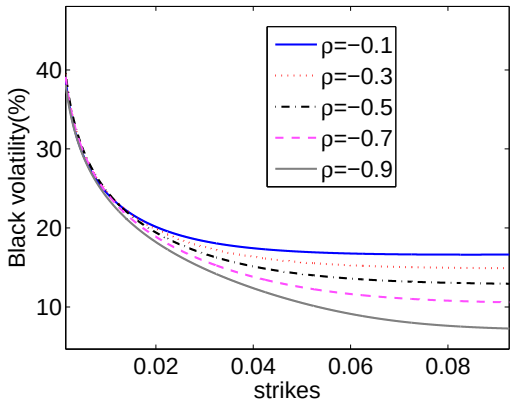

(d) Different values of ρ in Hagan's Black formula.

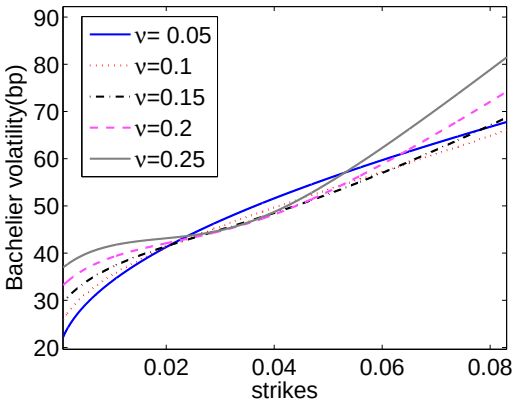

(e) Different values of ν in Hagan's Bachelier formula.

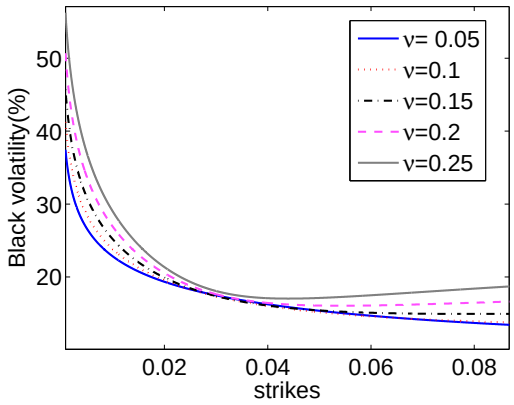

(f) Different values of ν in Hagan's Black formula.

Figure 2.4: Hagan's implied volatility for Bachelier's and Black's model for different values of the parameters. Fixed parameters are given by Table 2.1.

In Figures 2.3a–2.4f α, β, ρ and ν are varied respectively to investigate the impact of each parameter on the implied volatility curve as predicted by Hagan's formulas. One can indeed observe that α controls the overall height of the curve, β and ρ control the skewness of the volatility curve, and ν controls how much curvature the volatility curve exhibits. The SABR parameter β also influences the height of the volatility curve. This is since β can be seen as varying in type of distribution, $\beta = 0$ corresponds to a Bachelier's model and $\beta = 1$ corresponds to Black's model with a stochastic volatility. In general, one needs a higher volatility for the same price under Black's model compared to Bachelier's model. Figure 2.2 presents an example for the comparison between the volatilities of Black's and Bachelier's model. For this figure the Black volatility is approximately 200 times higher than the Bachelier volatility.

2.5.4 Arbitrage in Hagan's formulas

The drawbacks of Hagan's formulas is that they are not arbitrage-free. This is shown with Lemma 2.19 and butterfly option prices.

Lemma 2.19. *Let the price of a call (C) and put (P) be given by:*

$$C(K) := C(t,T,K) = \mathcal{D}(t)\mathbb{E}^A\left[(S_T - K)^+ \middle| \mathcal{F}_t\right],$$
$$P(K) := P(t,T,K) = \mathcal{D}(t)\mathbb{E}^A\left[(K - S_T)^+ \middle| \mathcal{F}_t\right],$$

for some function $\mathcal{D}(t)$. The prices satisfy the following relations to the probability density function f and the cumulative density function F:

$$\frac{\partial^2 C}{\partial K^2}(K) = \frac{\partial^2 P}{\partial K^2}(K) = \mathcal{D}(t)f(K), \tag{2.15}$$
$$\frac{\partial C}{\partial K}(K) = \mathcal{D}(t)(F(K) - 1), \tag{2.16}$$
$$\frac{\partial P}{\partial K}(K) = \mathcal{D}(t)F(K), \tag{2.17}$$

where S_t is a well-defined martingale process.

Proof. The proof can be found in Appendix A.2. □

Definition 2.20 (Butterfly Option)**.** A butterfly option is a portfolio of call options with pay-off $\mathrm{V_B}$ at maturity T:

$$\mathrm{V_B}(K,\Delta K) := \mathrm{V_B}(t,T,K,\Delta K) = C(t,T,K+\Delta K) - 2C(t,T,K) + C(t,T,K-\Delta K), \tag{2.18}$$

where $\Delta K > 0$. The quantity ΔK will be referred to as the *call spread* of a butterfly option.

Figure 2.5 presents an example of a pay-off at maturity of a butterfly option with. The value of a butterfly option is nonnegative. Assuming $\mathcal{D}(t) = 1$, the following relation between a butterfly option and the probability density function f of S_t holds:

$$f(K) = \frac{\partial^2 C}{\partial K^2}(K) \approx \frac{C(K+\Delta K) - 2C(K) + C(K-\Delta K)}{\Delta K^2} = \frac{\mathrm{V_B}(K,\Delta K)}{\Delta K^2}, \tag{2.19}$$

for $\Delta K \ll 1$.

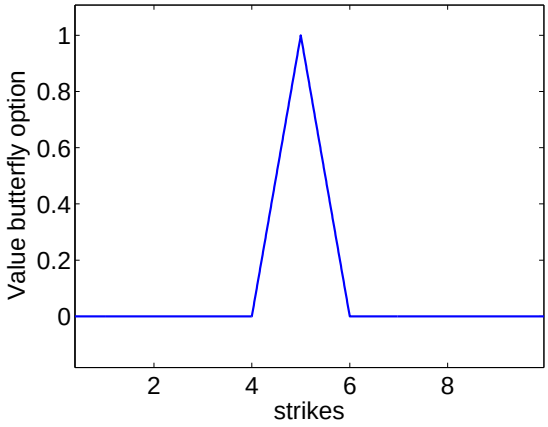

Figure 2.5: Example of a Pay-off of a butterfly option for different strikes with $\Delta K = 1$, $S_T = 5$.

General parameters		Hagan's Bachelier formula			
T	S_0	α	β	ρ	ν
30	0.02407	0.0987	1.000	-0.2174	0.5768

Table 2.2: Parameters for the construction of Figure 2.6.

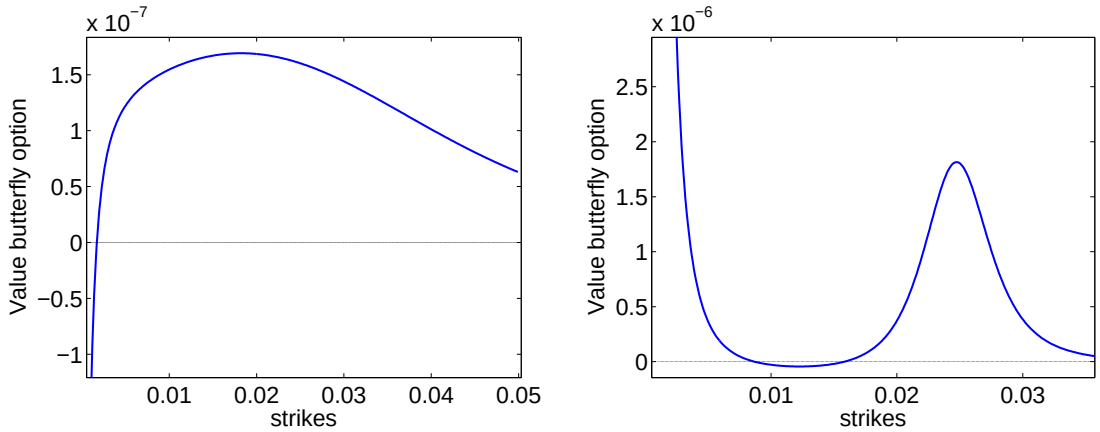

(a) Hagan's Black formula.

(b) Hagan's Bachelier formula.

Figure 2.6: Butterfly option prices implied by Hagan's formulas for a call spread $\Delta K = 1$ bp. Parameters are taken from Table 2.1 for Hagan's Black formula and Table 2.2 for Hagan's Bachelier formula.

By valuing butterfly options, it can be shown that Hagan's formulas contain arbitrage. For the butterfly options it Figures 2.6a and 2.6b shows examples of such cases.

The butterfly option can attain negative values for some strikes under Hagan's formulas. This implies that one would assign a negative value to a butterfly option when pricing it with Hagan's formulas. So, a guaranteed profit is assured for a butterfly option when its price is assigned with Hagan's formulas. This is an arbitrage opportunity which is called a *butterfly-arbitrage*. If this occurs, it implies that the underlying process is governed by a negatively valued probability density function due to the relation in Equation (2.19). This implied negatively

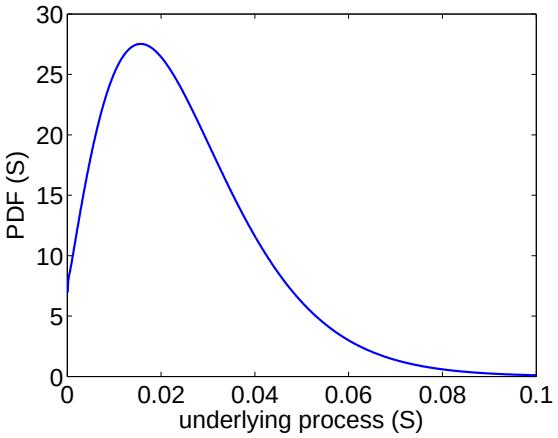

Figure 2.7: An arbitrage-free implied probability density function for Hagan's Black formula. Parameters are taken from Table 2.3.

General parameters		Hagan's Black formula			
T	S_0	α	β	ρ	ν
1	0.025	0.15	0.6	-035	0.1

Table 2.3: A parameter set for which Hagan's Black formula is arbitrage free.

valued probability density function is often referred to as a butterfly-arbitrage as well. Some practitioners prefer to reverse this statement, i.e. butterfly-arbitrage implies a negatively valued probability density function. Hagan's formulas do not always contain arbitrage. If Hagan's formulas do not imply butterfly arbitrage, they imply a well-defined process as a model for the financial quantity, like the swap rate. This underlying process has a positively valued probability density function with a point mass at zero which is aligned with the SABR model. Figure 2.7 presents an example of such an underlying probability density function implied by Hagan's formulas. Like the SABR model, this probability density function implies a point mass at zero. In this case, it is approximately equal to 0.004.

The implied negatively valued probability density function is caused by a discontinuity in Hagan's formulas, as noted by Doust [11]. This discontinuity causes the volatility curve to blow up to infinity for strikes near zero. In this case, call prices are too high for low strikes, such that they are either no longer convex and imply an underlying process with a negatively valued probability density function, or they remain convex but imply an underlying process for which the probability density function blows up at zero. A combination is also possible. Figures 2.6a and 2.6b are examples of such cases.

Another way to verify if an approach holds arbitrage, is via put-call parity. This is a well-known relation in finance that must hold to ensure no arbitrage is applied by the approach:

$$C(t,T,K) = P(t,T,K) + \mathcal{D}(t)(S_t - K). \tag{2.20}$$

In the case of swaptions $\mathcal{D}(t) = A(t)N$. If the relation (2.20) does not hold, one can construct arbitrage via a portfolio of a call option, a put option and a forward agreement. If S_t is a well-defined process and a martingale at time T, it can be proven that put-call parity holds. Hagan's formulas satisfy the put-call-parity. Only Hagan's Black formula implies a positive martingale process with an absorption at zero. To elaborate on this, let S_T be the process at time T implied

by Hagan's Black formula. The positive expectation is equal to the call price with strike equal to zero. The latter one is yet again equal to S_0 under Black's model, independent of the volatility. Hence:

$$\mathbb{E}\left[(S_T)^+\right] = C_{\text{Black}}(t, T, 0, \sigma) = S_0.$$

This follows from the fact that Black's model assumes a positive underlying process for the financial quantity, like the swap rate. This is in alignment with the SABR model for $\beta > 0$.

Hagan's Bachelier formula does not guarantee a martingale process with absorption at zero, since it holds $C_{\text{Bachelier}}(t, T, 0, \sigma) > S_0$ for $S_0 > 0$ and $\sigma > 0$. It only provides a positive process with a point mass at zero if $\sigma = 0$ for $K = 0$. This follows from the fact that Bachelier's model assumes a underlying process that can become negative. It is however in alignment with the SABR model for $\beta = 0$. To be fully aligned with the SABR model for $\beta > 0$, one should derive the call price under Bachelier's model, where the underlying process is stopped at zero. For this case, an analytical expression for the call price can be found in Park [31].

Other conditions to exclude arbitrage for approaches can be derived from other options or relations between derivatives. For example, arbitrage can occur by interpolation in the maturity of options. A condition for arbitrage in the direction of the maturity and tenor for a swaption is provided by Johnson et al. [24]. The focus in this thesis will be on arbitrage in the direction of the strikes. To ensure no arbitrage occurs in the interpolation in the tenor and maturity direction, one has to ensure first that the inter- and extrapolation of the market quotes in the strike dimension is arbitrage-free. It can be proven that if the approach implies a positively valued underlying density and the martingale property, the approach is arbitrage-free.

2.6 Summary

This chapter presented the mathematical background to price swaps and swaptions. It is explained how market prices are quoted and how they are related to Black's and Bachelier's model. The market quotes its prices in Black volatilities. Furthermore, the volatility curve stays approximately constant over time [19]. Hagan's formulas can capture the market volatility curve accurately and is therefore used by practitioners. However, it holds butterfly arbitrage, which is not desired. Therefore, more advanced approaches which are fast and arbitrage-free must be investigated and compared to Hagan's formulas. These will be investigated in the Chapters 3 and 4.

Chapter 3

Arbitrage-free approaches for pricing swaptions

Many alternative approaches to address the arbitrage issue in Hagan's formulas were recently proposed in the literature. In this chapter, two of these approaches will be discussed which seemed promising. A more detailed list of alternatives can be found in the bibliography. These approaches were selected since they are arbitrage-free and are computationally rapid. These approaches can be used in practice to parametrize the market volatility curve of swaptions in the strike direction for a fixed tenor and maturity. Approaches that are not computationally rapid, cannot be used in practice to parametrize the market volatility curve.

This chapter starts by explaining the approach by Hagan et al. [30] in Section 3.1, which will be referred to as Hagan's AF SABR. It is an approach based on solving a PDE for the marginal probability density function of a stochastic process. The PDE itself implies a well-defined process, making it arbitrage-free. Choosing the process implied by the PDE for the financial quantity will be referred to as Hagan's AF SABR model.[1] The PDE will be solved numerically by the approach of Le Floch et al. [15]. In this approach a change of variables is introduced to ensure that few discretization points have to be used such that the PDE can be solved computationally rapid. After the PDE is solved numerically, the probability density function has to be described between the discretization points. An alternative technique will be proposed compared to the technique of Le Floch et al. for more stable butterfly option prices. Lastly, Section 3.1 presents convergence results by Hagan's AF SABR and discusses whether Hagan's AF SABR model is in align with the SABR model.

After Hagan's AF SABR, the approach by Antonov et al. [3] is introduced in Section 3.2. This approach gives an analytically exact solution of a call price under the SABR model for $\rho = 0$, i.e. the uncorrelated case. Since this approach gives the analytical solution it is arbitrage-free. This solution is expressed as a two-dimensional integral and is approximated by an one-dimensional integral. The benefits and drawbacks of this one-dimensional integral will be discussed. Furthermore, it is discussed how to price call options under the correlated case in this approach, but as this approach is not arbitrage-free, it is not considered in this thesis.

This chapter concludes with a summary and discussion of Hagan's AF SABR and uncorrelated Antonov by comparison of these approaches.

[1] Hagan's AF SABR model should not be confused with Hagan's AF SABR. The first one is a model, the latter one is an approach to price options under this model.

3.1 Hagan's Arbitrage-Free SABR

As discussed in Section 2.4.2, the full SABR PDE is expensive to solve numerically. Hagan et al. reduced the dimension of this PDE by removing the dependency of the volatility α. This reduction of dimensionality is done by analyzing the dynamics of the SABR model using a small time expansion.

The result is an approximation of the marginal probability density function $Q(T,S) := \int_{-\infty}^{+\infty} f\left(S_T, \alpha_T | S_0, \alpha\right) \mathrm{d}\alpha_T$ and is described by the one-dimensional PDE:

$$\begin{cases} \frac{\partial Q}{\partial T} = \frac{\partial^2 (H(T,S)Q)}{\partial F^2}, \\ Q(T=0,S) = \delta(S - S_0). \end{cases} \tag{3.1}$$

with

$$\begin{aligned} &H(T,S) = \frac{1}{2} O^2(S) E(T,S), \\ &O(S) = \alpha \sqrt{1 + 2\rho\nu y(S) + \nu^2 y^2(S)} S^\beta, \; E(T,S) = e^{\rho\nu\alpha\Theta(S)(T-t)}, \\ &y(S) = \frac{S^{1-\beta} - S_0^{1-\beta}}{1-\beta}, \; \Theta(S) = \frac{S^\beta - S_0^\beta}{S - S_0}. \end{aligned}$$

The derivation of the PDE can be found in Appendix B.1.1. The resulting PDE is a one-dimensional PDE and therefore easier to solve numerically than the full SABR PDE. The PDE implies a well-defined process, since if one applies the Fokker-Planck equation to the process

$$\mathrm{d}S_t = \sqrt{H(T,S_t)}\, \mathrm{d}W_t, \tag{3.2}$$

one can observe that this process S_t implies the one-dimensional PDE derived by Hagan et al. The PDE therefore itself implies a nonnegative probability density function. This process S_t should not be confused with the SABR model and in the remainder of this section S_t will be the process that satisfies the SDE in Equation (3.2). This reduction of dimensionality creates a new model, which will be referred to as Hagan's AF SABR model, where AF is shorthanded for arbitrage-free. Pricing options under Hagan's AF SABR model by solving the PDE numerically will be referred to as Hagan's AF SABR.

The function $H(T,S)$ is only defined for $S \geq 0$ for the real line. Therefore, it is chosen to stop the process S_t on a point $S_{\min} \geq 0$. For numerically solving the PDE, the PDE has to be described on a finite domain. Therefore it is assumed that the process S_t is stopped at a $S_{\max}$ too. The probability density function will be therefore be written in the form:

$$Q(T,S) = \begin{cases} \mathcal{Q}^L(T)\delta(S - S_{\min}) & \text{for } S = S_{\min}, \\ Q^c(S,t) & \text{for } S_{\min} < S < S_{\max}, \\ \mathcal{Q}^R(T)\delta(S - F_{\max}) & \text{for } S = S_{\max}, \end{cases} \tag{3.3}$$

where δ is the Dirac function, $\mathcal{Q}^L$ and $\mathcal{Q}^R$ are the probability masses accumulated at $S_{\min}$ and $S_{\max}$ respectively. Q^c satisfies the one-dimensional PDE in Equation (3.1) on the interval $[S_{\min}, S_{\max}]$. $S_{\max}$ is chosen such that the probability that the process S_t hits zero is small, i.e. $\mathcal{Q}^R(T)$. This will be made more concrete after the transformation of variables in the next section.

The boundary conditions are given by

$$\lim_{S\to S_{\min}} H^2(F)Q^c(T,S) = 0, \quad \lim_{S\to S_{\max}} H^2(F)Q^c(T,S) = 0,$$
$$\frac{\mathrm{d}\mathcal{Q}^L}{\mathrm{d}T} = \lim_{S\to S_{\min}} \frac{1}{2}\alpha^2 \frac{\partial\left[H^2(S)Q^c\right]}{\partial S}, \quad \frac{\mathrm{d}\mathcal{Q}^R}{\mathrm{d}T} = -\lim_{S\to S_{\max}} \frac{1}{2}\alpha^2 \frac{\partial\left[H^2(S)Q^c\right]}{\partial S}.$$

The boundary conditions make sure that the total probability sums up to one and that the martingale property is preserved. For the derivation of the boundary conditions, see Hagan et al. [30]. In order to be alignment with the SABR model, it is chosen to set $S_{\min} = 0$ in the thesis. In the next section, when the transformation of variables is introduced, this will be made more concrete.

The limiting case for $y(S)$ can be computed with l'Hopital's rule:

$$\lim_{\beta\to 1} y(S) = \log\left(\frac{S}{S_0}\right).$$

Pricing options under Hagan's AF SABR model will be restricted by solving the PDE for the probability density function and approximating option prices with a numerical integration technique.[2] To solve the PDE, numerical techniques will be employed. To ensure that the PDE is solved a computationally rapid, the approach by Le Floch et al. will be followed in the next section.

3.1.1 A change of variable to efficiently solve the PDE numerically

The PDE can be solved computationally rapid with the transformation by Le Floch et al with numerical techniques, since fewer discretization points are needed for a similar accuracy compared to the original PDE derived by Hagan et al. The PDE for the probability density function will be derived for the variable

$$z(S) := \int_{S_0}^{S} \frac{1}{O(u)}\,\mathrm{d}u = -\frac{1}{\nu}\log\left(\frac{\sqrt{1-\rho^2+\left(\rho+\frac{\nu\tilde{y}(S)}{\alpha}\right)^2}-\rho-\frac{\nu-\nu\tilde{y}(S)}{\alpha}}{1-\rho}\right). \tag{3.4}$$

Reversely, the transformation implies:

$$S(z) = \left(S_0^{1-\beta} + (1-\beta)\tilde{y}(z)\right)^{\frac{1}{1-\beta}}, \quad \tilde{y}(z) = \frac{\alpha}{\nu}\left(\sinh(\nu z) + \rho(\cosh(\nu z) - 1)\right).$$

(a) Grid for variable z. (b) Grid for variable s.

Figure 3.1: Grid in z and s compared for the approach by Le Floch et al. The parameter used to construct this Figure are in Table 3.2.

[2] Other techniques, like Monte Carlo, can also be applied to the process S_t.

General parameters		SABR parameters			
T	S_0	α	β	ρ	ν
10	0.025	0.15	0.6	-035	0.1

Table 3.1: Parameter set to construct Figure 3.1.

The result of the transformation of variables is that by a uniform discretization of z, the discretization is more dense in S near S_0 and more coarse away from S_0. Furthermore, a reasonably sized interval of z, can lead to a wide interval in S. Thus fewer discretization points have to be used to solve the transformed PDE compared to the direct approach by Hagan et al. For example, see Figure 3.1.

The new probability density function under z is defined by:

$$\theta(T,z) := Q(T,S(z))O(S(z)),$$

where

$$\theta(T,z) = \begin{cases} \mathcal{P}_L(T)\delta(z-z^-) & \text{for, } z \le z^-, \\ \theta^c(T,z), & \text{for } z^- < z < z^+, \\ \mathcal{P}_R(T)\delta(z-z^+), & \text{for } z \ge z^+, \end{cases} \tag{3.5}$$

with

$$z^- := z(S_{\min}),\ z^+ := z(S_{\max}),$$

and $\mathcal{P}_L$ and $\mathcal{P}_R$ are the probability masses at z^- and z^+ respectively.

The PDE for $\theta(T,z)$ is given by:

$$\frac{\partial\theta(T,z)}{\partial T} = \frac{\partial}{\partial z}\left\{\frac{1}{O(z)}\frac{\partial}{\partial z}\left\{O(z)E(T,z)\theta(T,z)\right\}\right\}, \tag{3.6}$$

where $O(z) := O(S(z))$ and $E(T,z) := E(T,S(z))$. The derivation of this PDE is done in Appendix B.1.2. The PDE becomes singular at $S = 0$, since $O(z(0)) = 0$. Therefore, one must ensure in the discretization that $z > z(0)$.

The boundary conditions are given by

$$\frac{\partial\mathcal{P}_L(T)}{\partial T} = \frac{1}{C(z)}\frac{\partial}{\partial z}\left\{C(z)E(T,z)\theta(T,z)\right\}\Big|_{z=z^-},\ \frac{\partial\mathcal{P}_R(T)}{\partial T} = -\frac{1}{C(z)}\frac{\partial}{\partial z}\left\{C(z)E(T,z)\theta(T,z)\right\}\Big|_{z=z^+},$$
$$C(z)E(T,z)\theta(T,z)|_{z=z^-} = 0,\ C(z)E(T,z)\theta(T,z)|_{z=z^+} = 0.$$

The derivation of the boundary conditions is given in Appendix B.1.3.

It is claimed by Le Floch et al. and Hagan et al. that the new probability density function as function of z is close to a normal distribution. This can be concluded from the dynamics in Equation (3.2) [30]. $S_{\max}$ can be chosen such that $1 - F_{\mathcal{N}}(z^+)$ is small, where $F_{\mathcal{N}}$ is the cumulative density function of a normal distribution with mean zero and standard deviation $\sqrt{T}$. For example, one can choose $z^+ = 6\cdot\sqrt{T}$, this gives $1 - F_{\mathcal{N}}(z^+) = 9.9\cdot 10^{-10}$ for $T = 1$. It is suggested by Hagan et al. and Le Floch et al. to choose $\frac{z^+}{\sqrt{T}}$ between four and six.

Remark 3.1. *Le Floch et al. [15] made a consistent writing error in the function E, where H is written as* $H = \frac{1}{2}O^2E^2$, *so* $E = e^{\frac{1}{2}\rho\nu\alpha\Theta(S)T}$. *Thereafter, the square in the definition of H is forgotten. We tested our implementation by setting* $E = e^{\frac{1}{2}\rho\nu\alpha\Theta(S)T}$ *and could reproduce the results by Le Floch et al. In our implementation we set thereafter* $E = e^{\rho\nu\alpha\Theta(S)T}$, *since it did not impact the main results by Le Floch et al.*

3.1.2 Numerical scheme

The discretization is described for time and spatial directions in the approach of Le Floch et al. [15] in this section. It is investigated under which conditions the solution of the numerical scheme satisfies the necessary properties to be arbitrage-free.

Time t and the spatial direction z are discretized uniformly:

$$\begin{aligned} &t_i = i\Delta t, \quad i = 0, \dots, M, \quad T = M\Delta t, \\ &z_j = z^- + jh, \quad h = \frac{1}{J+1}\left(z^+ - z^-\right), \quad j = 0, \dots, J+1. \end{aligned}$$

Hence the discretization of S is given by $s_j = S(z_j)$, where it is chosen such that S_0 is centered between s_{j_0} and s_{j_0+1} for some j_0 in order to have the martingale property at time $t = 0$.[3]

The PDE can be written in a more convenient form

$$\frac{\partial\theta(T,z)}{\partial T} = \frac{\partial}{\partial z}\left\{\frac{\partial}{\partial S}\left\{O(z)E(T,z)\theta(T,z)\right\}\right\}, \tag{3.7}$$

where $S \equiv S(z)$ and $\frac{1}{O(z)}\frac{\partial}{\partial z} \equiv \frac{\partial}{\partial S}$. To describe the discretization in time, the discrete operator $\mathcal{L}(\theta)$ is introduced:

$$\begin{aligned} \mathcal{L}_{\mathrm{j}}^{\mathrm{n}}\left(\theta(z,t_n)\right) :=& \frac{1}{h}\frac{\hat{O}_{j-1}}{\hat{s}_j - \hat{s}_{j-1}}\hat{E}_{j-1}(t_n)\theta_{j-1}^n - \frac{1}{h}\left(\frac{\hat{O}_j}{\hat{s}_{j+1} - \hat{s}_j} + \frac{\hat{O}_j}{\hat{s}_j - \hat{s}_{j-1}}\right)\hat{E}_j(t_n)\theta_j^n \\ &+ \frac{1}{h}\frac{\hat{O}_{j+1}}{\hat{s}_{j+1} - \hat{s}_j}\hat{E}_{j+1}(t_n)\theta_{j+1}^n, \end{aligned}$$

where

$$\hat{s}_j = S\left(z_j - \frac{1}{2}h\right), \ \hat{O}_j = O\left(\hat{s}_j\right), \ \hat{\Theta}_j = \Theta(\hat{s}_j), \ \hat{E}_j(t_n) = E(\hat{s}_j, t_n), \ \theta_j^n \approx \theta(z_j, t_n),$$

The discrete operator $\mathcal{L}$ describeds a discretization for a finite volume technique, see Leveque[27] for information on this topic.

The Lawson-Swayne scheme is chosen to numerically solve the PDE, since it converges the fastest of the proposed schemes by Le Floch et al. and is unconditionally stable [15]. See Figure 3.2 for the convergence rates of the schemes compared, where the error in the probability density function is measured in the infinity norm and two norm.[4]

[3] s is introduced here as a dummy variable for the discretization of the process S_t and should not be confused with the time indication s as used in other chapters.

[4] For a vector $[a_1, \dots, a_M]$, the two-norm is given by $\sqrt{\sum_{i=1}^M |a_i|^2}$ and the infinity norm is given by $\max_{\{i=1,\dots,M\}} |a_i|$.

General parameters			SABR parameters			
T	S_0	J	α	β	ρ	ν
10	0.025	1000	0.2	0.9	-0.5	0.3

Table 3.2: Parameter set to construct Figure 3.1.

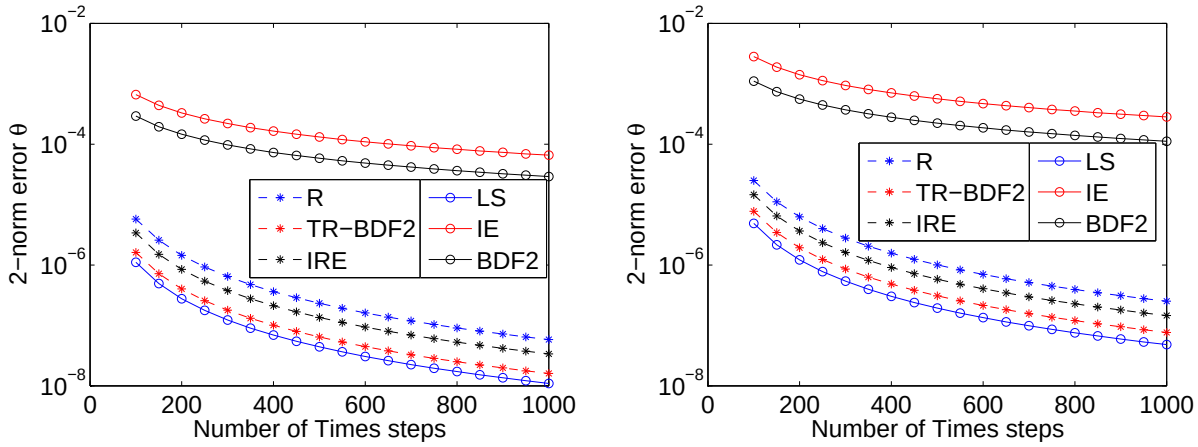

(a) Infinity-norm. (b) Two-norm.

Figure 3.2: Convergence numerical schemes. Parameters are taken from Table 3.2.

Figures 3.2a-3.2b employ the following abbreviations: Lawson Swayne (LS), implicit Euler (IE), backward differentiation formula (BDF2), Rannacher (R), trapezium rule backward differentiation formula (TR-BDF2) and implicit Richardson extrapolation (IRE). For a more detailed description of these schemes, see Le Floch et al. [15].

The Lawson-Swayne scheme is given by:

$$\begin{aligned}
\theta_j^{n+b} &= \theta_j^n + b\Delta t\, \mathcal{L}_{\mathrm{j}}^{\mathrm{n+b}}\left(\theta_j^{n+b}\right), \\
\theta_j^{n+2b} &= \theta_j^{n+b} + b\Delta t\, \mathcal{L}_{\mathrm{j}}^{\mathrm{n+2b}}\left(\theta_j^{n+2b}\right), \\
\theta_j^{n+1} &= (\sqrt{2}+1)\theta_j^{n+2b} - \sqrt{2}\theta_j^{n+b},
\end{aligned}$$

where $b = 1 - \frac{\sqrt{2}}{2}$. The Lawson-Swayne scheme consists of applying the implicit Euler scheme twice with time stepping $b\Delta t$, followed by an interpolation in time.

The discretization for the boundaries is based on a second order approximation in spatial direction and is given by:

$$\frac{\hat{O}_0}{\hat{s}_1-\hat{s}_0}\hat{E}_0(t_n)\theta_0^n = -\frac{\hat{O}_1}{\hat{s}_1-\hat{s}_0}\hat{E}_1(t_n)\theta_1^n, \qquad \frac{\hat{O}_{J+1}}{\hat{s}_{J+1}-\hat{s}_J}\hat{E}_{J+1}(t_n)\theta_{J+1}^n = -\frac{\hat{O}_J}{\hat{s}_{J+1}-\hat{s}_J}\hat{E}_J(t_n)\theta_J^n.$$

For the discretization for $\mathcal{P}_L$ and $\mathcal{P}_R$, the operators $\mathcal{L}_L$ and $\mathcal{L}_R$ are introduced:

$$\begin{aligned}
\mathcal{L}_L^n(\mathcal{P}_L^n, \theta^n) &= \frac{\hat{O}_1}{\hat{s}_1-\hat{s}_0}\hat{E}_1(t_n)\theta_1^n - \frac{\hat{O}_0}{\hat{s}_1-\hat{s}_0}\hat{E}_0(t_n)\theta_0^n, \\
\mathcal{L}_R^n(\mathcal{P}_R^n, \theta^n) &= -\frac{\hat{O}_{J+1}}{\hat{s}_{J+1}-\hat{s}_J}\hat{E}_{J+1}(t_n)\theta_{J+1}^n + \frac{\hat{O}_J}{\hat{s}_{J+1}-\hat{s}_J}\hat{E}_J(t_n)\theta_J^n,
\end{aligned}$$

where $\mathcal{P}_L^n \approx \mathcal{P}^L(t^n)$ and $\mathcal{P}_L^n \approx \mathcal{P}^R(t^n)$. The time stepping procedure is defined by the scheme, as it is for θ. For example, the discretization of $\mathcal{P}^L(T)$ for the implicit Euler scheme is given by:

$$\mathcal{P}_L^{n+1} - \mathcal{P}_L^n = \Delta t \left(\frac{\hat{O}_1}{\hat{s}_1 - \hat{s}_0} \hat{E}_1(t_{n+1}) \theta_1^{n+1} - \frac{\hat{O}_0}{\hat{s}_1 - \hat{s}_0} \hat{E}_0(t_{n+1}) \theta_0^{n+1} \right).$$

It is important to know that under the discretization described as above, the numerical solution of the PDE is arbitrage-free. The solution of the PDE is arbitrage-free if it implies the martingale property and is nonnegative. Therefore, it is proven in the following two lemmas under which conditions the probability density function integrates to one, is nonnegative and is such that the martingale property is satisfied.

Lemma 3.2. *Under the discretization described in this section and under the assumption that*

$$\int_{s_{j-1}}^{s_j} Q(T,u)\,\mathrm{d}u = h\theta_j^n, \ \int_{s_{j-1}}^{s_j} uQ(T,u)\,\mathrm{d}u = h\hat{s}_j\theta_j^n,$$

it holds that:

$$1 = \sum_{i=1}^{J} h\theta_i^n + \mathcal{P}_L^n + \mathcal{P}_R^n, \ S_0 = \sum_{i=1}^{J} h\theta_i^n s_i + \mathcal{P}_L^n S_{\min} + \mathcal{P}_R^n S_{\max}.$$

Proof. The proof is given for the implicit Euler scheme. For other schemes the proof is similar or a direct result from this lemma.
The initial conditions are chosen such that for $n = 0$ it holds that:

$$1 = \sum_{i=1}^{J} h\theta_i^0 + \mathcal{P}_L^0 + \mathcal{P}_R^0, \ S_0 = \sum_{i=1}^{J} h\theta_i^0 s_i + \mathcal{P}_L^0 S_{\min} + \mathcal{P}_R^0 S_{\max}.$$

If $n \geq 1$, for both cases, it holds that:

$$\begin{aligned}
&\Delta t \left(\sum_{i=1}^{J} h\theta_i^n + \mathcal{P}_L^n + \mathcal{P}_R^n - \sum_{i=1}^{J} h\theta_i^{n-1} - \mathcal{P}_L^{n-1} - \mathcal{P}_R^{n-1} \right) \\
&= \sum_{j=1}^{J} h\mathcal{L}_j^n\theta_j^n + \left\{ \frac{\hat{O}_1}{\hat{s}_1 - \hat{s}_0} \hat{E}_1(t_n)\theta_1^n - \frac{\hat{O}_0}{\hat{s}_1 - \hat{s}_0} \hat{E}_0(t_n)\theta_0^n \right\} + \left\{ -\frac{\hat{O}_{J+1}}{\hat{s}_{J+1} - \hat{s}_J} \hat{E}_{J+1}(t_n)\theta_{J+1}^n + \frac{\hat{O}_J}{\hat{s}_{J+1} - \hat{s}_J} \hat{E}_J \right\} \\
&= \sum_{j=1}^{J} \left\{ \frac{\hat{O}_{j-1}}{\hat{s}_j - \hat{s}_{j-1}} \hat{E}_{j-1}(t_n)\theta_{j-1}^n - \left(\frac{\hat{O}_j}{\hat{s}_{j+1} - \hat{s}_j} + \frac{\hat{O}_j}{\hat{s}_j - \hat{s}_{j-1}} \right) \hat{E}_j(t_n)\theta_j^n + \frac{\hat{O}_{j+1}}{\hat{s}_{j+1} - \hat{s}_j} \hat{E}_{j+1}(t_n)\theta_{j+1}^n \right\} \\
&+ 2\frac{\hat{O}_1}{\hat{s}_1 - \hat{s}_0} \hat{E}_1^n\theta_1^n + 2\frac{\hat{O}_K}{\hat{s}_{J+1} - \hat{s}_J} \hat{E}_J^n\theta_J^n \\
&= 0.
\end{aligned}$$

And:

$$
\begin{aligned}
&\Delta t \left(\sum_{i=1}^{J} h\theta_i^n \hat{s}_i + \mathcal{P}_L^n S_{\min} + \mathcal{P}_R^n S_{\max} - \sum_{i=1}^{J} h\theta_i^{n-1} \hat{s}_i - \mathcal{P}_L^{n-1} S_{\min} - \mathcal{P}_R^{n-1} S_{\max} \right) \\
&= \sum_{j=1}^{J} h\hat{s}_i \mathcal{L}_j^n \theta_j^n + 2\frac{\hat{O}_1}{\hat{s}_1 - \hat{s}_0} \hat{E}_1^n \theta_1^n S_{\min} + 2\frac{\hat{O}_K}{\hat{s}_{J+1} - \hat{s}_J} \hat{E}_J^n \theta_J^n S_{\max} \\
&= \sum_{j=1}^{J} \left\{ \frac{\hat{O}_{j-1}}{\hat{s}_j - \hat{s}_{j-1}} \hat{E}_{j-1}(t_n) \theta_{j-1}^n \hat{s}_i - \left(\frac{\hat{O}_j}{\hat{s}_{j+1} - \hat{s}_j} + \frac{\hat{O}_j}{\hat{s}_j - \hat{s}_{j-1}} \right) \hat{E}_j(t_n) \theta_j^n \hat{s}_i \right. \\
&\quad \left. + \frac{\hat{O}_{j+1}}{\hat{s}_{j+1} - \hat{s}_j} \hat{E}_{j+1}(t_n) \theta_{j+1}^n \hat{s}_j \right\} + 2\frac{\hat{O}_1}{\hat{s}_1 - \hat{s}_0} \hat{E}_1^n \theta_1^n F_0 + 2\frac{\hat{C}_J}{\hat{s}_{J+1} - \hat{s}_J} \hat{E}_J^n \theta_J^n \hat{s}_{J+1} \\
&\quad = 0
\end{aligned}
$$

As a consequence:

$$
1 = \sum_{i=1}^{J} h\theta_i^n + \mathcal{P}_L^n + \mathcal{P}_R^n, \;\; S_0 = \sum_{i=1}^{J} h\theta_i^n \hat{s}_i + \mathcal{P}_L^n S_{\min} + \mathcal{P}_R^n S_{\max}.
$$

□

Lemma 3.3. *If $\theta^n \geq 0$ for $j = 1, \ldots, J$ and if*

$$
1 + \frac{\Delta t}{h} \left(\frac{\hat{O}_j}{\hat{s}_{j+1} - \hat{s}_j} + \frac{\hat{O}_j}{\hat{s}_j - \hat{s}_{j-1}} \right) \hat{E}_j(t_n) > \frac{\Delta t}{h} \left(\frac{\hat{O}_{j-1}}{\hat{s}_j - \hat{s}_{j-1}} \hat{E}_{j-1}(t_n) + \frac{\hat{O}_{j-1}}{\hat{s}_j - \hat{s}_{j-1}} \hat{E}_{j-1}(t_n) \right), \tag{3.8}
$$

then the implicit Euler scheme gives $\theta^{n+1} \geq 0$.

Proof. A proof can be found in Appendix B.2. □

In general, the conditions in Equation (3.8) will hold and the implicit Euler scheme will directly provide an arbitrage-free probability density function.[5] If the time stepping is not too large, the Lawson Swayne scheme will provide an arbitrage-free probability density function too. The Lawson Swayne scheme consists of applying the implicit Euler scheme twice, followed by an interpolation in time. The first steps are arbitrage-free if the conditions in Equation (3.8) will hold. The main problem lies in the interpolation step, where $\theta_j^{n+1} = (\sqrt{2}+1)\theta_j^{n+2b} - \sqrt{2}\theta_j^{n+b}$. In this case, one has to constrain the discretization such that for each time step it holds that $(\sqrt{2}+1)\theta_j^{n+2b} \geq \sqrt{2}\theta_j^{n+b}$ for $j = 1, \ldots, J$. Refining the time step ensures that this will hold. Arbitrage can therefore only occur if the discretization is not fine enough. For most practical problems, a time step of one-tenth of a year is used, i.e. $\Delta t = 0.1$. This results in a positively valued probability density function in practice.

3.1.3 Numerical integration for option pricing

The probability density function is only known on the discretization points after the solution of the PDE is approximated. For integration, it is desired to describe it outside these discretization points too. Call and put prices are computed by Le Floch et al. by integrating with the mid-point

[5] A situation in which the condition in Equation (3.8) did not hold was not encountered during the thesis.

rule where it is assumed that the numerical probability density function is piecewise constant on each discretized interval. The call price with strike K and maturity T is:

$$\frac{C(0,T,K)}{\mathcal{D}(0)} = \begin{cases} S_0 - K, & \text{for } z^* \leq z^-, \\ \frac{h}{4(s_k - \hat{s}_k)}(s_k - K)^2\theta_k^M & \\ + \sum_{j=k+1}^{J-1}(\hat{s}_j - K)h\theta_j^M + (S_{\max} - K)\mathcal{P}_R, & \text{for } z^- < z^* < z^+, \\ 0, & \text{for } z^* \geq z^+, \end{cases} \tag{3.9}$$

where $z_{k-1} < z^* \leq z_k$ with $z^* = z(K)$ and $\mathcal{D}(t)$ denotes a function known at time t. In the case of a swaption, the function $\mathcal{D}$ equals the annuity times the notional. The downside of this approach for integration is that butterfly option prices with a small call spread are not stable. For example, consider Figure 3.3a. The call spread between the butterfly options is 1 bp. The butterfly option prices are normalized such that they approximate the probability density function.

General parameters					SABR parameters			
T	S_0	M	J for flat PDF	J for linear PDF	α	β	ρ	ν
10	0.025	100	3000	200	0.05	0.2	0.3	0.17

Table 3.3: Parameter set to construct Figure 3.3.

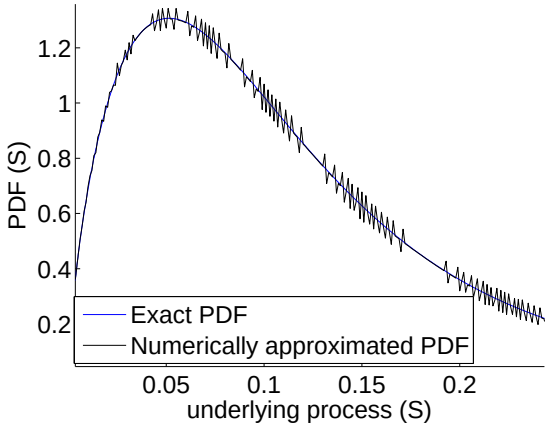

(a) Probability density function is flat continued.

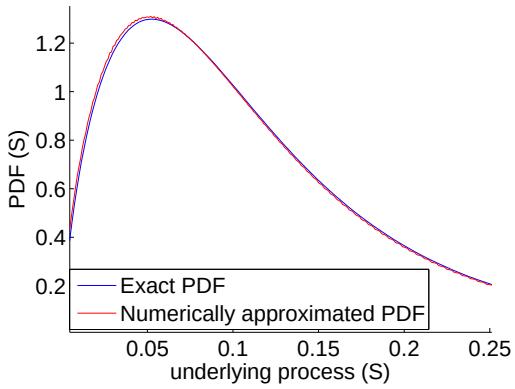

(b) Probability density function is linear continued.

Figure 3.3: Stability of the probability density function implied by butterfly options. Parameters are taken from Table 3.3.

Therefore, a different approach is chosen, which gives more stable butterfly option prices. It is chosen to use a linear continuation of $Q(T,S) = a + bS$ on each interval $[s_{j-1}, s_j]$.[6] The coefficients a and b are fixed such that in each interval it holds

$$\int_{s_{j-1}}^{s_j} Q(T,u)\,\mathrm{d}u = h\theta_j^n, \quad \int_{s_{j-1}}^{s_j} uQ(T,u)\,\mathrm{d}u = h\hat{s}_j\theta_j^n.$$

[6]This is a known technique to describe the slope for finite volume techniques, See Leveque [27] for more information.

These constraints make sure that the numerical probability density function integrates to one and is such that the martingale property is satisfied, as already discussed in Lemma 3.2.

Equation (3.10) gives the linear representation of $Q(T,S)$ on the interval $[s_{j-1}, s_j]$:

$$Q(T,S) \approx \frac{h\theta_j}{s_j - s_{j-1}} \left(1 + 3 \cdot (2S - s_j - s_{j-1}) \cdot \frac{2\hat{s}_j - s_j - s_{j-1}}{(s_j - s_{j-1})^2}\right). \tag{3.10}$$

As a consequence:

$$\int_K^{s_k} (u-K)Q(T,u)\,\mathrm{d}u \approx \frac{h\theta_k (s_k - K)^2}{2(s_k - s_{k-1})} \left(1 + (s_k + 2K - 3s_{k-1}) \cdot \frac{2\hat{s}_k - s_k - s_{k-1}}{(s_k - s_{k-1})^2}\right),$$
$$\int_{s_{k-1}}^K (K-u)Q(T,u)\,\mathrm{d}u \approx \frac{h\theta_k (K - s_{k-1})^2}{2(s_k - s_{k-1})} \left(1 - (3s_k - 2K - s_{k-1}) \cdot \frac{2\hat{s}_k - s_k - s_{k-1}}{(s_k - s_{k-1})^2}\right),$$

Assuming $s_{k-1} < K < s_k$, it can be easily computed that:

$$\begin{aligned}
\frac{C(0,T,K)}{\mathcal{D}(0)} \approx & \frac{h\theta_k^M (s_k - K)^2}{2(s_k - s_{k-1})} \left(1 + (s_k + 2K - 3s_{k-1}) \cdot \frac{2\hat{s}_k - s_k - s_{k-1}}{(s_k - s_{k-1})^2}\right) \\
& + \sum_{j=k}^{N} h\theta_j^M (s_j - K) + (S_{\max} - K)\mathcal{P}_R^M, \\
\frac{P(0,T,K)}{\mathcal{D}(0)} \approx & \frac{h\theta_k^M (K - s_{k-1})^2}{2(s_k - s_{k-1})} \left(1 - (3s_k - 2K - s_{k-1}) \cdot \frac{2\hat{s}_k - s_k - s_{k-1}}{(s_k - s_{k-1})^2}\right) \\
& + \sum_{j=1}^{k-1} h\theta_j^M (s_j - K) + (K - S_{\min})\mathcal{P}_L^M.
\end{aligned}$$

See Figure 3.3b for the more stable butterfly options.

This approach does not directly imply a nonnegative probability density function. This is easily verified, since the extrema of a linear function on a finite interval are on the boundaries of the interval. To have a nonnegative probability density function, it must hold that $\min\{a + bs_{j-1}, a + bs_j\} \geq 0$ for each interval $[s_{j-1}, s_j]$, where a and b can be deduced from the linear representation of $Q(T,S)$. Refining the grid or switching to the proposed integration technique by Le Floch et al. provides this. Switching between the proposed integration techniques is possible since the integration techniques coincide on the discretization points s_j. For an interval $[s_{j-1}, s_j]$ it holds for both integration techniques that $\int_{s_{j-1}}^{s_j} Q(T,u)\,\mathrm{d}u = h\theta_j$ and $\int_{s_{j-1}}^{s_j} uQ(T,u)\,\mathrm{d}u = h\hat{s}_j\theta_j$. This ensures that if the linear continuation of $Q(T < S)$ becomes negative on a interval $[s_{j-1}, s_j]$, the flat continuation of $Q(T,S)$ can be used on this interval without the need to completely switch to a flat continuation of Q.

3.1.4 Results

The convergence of call prices is discussed by the direct approach of Hagan et al. and the approach by Le Floch et al. Furthermore, the volatility curve behavior is investigated. The set of parameters are presented in Table 3.4. These parameters are close to the SABR parameters calibrated in Section 2.5.4, which generated arbitrage in Hagan's formulas. $S_{\max}$ was chosen equal to $S_{\max} = S_0\left(10 + 5\alpha\sqrt{T}\right) \approx 28\%$ for the approach of Hagan et al. [30]. This is a

heuristic rule for $S_{\max}$ which worked in most practical cases, without setting $S_{\max} = S(z^+)$ with $4\sqrt{T} < z^+ < 6\sqrt{T}$ or higher, this would require $0.33 < S_{\max} < 1$. In this case it holds that $S_{\max} < S(z^+)$ and thus fewer discretization points are needed.

General parameters			SABR parameters			
T	S_0	$\mathcal{D}(0)$	α	β	ρ	ν
10	0.025	1	0.05	0.6	-0.35	0.13

Table 3.4: Parameter set for the convergence investigation.

Table 3.5 presents the convergence of a call price with strike $K = S_0$ for the approach of Hagan et al. using the BDF-2 scheme [15]. The results in Table (3.5) are compared to the results for $M = 1200$ and $J = 1600$, where M is the number of time steps and J is the number of spatial grid points. The reference value is therefore 0.0111254. The convergence was tested for larger sets of α, β, ν, ρ, T and the strike K and the conclusion was that the convergence was similar as in Table 3.5.

$J \backslash M$	150	300	600
100	0.455	0.454	0.454
200	0.150	0.149	0.149
400	0.0554	0.0548	0.0547
800	0.0208	0.0202	0.0200

Table 3.5: Error call price (bp) for a direct approach of Hagan et al. with the parameter set in Table 3.4.

The convergence of a call price is investigated for the set in Table 3.4 with the approach by Le Floch et al. and the Lawson and Swayne scheme with the linear continuation of $Q(T, S)$. Table 3.6a presents the results of the convergence of a call price for different set of strikes: $K = S_0$, $K = 0.005$ and $K = 0.1$. The results in Table 3.6a are compared to the results for $M = 1200$ and $J = 1600$. The reference value for $K = S_0$ is 0.0111268, which is approximately the same as the result of solving the untransformed PDE by Hagan et al. The result of the approach by Le Floch et al. is more accurate. The convergence is similar for different sets of α, β, ν, ρ, T.

As one can observe from Tables 3.5 and 3.6, solving the transformed PDE by Le Floch et al. provides faster convergence for option pricing. A small time step does not have much influence on the convergence of option prices. In general if α an ν are chosen to be large (in this example $\alpha = 0.3$, $\nu = 0.4$), the time discretization plays a more dominant role, but in most practical problems the discretization in z has the dominant role in convergence. However, one cannot take a too large time stepping with the Lawson Swayne scheme since this can lead to a negatively valued numerical probability density function as explained in Section 3.1.2.

Finally, the implied volatility curve implied by Hagan's AF SABR model is investigated. It is investigated whether the impact of the SABR parameters α, β, ρ, ν under Hagan's AF SABR model have a similar impact on the volatility curve as the SABR model. The results for a variation in α, β, ρ, ν are presented in Figures 3.4a–3.4d, respectively. As can be observed, the parameters in Hagan's AF SABR model have the same implied volatility curve characteristics as the SABR model. This makes Hagan's AF SABR model in alignment with the SABR model.

$J \backslash M$	150	300	600
100	$0.689 \cdot 10^{-2}$	$0.693 \cdot 10^{-2}$	$0.695 \cdot 10^{-2}$
200	$0.147 \cdot 10^{-2}$	$0.152 \cdot 10^{-2}$	$0.154 \cdot 10^{-2}$
400	$0.272 \cdot 10^{-3}$	$0.324 \cdot 10^{-3}$	$0.337 \cdot 10^{-3}$
800	$0.141 \cdot 10^{-5}$	$0.507 \cdot 10^{-4}$	$0.637 \cdot 10^{-4}$

(a) $K = S_0$

$J \backslash M$	150	300	600
100	$0.352 \cdot 10^{-2}$	$0.353 \cdot 10^{-2}$	$0.353 \cdot 10^{-2}$
200	$0.780 \cdot 10^{-3}$	$0.0789 \cdot 10^{-3}$	$0.791 \cdot 10^{-3}$
400	$0.111 \cdot 10^{-3}$	$0.119 \cdot 10^{-3}$	$0.121 \cdot 10^{-3}$
800	$0.151 \cdot 10^{-4}$	$0.238 \cdot 10^{-4}$	$0.260 \cdot 10^{-4}$

(b) $K = 0.005$

$J \backslash M$	150	300	600
100	$0.183 \cdot 10^{-1}$	$0.183 \cdot 10^{-1}$	$0.183 \cdot 10^{-1}$
200	$0.0438 \cdot 10^{-2}$	$0.0444 \cdot 10^{-2}$	$0.445 \cdot 10^{-2}$
400	$0.924 \cdot 10^{-3}$	$0.980 \cdot 10^{-3}$	$0.995 \cdot 10^{-3}$
800	$0.130 \cdot 10^{-3}$	$0.186 \cdot 10^{-3}$	$0.200 \cdot 10^{-3}$

(c) $K = 0.1$

Table 3.6: Error call price (bp) for different strikes K with the parameter set in Table 3.7.

3.1.5 Discussion of the approach

Hagan's AF SABR is arbitrage-free since it implies a well-defined process and therefore creates Hagan's AF SABR model. In this section the approach by Le Floch et al. was followed for a fast implementation.[7] An alternative integration technique was proposed to produce more stable option prices. Convergence properties were investigated showing that a coarse discretization led to fast convergence in option prices under Hagan's AF SABR. Furthermore, the impact of the SABR parameters α, β, ρ, ν on the implied volatility curve was investigated and it was concluded that the impact of the parameters was similar to the impact of the parameters by the SABR model. A downside of this approach is that the approach becomes more expensive for longer maturities. Therefore, an approach that does not become more expensive for longer maturities is investigated.

3.2 An exact solution of the SABR model

It will be shown how analytical expressions of options under the SABR model can be derived for the uncorrelated case, following the approach by Antonov et al. [3]. A global overview of this derivation of a call price under the SABR model for the uncorrelated case will be given and it will be discussed how this relates to the correlated case. The final result is a two-dimensional integral for a call price. Since this is the exact solution of a call price under the SABR model, this approach is arbitrage-free. Antonov et al. approximated this two-dimensional integral by a one-dimensional integral to speed up the approach. This approach a drawback, which will be discussed. Approximating this one-dimensional integral numerically for the uncorrelated case will be referred to as uncorrelated Antonov.

[7] In the convergence section, the CPU time for $\Delta t = 0.1$ and $J = 200$ with the approach by Le Floch et al. was approximetely 0.1 s. in an Matlab implementation.

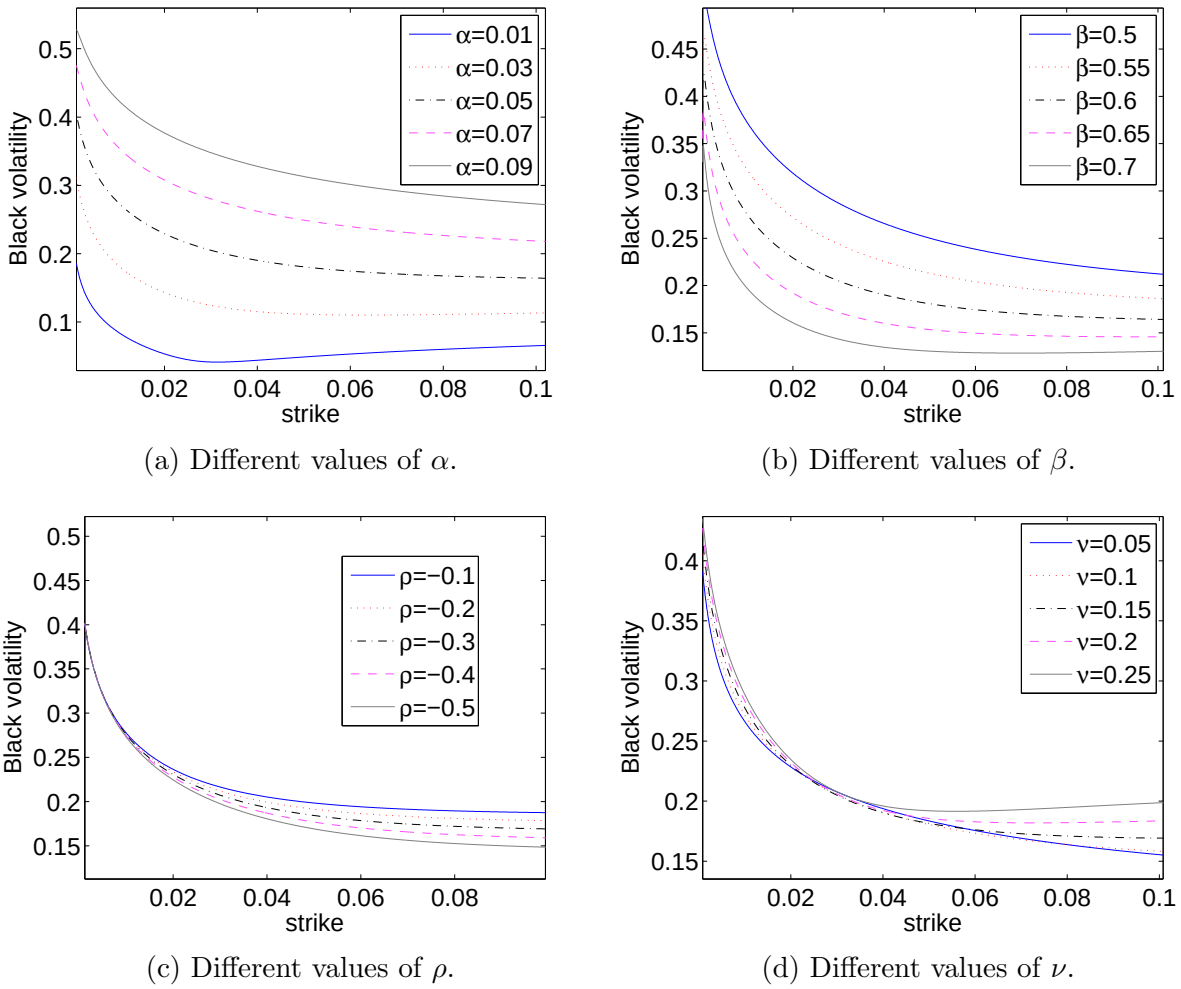

(a) Different values of α.

(b) Different values of β.

(c) Different values of ρ.

(d) Different values of ν.

Figure 3.4: Implied Black volatility curve. The fixed parameters are taken from Table 3.4.

3.2.1 Price derivation under the SABR model

The dynamics of the SABR model for the uncorrelated case are given by:

$$\begin{cases} \mathrm{d}S_t = \alpha_t S_t^{\beta}\,\mathrm{d}W_t^1 & S(0) = S_0 > 0, \\ \mathrm{d}\alpha_t = \nu\alpha_t\,\mathrm{d}W_t^2 & \alpha(0) = \alpha_0 > 0, \\ \mathrm{d}W_t^1\,\mathrm{d}W_t^2 = 0. \end{cases}$$

To price a call option, Lemma 3.4 is introduced. It illustrates in which manner one can switch from the SABR process to a CEV process by changing to an alternative time.[8]

Lemma 3.4. *Suppose that a continuous function $g : [0,\infty) \to \mathbb{R}$ satisfies $g(s) > 0$ for all $s > 0$ and*

$$\int_0^t g^2(s)\,\mathrm{d}s \to \infty \text{ as } t \to \infty.$$

Let

$$\tau_t = \inf\left\{u : \int_0^u g^2(s)\,\mathrm{d}s \geq t\right\} \text{ and } Y_t = \int_0^{\mathcal{S}_t} g(s)\,\mathrm{d}W_s,$$

then the process $\{Y_t : 0 \leq t\}$ is a standard Brownian motion.

[8]The CEV process was investigated in more detail in Section 2.4.1.

Proof. A proof can be found in Steele [38]. □

Similarly as in the lemma, let τ be defined by $\tau := \tau_t = \int_0^t \alpha_s^2 \, \mathrm{d}s$. Define $W_\tau^3 := W_{\tau_t}^1$, then it holds that $W_\tau^3 \sim \text{Norm}\left(0, \int_0^t \alpha_s^2 \, \mathrm{d}s\right)$, where Norm indicates a normal distribution. This relation holds since W_t^1 and W_t^2 are independent and knowing τ_s for $0 \leq s \leq t$ is equivalent to knowing α_s for $0 \leq s \leq t$. Define $X_\tau := S_{\tau_t}$; it follows that X_τ is a CEV process given τ and therefore

$$\mathrm{d}X_u = X_u^\beta \, \mathrm{d}W_u^3.$$

A more detailed proof can be found in Islah [20]. This does not hold if $\rho \neq 0$, since then W_τ^3 would not be a standard Brownian motion under time τ due to the correlation effect between the Brownian motion W_t^1 and W_t^2. In the case of $\rho \neq 0$, one has also to know α_t. If one knows α_s and τ_s for $0 \leq s \leq t$, it holds that α_s is a given function such that W_τ^3 is a standard Brownian motion. This can be best understood by writing the solution for α_t for the general case, in the following manner:

$$\begin{aligned}\alpha_t =& \alpha_0 \exp\left(-\frac{\nu^2 t}{2} + \nu W_t^2\right) \\ =& \alpha_0 \exp\left(-\frac{\nu^2(1-\rho^2)t}{2} + \nu\sqrt{1-\rho^2}\tilde{W}_t^2\right) \exp\left(-\frac{\nu^2\rho^2 t}{2} + \nu\rho W_t^1\right),\end{aligned}$$

where W_t^1 and $\tilde{W}_t^2$ are two independent Brownian motions, i.e. W_t^2 is written as $W_t^2 = \rho W_t^1 + \sqrt{1-\rho^2}\tilde{W}_t^2$. Hence, in the correlated case one also needs to know

$$\exp\left(-\frac{\nu^2\rho^2 t}{2} + \nu\rho W_t^1\right).$$

The probability density function of τ is derived by Antonov et al. for the uncorrelated case. Using the conditional expectation, the call price can be derived under the SABR model with absorption at zero and $\rho = 0$ [3]:

$$\frac{C(0,t,K)}{\mathcal{D}(0)} = (S_0 - K)^+ + \frac{2}{\pi}\left\{\int_{s^-}^{s^+} \frac{\sin(\eta\phi(s))}{\sinh(s)}\mathcal{H}(t\nu^2, s)\,\mathrm{d}s + \sin(\eta\pi)\int_{s^+}^{\infty} \frac{e^{-\eta\Psi(s)}}{\sinh(s)}\mathcal{H}(t\nu^2, s)\,\mathrm{d}s\right\},$$

where

$$\begin{aligned}&\mathcal{H}(t,s) = 2\sqrt{2}\frac{e^{-\frac{t}{8}}}{t\sqrt{2\pi t}}\int_s^\infty u e^{-\frac{u^2}{2t}}\sqrt{\cosh(u) - \cosh(s)}\,\mathrm{d}s, \\ &\phi(s) = 2\tan^{-1}\left(\sqrt{\frac{\sinh^2(s) - \sinh^2(s^{-1})}{\sinh^2(s^+) - \sinh^2(s)}}\right),\ \Psi(s) = 2\tanh^{-1}\left(\sqrt{\frac{\sinh^2(s) - \sinh^2(s^+)}{\sinh^2(s) - \sinh^2(s^-)}}\right), \\ &s^- = \sinh^{-1}\left(\frac{\nu|q-q_0|}{\alpha_0}\right),\ s^+ = \sinh^{-1}\left(\frac{\nu(q+q_0)}{\alpha_0}\right), \\ &\eta = \left|\frac{1}{2(\beta-1)}\right|,\ q = \frac{K^{1-\beta}}{1-\beta},\ q_0 = \frac{S_0^{1-\beta}}{1-\beta},\end{aligned}$$

and $\mathcal{D}(t)$ denotes a function known at time t. In the case of a swaption, the function equals the annuity times the notional.

For practical purposes, the integral

$$\int_{s^+}^{\infty} \frac{e^{-\eta\Psi(s)}}{\sinh(s)}\mathcal{H}(t\nu^2, s)\,\mathrm{d}s,$$

has to be limited to a definite integral such that it can be approximated, i.e.

$$\int_{s^+}^{\infty} \frac{e^{-\eta\Psi(s)}}{\sinh(s)}\mathcal{H}(t\nu^2, s)\,\mathrm{d}s \approx \int_{s^+}^{s^{\text{bound}}} \frac{e^{-\eta\Psi(s)}}{\sinh(s)}\mathcal{H}(t\nu^2, s)\,\mathrm{d}s,$$

for some large s^{bound}. Noting that $\frac{1}{\sinh(s)} \sim \frac{e^{-s}}{2}$, indicates that this part of the integral converges. Approximating $\Psi(s) \approx s$ for large s, one can approximate $\frac{e^{-\eta\Psi(s)}}{\sinh(s)} \approx \frac{e^{-s(\eta+1)}}{2}$.[9] Lastly, $\mathcal{H}(t, s)$ can be bounded and then approximated by the expected value of $\mathbb{E}\left[Z1_{\{Z\geq s\}}\right]$ with $Z \sim \text{Norm}(\mu, \sigma^2)$. This follows from the relations $\sqrt{\cosh(u) - \cosh(s)} \leq \sqrt{\cosh(u)} \approx \frac{e^{\frac{u}{2}}}{\sqrt{2}}$ for large u. This expectation converges rapidly to zero. Combining these facts, can give a crude approximation for s^{bound} to have a accurate approximation of

$$\int_{s^+}^{\infty} \frac{e^{-\eta\Psi(s)}}{\sinh(s)}\mathcal{H}(t\nu^2, s)\,\mathrm{d}s \approx \int_{s^+}^{s^{\text{bound}}} \frac{e^{-\eta\Psi(s)}}{\sinh(s)}\mathcal{H}(t\nu^2, s)\,\mathrm{d}s.$$

An approximation for the two-dimensional integral

Antonov et al. derived an approximation for the function $\mathcal{H}(t, s)$ in an analytical expression. As a consequence only a one-dimensional integral has to be approximated. Their approximation is given by

$$\mathcal{H}(t, s) \approx \sqrt{\frac{\sinh(s)}{s}} e^{-\frac{s^2}{2t}} \left(R(t, s) + \delta R(t, s)\right),$$

where

$$R(t, s) = 1 + \frac{3t\kappa(s)}{8s^2} - \frac{5t^2(-8s^2 + 2\kappa^2(s) + 24\kappa(s))}{128s^4} + \frac{35t^3(-40s^2 + 3\kappa^3(s) + 24\kappa^2(s) + 120\kappa(s))}{1024s^6},$$

$$\kappa(s) = s\coth(s) - 1,\ \delta R(t, s) = e^{\frac{t}{8}} - \frac{3072 + 384t + 24t^2 + t^3}{3072}.$$

A detailed derivation for this approximation is given by Van der Have [42]. This approximation of $\mathcal{H}(t, s)$ is based on an expansion of s^{-1} and gives $\sqrt{\frac{\sinh(s)}{s}} e^{-\frac{s^2}{2t}} R(t, s)$. This approximation is therefore not accurate when $s \approx 0$. For $K = S_0$, it can be easily verified that $s^- = 0$. To have a satisfactory result, Antonov et al. proposed to add the term $\delta R(t, s)$ to the approximation of $R(t, s)$ such that $\mathcal{H}(t, 0) = 1$. Furthermore, they proposed a fourth-order Taylor expansion for small s for $R(t, s)$ and $\sqrt{\frac{\sinh(s)}{s}}$, to ensure that these functions are accurate approximated for small s. The fraction $\frac{\sinh(s)}{s}$ cannot be evaluated accurately by a numerical program, since both the numerator as denominator go to zero as s goes to zero. Similar problems hold for $R(t, s)$. Using the Taylor expansion ensures that a numerical program uses a accurate approximation for small s of these terms.

In order to approximate the one-dimensional integral, a numerical integration technique has to be chosen. The composite Simpson's rule is chosen for this thesis to provide accurate results. The composite Simpson's rule applies the Simpson's rule on multiple intervals $[x_i, x_{i+1}]$ for some

[9] This is a crude approximation, since $\Psi(s) > \mathcal{O}(s)$ for large s.

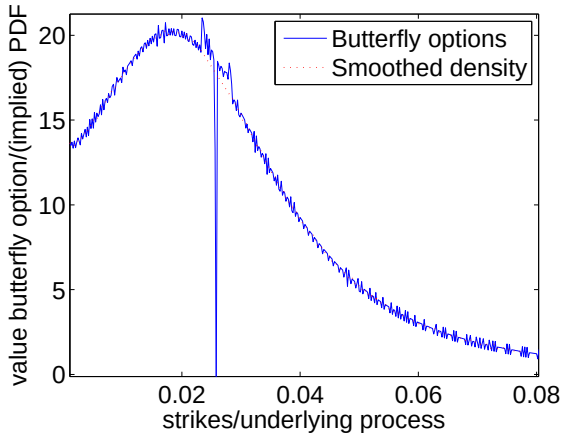

(a) The implied probability density function.

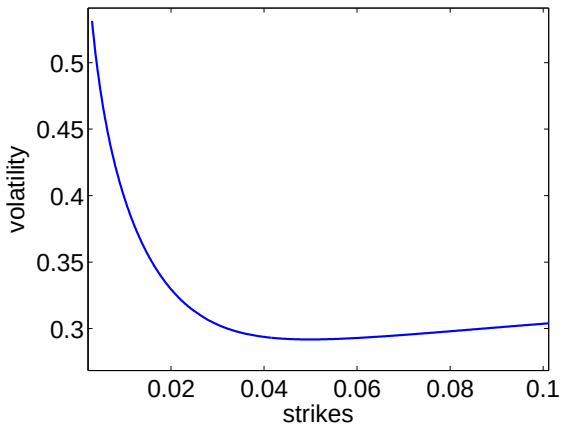

(b) The implied Black volatility curve.

Figure 3.5: An application of uncorrelated SABR implied by the approach of Antonov et al. Parameters are taken from Table 3.7.

discretization $c = x_1 < \ldots < x_N = d$ of the interval $[c, d]$. For an interval $[a, b]$, Simpson's rule is given by:

$$\int_a^b g(x)\,\mathrm{d}x \approx \frac{b-a}{6}\left[g(a) + 4g\left(\frac{a+b}{2}\right) + g(b)\right].$$

The error is given by

$$\frac{1}{90}\left(\frac{b-a}{2}\right)^5 \left|g^{(4)}(\zeta)\right|, \text{ for some } \zeta \in [a, b].$$

An example of the result of the approach by Antonov et al. is presented in Figure 3.5. Figure 3.5a presents the probability density function implied by a second order numerical approximation using call prices, i.e. $f(K) = \frac{1}{\mathcal{D}(0)}\frac{\partial^2 C}{\partial K^2}(K) \approx \frac{1}{\mathcal{D}(0)}\frac{C(K+\epsilon)-2C(K)-C(K-\epsilon)}{\epsilon^2}$ as discussed in Section 2.5.4. The choice was made to set $\epsilon = 2$bp, i.e. normalized butterfly options with a call spread of 2bp.

General parameters		SABR parameters		
T	S_0	α	β	ν
10	0.02576	0.06	0.55	0.33

Table 3.7: Parameter set for Figure 3.5. This set follows from a calibration result.

The saw tooth behavior for strikes away from $K = S_0$ can be reduced by refining the step size used for the numerical integration. The probability density function is also computed by a numerical approximation with call prices where the difference in strike is 5bp. The call prices are computed for strikes away from S_0. Call prices with strikes near S_0 are obtained by a spline interpolation. This numerical approximation of the probability density function in Figure 3.5a is referred to as the smoothed density.

Due to the approximation of $R(t, s)$ and $\sqrt{\frac{\sinh(s)}{s}}$ by a Taylor expansion for small s, the instability of the approximation of $\mathcal{H}(T, S)$ is not directly observed in the call prices. Figure

3.5b presents the Black volatility implied by the call prices used to produce the butterfly option prices in Figure 3.5a. The volatility curve seems to not suffer for strikes around $K = S_0$.

3.2.2 An approach by Antonov et al. for the correlated case

In order to price options for the correlated case, a mapping is derived by Antonov et al, based on a small time expansion. The mapping is used to get from the general case of the SABR model to a mimicking model, i.e. the uncorrelated SABR model:

$$\begin{cases} \mathrm{d}\tilde{S}_t = \tilde{\alpha}_t S_t^{\tilde{\beta}} \,\mathrm{d}\tilde{W}_t^1, & \tilde{S}(0) = S_0 > 0, \\ \mathrm{d}\tilde{\alpha}_t = \tilde{\nu}\tilde{\alpha}_t \,\mathrm{d}\tilde{W}_t^2, & \tilde{\alpha}(0) = \tilde{\alpha}_0 > 0, \\ \mathrm{d}\tilde{W}_t^1 \,\mathrm{d}\tilde{W}_t^2 = 0. \end{cases}$$

For the call price with strike K, the following parameters are used for the mimicking model to price a call option:

$$\tilde{\beta} := \tilde{\beta}(\beta),\ \tilde{\alpha} := \tilde{\alpha}(\alpha_0, \beta, \rho, \nu, S_0, K),\ \tilde{\nu} := \tilde{\nu}(\alpha_0, \beta, \rho, \nu, S_0).$$

The function $\tilde{\alpha}, \tilde{\beta}, \tilde{\rho}$ are given by Antonov et al. [7]. This mapping is based on a small time expansion like Hagan et al. [29] and is not guaranteed to be arbitrage-free [3]. The difference in these approaches is that Antonov et al. map the SABR model to an uncorrelated SABR model. Hagan et al. map the SABR model to Black's and Bachelier's model.

In this thesis only arbitrage-free approaches are investigated to compare to Hagan's formulas. Therefore, the approach by Antonov et al. will be limited to the uncorrelated case and called uncorrelated Antonov. It will be investigated whether it can capture market volatility curves accurately with this limitation. For the SABR model it holds that β and ρ have a similar impact on the volatility curve. Therefore, the hypothesis is that setting ρ equal to zero, the approach of Antonov et al. can capture the market quotes accurately.

3.2.3 Discussion of the approach

Antonov et al. derived a two-dimensional integral for a call price under the SABR model for the uncorrelated case. Approximating this two-dimensional integral is an arbitrage-free approach. A one-dimensional integral is derived as an approximation for the two-dimensional integral. This approximation works very accurately for call prices, but not for butterly option prices with a strike near S_0. For real pricing the two-dimensional integral should be used to approximate the call prices. The one-dimensional integral can be used to fit the market volatility curve.

The main advantage of the approach of Antonov et al. is the approximation in the form of a one-dimensional integral, as it is fast enough for market applications.[10] However, it is still not as fast as Hagan's formulas and does not directly parametrize the volatility curve. Another advantage of the approach is that it does not become more expensive for longer maturities. A disadvantage of the approach by Antonov et al. is that it must be limited to the the uncorrelated case to ensure it is arbitrage-free.

[10]The CPU time for one call price was approximately 20ms. in a Matlab implementation.

3.3 Summary

This chapter gave an overview of two approaches in literature that looked very promising compared to other approaches recently proposed. Hagan's AF SABR is a reduction of dimensionality of the SABR model. Pricing options can therefore be done fast and in a arbitrage-free fashion. It is however an approach that becomes computationally expensive for longer maturities. The approach of Antonov et al. is an exact solution of a call price under the SABR model for the uncorrelated case and it is therefore arbitrage-free for this case. An approximation is made for the two-dimensional integral in the form of a one-dimensional integral. This one-dimensional integral numerically can be approximated numerically rapid. This approach does not become more expensive for longer maturities. Preferably, it would be optimal to have an approach that is (almost) computationally rapid as Hagan's formulas and does not become more expensive for longer maturities, is not limited to a special case (like $\rho = 0$), is consistent with the SABR model and is arbitrage-free. Ideally, it should give a parameterization of the volatility curve. Therefore, in the next chapter an approach is investigated that removes the arbitrage in Hagan's formulas in a sophisticated fashion.

Chapter 4

The Stochastic Collocation Method

This chapter explains the approach by Grzelak et al. [25], the stochastic collocation method (SCM). The SCM is a general approach introduced by Grzelak et al. [26] to efficiently do Monte Carlo simulations for a random variable with an computationally expensive distribution. To achieve this, the expensive random variable is mapped to a simpler random variable. This mapping is approximated by a Lagrange polynomial in the approaches of Grzelak et al. [25, 26]. In the approach by Grzelak et al. [25] this mapping is used to transform the negative part of the probability density function implied by Hagan's formulas into a positively valued probability density function. Following this approach ensures that butterfly arbitrage is removed in Hagan's formulas.

Error estimations will be derived when applying the SCM with a Lagrange polynomial to provide an indication for the convergence of this approach. Different interpolation techniques will be compared to a Lagrange polynomial to see whether if another interpolation technique gives more satisfactory results. In the approach of Grzelak et al. [25], the process implied by Hagan's formulas is mapped to a normal distribution. In this thesis the process implied by Hagan's formulas will be mapped to a gamma distribution too. It will be discussed which distribution should be used in which case. Lastly, this approach will be reformulated to ensure the martingale property holds to make this approach completely arbitrage-free. This chapter ends with a summary and conclusion.

4.1 Introduction of the Stochastic Collocation Method

For the SCM it is assumed that X and Y are two well-defined random variables. X has a computationally simple distribution, like a standard normal random variable, Y has a computationally expensive distribution, like the process S_t of the SABR model. However, it is assumed that the cumulative density function (CDF) of Y is known or can be approximated accurately.

The main goal of this approach is to compute the expectations of Y as rapidly as the expectations of X. To do so, Y will be approximated as a function of X, i.e. $Y \approx g_N(X)$. This approximation of the relation between X and Y will be based on the relation:

$$F_Y(Y) \sim U(0,1) \sim F_X(X), \tag{4.1}$$

where F is the CDF of a random variable and $U(0,1)$ is the uniform distribution. Using the relation in Equation (4.1), one can observe that the exact mapping m, satisfies the relation:

$$y = m(x) = F_Y^{-1}(F_X(x)).$$

This mapping is one-to-one if X and Y are defined on the same Borel set, and therefore monotonic. The goal is to approximate the mapping m without performing many inversions of F_Y and preserve monotonicity. Ideally, there should be a close relation between X and Y, preferably linear. This results in few inversions, but the existence of such a X is not guaranteed for an expensive random variable Y.

In order to approximate m, one uses a set of collocation points. This is a set of points $\{\tilde{x}_i\}_{i=1}^N$ for X and $\{\tilde{y}_i\}_{i=1}^N$ for Y, for which the mapping is exact, i.e. $\tilde{y}_i = m(\tilde{x}_i)$. It follows from the mapping that $\{\tilde{x}_i\}$ and $\{\tilde{y}_i\}$ are sorted, i.e. $\tilde{x}_1 < \ldots < \tilde{x}_N$ and $\tilde{y}_1 < \ldots < \tilde{y}_N$.

A Lagrange polynomial g_N is used to inter- and extrapolate the collocation points in this approach [25, 26]. Other inter- and extrapolation techniques can be used, but it is known that the Lagrange polynomial converges exponentially to the mapping on the interval $[\tilde{x}_1, \tilde{x}_N]$. This will be discussed in more detail in Section 4.6 and Section 4.8 for the SCM.

A Lagrange polynomial that interpolates between the points $\{(x_i, y_i)\}_{i=1}^N$ can be written as

$$g_N(x) = \sum_{i=1}^{N} y_i \lambda_i(x), \;\; \lambda_i(x) = \Pi_{j=1, j\neq i}^{N} \frac{x - x_j}{x_i - x_j}.$$

The Lagrange polynomial can also be expressed by a monic polynomial:

$$g_N(x) = a_0 + a_1 x + \ldots + a_N x^{N-1},$$

where N is the number of collocation points. In this case, the coefficients a_i can be determined by solving the Vandermonde equation $\mathcal{V}(\mathbf{x})\mathbf{a} = \mathbf{y}$, where

$$\mathcal{V}(\mathbf{x}) = \begin{pmatrix} 1 & x_1 & \ldots & x_1^{N-1} \\ \vdots & \vdots & \ldots & \vdots \\ 1 & x_N & \ldots & x_N^{N-1} \end{pmatrix}, \; \mathbf{a} = \begin{pmatrix} a_0 \\ \vdots \\ a_{N-1} \end{pmatrix}, \; \mathbf{y} = \begin{pmatrix} y_1 \\ \vdots \\ y_N \end{pmatrix}.$$

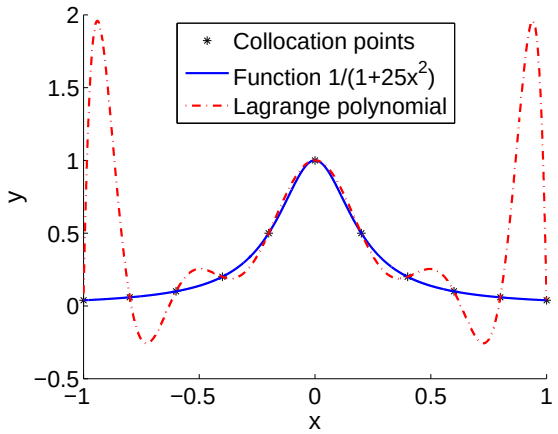

Figure 4.1: Runge oscillation for a Lagrange polynomial.

A drawback of a Lagrange polynomial, is that it can suffer from Runge oscillation as in Figure 4.1. In this figure the function $\frac{1}{1+25x^2}$ is approximated by a 9th order Lagrange polynomial on

the interval $[-1, 1]$. The collocation points are chosen according to a uniform discretization of the interval. It is therefore desired for the Lagrange polynomial to be stable (no Runge oscillation). In order to have a stable Lagrange polynomial, one has to use a set of collocation points that provide a stable interpolation. Grzelak et al. showed that if it is chosen to relate the Lagrange polynomial to the orthogonal polynomials, this will provide a stable interpolation in the SCM.

Definition 4.1 (Orthogonal Polynomials)**.** A sequence of orthogonal polynomials $\{p_n\}_{n=0}^{N}$ with $\deg(p_n) = n$ is said to be orthogonal in L^2 with respect to the probability density function $f_X(X)$ of X, if the following holds:

$$\mathbb{E}\left[p_i(X)p_j(X)\right] = \int_{\mathcal{R}(X)} p_i(X)p_j(X)f_X(x)\,\mathrm{d}x = \delta_{ij}\mathbb{E}\left[p_i^2(X)\right],\ i,j = 0,\ldots,N,$$

where $\mathcal{R}(X)$ is the support of X and δ_{ij} the Kronecker delta function.

The collocation points of X will be computed first. The location of the collocation points of X are chosen such that the Lagrange polynomial is equal to a weighted summation of the orthogonal polynomials under the probability measure of X. These collocation points are related to the Gaussian quadrature points. Grzelak et al. [26] gives an algorithm to compute these collocation points. Theorem 4.2 shows that the orthogonal polynomials are completely determined by the moments of X and one can compute these polynomials from the moments. As a result, the collocation points are chosen such that the moments of Y and the Lagrange polynomial g_N are matched, i.e.

$$\mathbb{E}\left[Y^i\right] = \mathbb{E}\left[g_N^i(X)\right],\ \text{for } i = 0,\ldots,N-1.$$

Theorem 4.2 (Recurrence In Orthogonal Polynomials)**.** *For any given probability density function $f_X(\cdot)$, a unique sequence of monic orthogonal polynomials $p_n(X)$ exists, with $\deg(p_n(X)) = n$, which can be constructed as follows,*

$$p_{i+1}(x) = (x - a_i)p_i(x) - b_i p_{i-1},\ i = 2,\ldots,N-1$$

where $p_0(x) \equiv 0$, $p_1(x) \equiv 1$ and where a_i and b_i are the recurrence coefficients,

$$a_i = \frac{\mathbb{E}\left[Xp_i^2(X)\right]}{\mathbb{E}\left[p_i^2(X)\right]},\ \text{for } i = 1,\ldots,N-1,$$
$$b_i = \frac{\mathbb{E}\left[p_i^2(X)\right]}{\mathbb{E}\left[p_{i-1}^2(X)\right]},\ \text{for } i = 2,\ldots,N-1.$$

Proof. A proof can be found in Favard [16]. □

These collocation points will be referred to as the optimal collocation points. For example, in the special case that X is chosen to be normally distributed, the optimal collocation points $\{\tilde{x}_i\}$ are $\sqrt{2}$ times the Gaussian quadrature points. The collocation points $\{\tilde{y}_i\}$ follow from the relation in Equation (4.1) by evaluationg $\tilde{y}_i = F_Y^{-1}(F_X(\tilde{x}_i))$. Therefore, F_Y must be inverted accurately.

To illustrate in more detail an application of the SCM, a CEV process is considered in the next section and in which manner the SCM can be applied.

4.2 Application of the SCM to a CEV process

It will be shown how the SCM can be applied to a CEV process, where it will be mapped to a normal distribution. The CEV process has an absorption at zero. Therefore, the random variables are not defined on the same Borel set, i.e. a CEV process does not become negative, whereas a normal distribution can become negative.

As introduced in Section 2.4.1, the cumulative density function $F_{\text{CEV}}(t, y)$ of a CEV process is given by:

$$F_{\text{CEV}}(t, y) = 1 - F_{\chi^2(b,c(y))}(a),$$

where

$$a = \frac{S_0^{2(1-\beta)}}{(1-\beta)^2\sigma^2 t},\ b = \frac{1}{1-\beta},\ c(y) = \frac{y^{2(1-\beta)}}{(1-\beta)^2\sigma^2 t}.$$

$F_{\chi^2(b,c)}$ is the cumulative density function of the non-central chi-squared distribution with b degrees of freedom and the non-centrality parameter $c(y)$.

In this example, the set of parameters is provided by Table 4.4.

General parameters		CEV parameters	
T	S_0	σ	β
2	0.07	0.05	0.6

Table 4.1: CEV parameter for the example in Tables 4.2 and 4.3 .

For convenience it is written $F_{\text{CEV}}(T, y) = F_{\text{CEV}}(y)$. The probability of hitting zero is $\mathbb{P}(S_T = 0) = F_{\text{CEV}}(0) = 0.6456$. In this example, X is chosen to be the standard normal variable and five collocation points will be used. The optimal collocation points of X are provided by Table 4.2.

Variable	Optimal collocation points					Absorption point
	$\tilde{x}_1$	$\tilde{x}_2$	$\tilde{x}_3$	$\tilde{x}_4$	$\tilde{x}_5$	x^*
$\tilde{x}_i$	-2.857	-1.3556	0	1.3556	2.857	0.3736
$F_X(\tilde{x}_i)$	0.0021	0.0876	0.5	0.9124	0.9979	0.6456
$y_i = F^{-1}_{\text{CEV}}(F_X(\tilde{x}_i))$	-	-	-	0.2770	0.9901	0

Table 4.2: Mapping specifications for the parameters of Table 4.1.

In this example, the CEV process has a cumulative density function with the properties $F_{\text{CEV}}(T, y) = 0$ for $y < 0$ and $F_{\text{CEV}}(T, y) \geq 0.6456$ for $y > 0$. Therefore, the values of the CEV process cannot be determined for $\tilde{y}_1$, $\tilde{y}_2$ and $\tilde{y}_3$. These points are therefore called *virtual* collocation points. These points cannot be used to construct a mapping between the CEV process and the normal distribution.

For this example, if the Lagrange polynomial would be used to extrapolate the approximation of the mapping for $x < x_4$, the SCM would be not able to model the absorption point. In order to get a satisfactory extrapolation of the mapping, g_N is linearly extrapolated. An x^* is found for which it holds that $F_X(x^*) = F_{\text{CEV}}(0)$ and g_N is linearly extrapolated for $[x^*, x_4)$ such that

$g_N(x^*) = 0$. It can be found that $x^* = 0.3736$. This results in the CDF being exact at x^* and that the point mass of the CEV process can be modeled with g_N. The result of the mapping is given in Figure 4.2a and the CDFs are compared in Figure 4.2b. For this example, the point x^* will be seen as a collocation point too and x^*, x_4, and x_5 are considered here to be the collocation points.

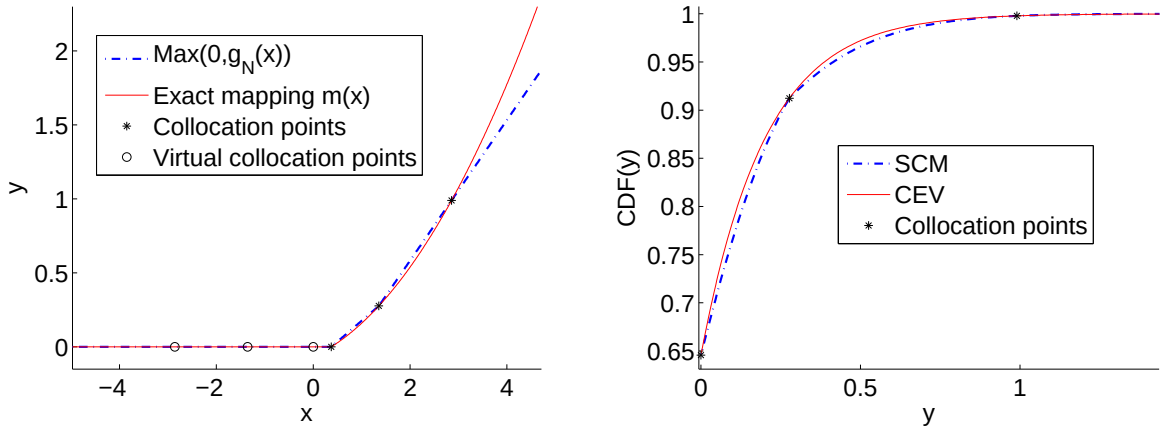

(a) The mapping and approximation of the mapping between the normal distribution (x) and the CEV process (y).

(b) The cumulative density function of the CEV process and implied by the SCM.

Figure 4.2: Application of the SCM to a CEV process.

Figure 4.2a shows that the mapping is not accurate when using these collocation points. This is because the variables are not defined on the same Borel set. To improve the approximation of the mapping function, the concept of grid-stretching will be used. It will be explained what this concept is and how it can be applied to the example of the CEV process.

4.2.1 An improvement through the concept of grid-stretching

As in the previous example, the optimal collocation points $\{\tilde{x}_i\}$ are determined and some of these optimal collocation points are virtual. They cannot be replicated by Y and an approximation of the mapping cannot be determined by these points.

Another problem with the optimal collocation points can be that they imply $F_X(\tilde{x}_i) > 1 - \epsilon$ or $F_X(\tilde{x}_i) < \epsilon$ for some i with $\epsilon \ll 1$. The collocation points of Y are determined by inverting F_Y, i.e. $\tilde{y}_i = F_Y^{-1}(F_X(\tilde{x}_i))$. Inverting F_Y cannot always be done accurately, for example if F_Y is a numerical approximation. This depends on the accuracy that the numerical approximation can achieve.

Therefore, a $\pi_{\min}$ is defined which can be inverted accurately and which Y can replicate, i.e. there exists a y such that $F_Y(y) = \pi_{\min}$. A $\pi_{\max}$ is defined such that $F_Y^{-1}(\pi_{\max})$ can be inverted accurately.[1] After defining $\pi_{\min}$ and $\pi_{\max}$, the optimal collocation points $\{\tilde{x}_i\}$ are linearly mapped to a set of collocation points $\{x_i\}$ such that $F_X(x_1) = \pi_{\min}$ and $F_X(x_N) = \pi_{\max}$, i.e. $x \to a\tilde{x} + b$. This is just a linear replacement of the optimal collocation points.

[1] Note that $\pi_{\min}$ and $\pi_{\max}$ are real numbers between 0 and 1 and should not be confused with the number π.

Variable	Grid-stretched collocation points				
	x_1	x_2	x_3	x_4	x_5
x_i	0.374	1.026	1.615	2.205	2.857
$F_X(x_i)$	0.6456	0.8476	0.9469	0.9863	0.9979
$y_i = F^{-1}_{\text{CEV}}(F_X(x_i))$	0	0.1680	0.3748	0.6360	0.9901

Table 4.3: Mapping specifications with grid-stretching for the parameters of Table 4.1.

In the case that X is chosen to be a normal distribution, grid-stretching can be seen as using the optimal collocation points from a different normal distribution $\tilde{X}$. This is due to the relation $X \sim \mu + \sigma Z$, where $X \sim \text{Norm}(\mu, \sigma^2)$ and $Z \sim \text{Norm}(0, 1)$. Grid-stretching preserves stability of the Lagrange polynomial since it is a linear replacement of the optimal collocation points, but the Lagrange polynomial loses its theoretical optimality for the degree of integration. Using the optimal collocation points and grid-stretching will be considered as the standard approach in the remainder of this thesis.

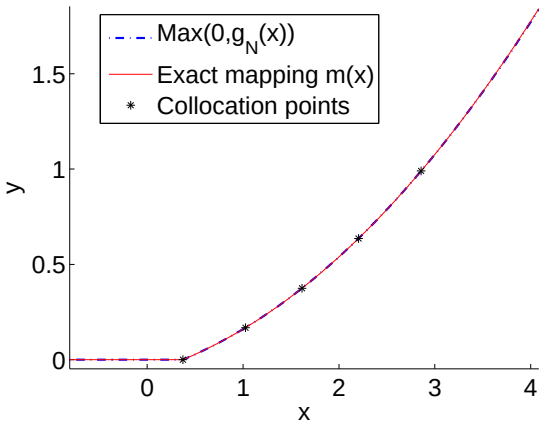

(a) The mapping and approximation of the mapping between the normal distribution (x) and the CEV process (y).

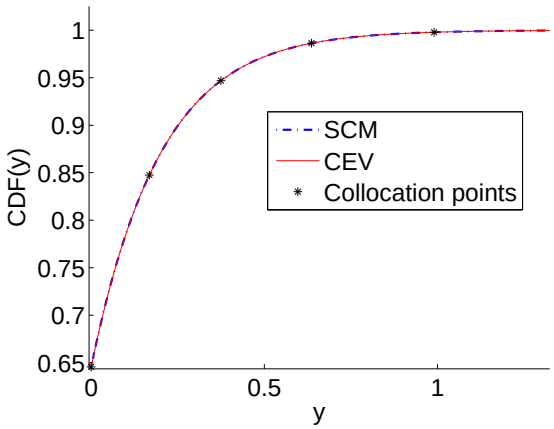

(b) The cumulative density function of the CEV process and implied by the SCM.

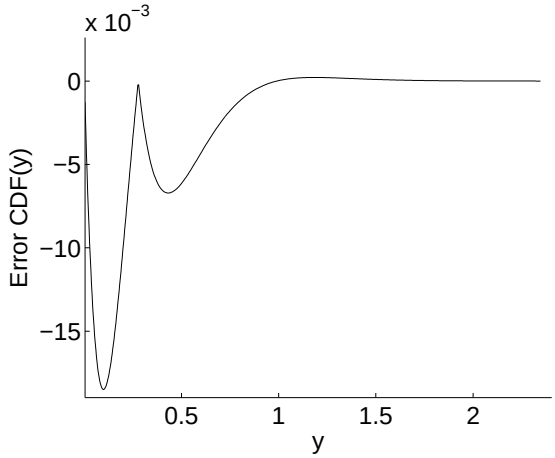

(c) Error made by the SCM without grid-stretching.

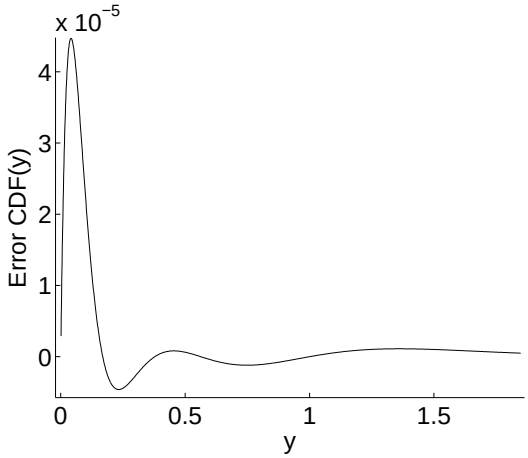

(d) Error made by the SCM with grid-stretching.

Figure 4.3: Application of the SCM to a CEV process.

The example of the CEV process is reconsidered with grid-stretching. It is chosen to set $\pi_{\min} = F(S_T = 0)$ so that the absorption point can be modeled accurately. The resulting collocation points are in Table 4.3, where it is chosen to let $\pi_{\max}$ be defined by the optimal collocation point, i.e. only x_1, x_2, x_3, x_4 are mapped linearly during grid-stretching. The result of the mapping is given in Figure 4.3a and the CDFs are compared in Figure 4.3b. The difference between the exact case and the approximation is not visible in these figures. Therefore, the error in the CDF is presented in Figure 4.3d and compared to the case without grid-stretching in Figure 4.3c. It can be concluded that grid-stretching can improve the accuracy.

This example provided a well-defined random variable. In the next section the concept of applying the SCM to Hagan's formulas will be explained.

4.3 Application of the SCM to Hagan's formulas

It will be explained how the SCM can be applied to Hagan's formulas in a similar fashion as in the example for the CEV process. It assumed that S is the random variable implied by Hagan's formulas. This random variable S will be referred to as Hagan's implied random variable. When the SCM can be applied to the general case, Y will be used as with the CEV process and not S.

Since this random variable S can imply a negatively valued "probability density function", one cannot construct a mapping based on the CDF. This chapter is limited to the cases for which S implies a negatively valued probability density function. The concept of transforming the negative part of the probability density function to a positively valued probability density function will be explained. When the probability density function remains positive, there is no arbitrage and the SCM does not have to be applied to Hagan's formulas.

Define $s^- > 0$ such that the probability density function of S is only positive on the interval (s^-, ∞) and negative on $[0, s^-]$. The cumulative density function is not well-defined on $[0, s^-]$, since on this interval it is decreasing. Therefore, it is chosen to use the survival density function (SDF) G, and not the cumulative density function to construct the mapping. The mapping will be based on the relation:

$$G_S(S) \sim U(0,1) \sim G_X(X), \tag{4.2}$$

where the survival density function G is defined as:

$$G(x) := \int_x^{+\infty} f(x)\,\mathrm{d}x.$$

For a well-defined process, the relation $G(x) = 1 - F(x)$ holds. For the implied SDF of S, it has the natural limit $\lim_{s\to+\infty} G_S(s) = 0$ [25], and in general the probability density function stays positive for high values of the underlying process. Therefore, the SDF can be used for most practical problems.[2] Figure 4.4 presents an example of the (implied) probability density function and survival density function of S in the figure on the left and right respectively. In this example, the set of parameters is provided by Table 4.4.

General parameters		SABR parameters			
T	S_0	α	β	ρ	ν
10	1	0.25	0.6	-0.8	0.3

Table 4.4: SABR parameter for Figure 4.4.

[2]Hagan's formulas can imply a negatively valued probability density function for high values of the underlying process too according to some articles, but this was not encountered during the thesis.

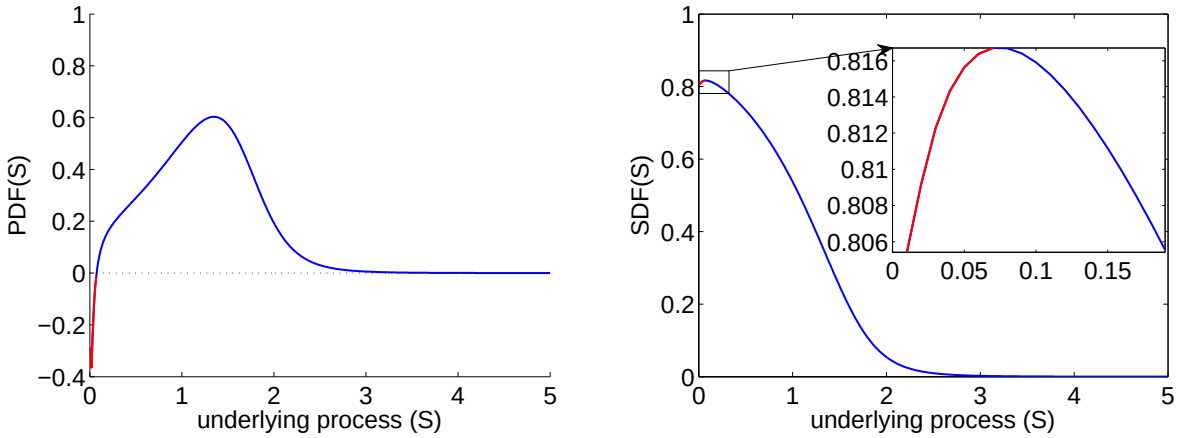

(a) (Implied) PDF. (b) (Implied) SDF.

Figure 4.4: Hagan's Black formula.

From Lemma 2.19, it is known that G_S can be computed using the relation:[3]

$$G_S(s) = -\frac{1}{\mathcal{D}(t)} \frac{\partial C}{\partial K}(K)\bigg|_{K=s}, \tag{4.3}$$

where $C(K) = C(t, T, K)$ is the price of a call option with strike K at time t and with maturity T and $\mathcal{D}(t)$ is a function known at time t. In the case of a swaption, the function $\mathcal{D}(t)$ is equal to the notional times the annuity. This relation will be used on an interval $[s^*, +\infty)$ with $s^* \geq s^-$. A derivation of the SDF and the PDF implied by Hagan's formulas is done in Appendix C.1. For convenience, this chapter limits the results to Hagan's Black formula, the results for Hagan's Bachelier formula can be obtained in an equivalent fashion.

As in the CEV example, first the optimal collocation points $\{\tilde{x}_i\}$ are determined. Then, grid-stretching will be applied based on the SDF. The optimal collocation points of Y can imply $G_X(\tilde{x}_i) < \epsilon$ or $G_X(\tilde{x}_i) > 1-\epsilon$ for some i with $\epsilon \ll 1$. The collocation points of Y are determined by inverting G_S, i.e. $\tilde{s}_i = G_S^{-1}(G_X(\tilde{x}_i))$. This inversion can not always be replicated by S, since like the CEV process S has a point mass at zero. For example, the SABR parameters imply that $G_S(s) \leq 0.817$ in Figure 4.4. It can also not be guaranteed that G_S can be accurately inverted if $G_X(\tilde{x}_i) < \epsilon$ or $G_X(\tilde{x}_i) > 1 - \epsilon$.

Therefore a $\zeta_{\max}$ is defined which S can replicate, i.e. there exists a s such that $G_S(s) = \zeta_{\max}$. A $\zeta_{\min}$ is defined such that $G_S^{-1}(\zeta_{\min})$ can be accurately inverted. These $\zeta_{\min}$ and $\zeta_{\max}$ relate to $\pi_{\max}$ and $\pi_{\min}$ respectively for the example with the CEV process, i.e. $\zeta_{\min} = 1 - \pi_{\max}$ and $\zeta_{\max} = 1 - \pi_{\min}$.

After defining $\zeta_{\min}$ and $\zeta_{\max}$, the optimal collocation points $\{\tilde{x}_i\}$ are linearly mapped to a set of collocation points $\{x_i\}$ such that $G_X(x_1) = \zeta_{\max}$ and $G_X(x_N) = \zeta_{\min}$. This approach is equivalent to the standard approach and therefore will also be referred to as the standard approach.

[3] In Lemma 2.19 it was derived that $\frac{\partial C}{\partial K}(K) = F(K) - 1$ for a *well-defined* process. In the proof, this involved using the relation $G(x) = 1 - F(X)$, i.e. $\frac{\partial C}{\partial K}(K) = -G(K) = F(K) - 1$. For Hagan's formulas the relation $\frac{\partial C}{\partial K}(K) = -G(K)$ should be used, since Hagan's formulas do not guarantee to imply a well-defined random variable.

After applying the standard approach, the collocation points $\{s_i\}$ and the Lagrange polynomial are determined, as in Section 4.1. S can be approximated by $g_N(X)$ and extrapolated outside $[x_1, x_N]$ by g_N. The Lagrange polynomial provides a natural extension to S.

Before examples of the SCM to Hagan's formulas are given, first a detailed investigation of the properties of the SCM are investigated to understand the approach better.

4.4 Properties of the SCM

4.4.1 The probability density function implied by the SCM

In the application of the SCM to Hagan's formulas, Hagan's implied random variable S is replaced by the variable $g_N(X)$ for $s < s^*$. In order to obtain a well-defined SDF, there should be a one-to-one correspondence between X and $g_N(X)$. Thus g_N has to be one-to-one. If g_N is a Lagrange polynomial it should be (strictly) monotonic. In order for $g_N(X)$ to be monotonic, it must hold that

$$\frac{\mathrm{d}g_N}{\mathrm{d}x}(x) \geq 0 \ \forall \ x \in \mathcal{R}(X),$$

where $\mathcal{R}(X)$ is the range of X.

If g_N is strictly monotonic, the implied probability density function of $g_N(X)$ is well-defined, since then the following holds:

$$G_X(x) = G_{g_N}(g_N(x)) \Rightarrow f_{g_N}(g_N(x)) = f_X(x) \left(\frac{\mathrm{d}g_N}{\mathrm{d}x}(x) \right)^{-1}.$$

Section 4.5 presents in detail an algorithm to test that the Lagrange polynomial is strictly monotonic. If the Lagrange polynomial is strictly monotonic, it holds that $\frac{\mathrm{d}g_N}{\mathrm{d}x}(x) > 0 \ \forall \ x \in \mathbb{R}$. If g_N is not strictly monotonic, i.e. there exists a point x^* for which it holds $\frac{\mathrm{d}g_N}{\mathrm{d}x}(x^*) = 0$, it implies that $\lim_{x \to x^*} f_{g_N}(g_N(x)) = \infty$. If g_N is not monotonic, the relationship between X and S is not one-to-one and the relationship between the probability density functions described above does not hold anymore. Using this relationship implies then a negative probability density function and thus arbitrage. Furthermore, for option pricing an inversion of g_N is needed, thus it is required that g_N is monotonic. In the remainder of the thesis, g_N is required to be strictly monotonic.

The mapping or the Lagrange polynomial g_N do not have to be strictly monotonic on the entire real line. As with the CEV process, Y can be a process with an absorption at zero. For this example, this is done by considering $g_N(x)1_{\{g_N(x) \geq 0\}}$. This is a powerful feature of the method. In this thesis only the case of absorption at zero will be discussed for Hagan's formulas since this is in alignment with the SABR model. Furthermore, this is most natural for Hagan's Black Formula, since then:

$$\mathbb{E}\left[(S_T)^+\right] = C_{\text{Black}}(0, T, 0, \sigma) = S_0,$$

as described in more detail in Section 2.5.4. This will be investigated in more detail in Section 4.9. First, Lemma 4.3 will be given, under which conditions the probability density function of the variable $h(X)$ integrates to one, where h is a differentiable function. The Lagrange polynomial is a special case of a differentiable function. A distinction between absorption and no absorption is made in lemma 4.3.

Lemma 4.3. *Let $\bar{h}_1, h_2$ be differentiable functions, and assume $\frac{\mathrm{d}\bar{h}_1}{\mathrm{d}x} > 0$ on $[x^*, \infty]$ and $\frac{\mathrm{d}h_2}{\mathrm{d}x}(x) > 0$ for all $x \in \mathbb{R}$. Define $h_1(X) = \bar{h}_1(x)1_{\{X>x^*\}}$. Let X be a random variable. Define $Y_1 := h_1(X)$ with an absorption point at $y^* = \bar{h}_1(x^*)$ with point mass $F_X(x^*)$. Define $Y_2 = h_2(x)$. Then the probability density functions of Y_1 and Y_2 integrate to one.*

Proof. First, it is noted that:

$$f_{Y_1}(y) = \frac{f_X(x)}{\frac{\mathrm{d}h_1}{\mathrm{d}x}(x)},$$

on (x^*, ∞). It follows by the monotonicity of h_1 on $[x^*, \infty)$ that $\lim_{x\to\infty} h_1(x) = \infty$. Hence by change of variables from $y = h_1(x)$ to x:

$$\begin{aligned}
\int_{-\infty}^{+\infty} f_{Y_1}(y)\,\mathrm{d}y &= \int_{y^*}^{+\infty} f_{Y_1}(Y)\,\mathrm{d}y \\
&= F_X(x^*) + \int_{(y^*)^+}^{\infty} f_Y(Y)\,\mathrm{d}y \\
&= F_X(x^*) + \int_{x^*}^{\infty} \frac{f_X(x)}{\frac{\mathrm{d}h_1}{\mathrm{d}x}(x)} \frac{\mathrm{d}h_1}{\mathrm{d}x}(x)\,\mathrm{d}x \\
&= F_X(x^*) + \int_{x^*}^{+\infty} f_X(X)\,\mathrm{d}x = 1.
\end{aligned}$$

The proof for Y_2 is done in a similar fashion, where compared to the absorption case, one uses the fact $\lim_{x\to-\infty} h_2(x) = -\infty$ in the change of variables. □

Thus if $h = g_N$ is a Lagrange polynomial or any other function that is strictly monotonic and X is a random variable, then it holds that $Y = h(X)$ is a well-defined random variable for which the probability density function can trivially be determined. One could also extend the process Y to a process with absorption at zero.

Applying the SCM on the Hagan's implied random variable, it is not guaranteed that the new process $g_N(X)$ satisfies the martingale property, i.e. $\mathbb{E}\left[g_N(X)\right] \neq S_0$. This is not constraint in the approach by Grzelak et al. In the example of Table 4.4 and choosing six collocation points and setting $\zeta_{\max} = 0.8$ and $\zeta_{\min} = 0.0001$ gave $\mathbb{E}\left[(g_N)^+(X)\right] = 1.0018 > 1 = S_0$. Without the martingale property, put-call-parity does not hold which generates an arbitrage opportunity. This can be obtained by setting this as a constraint on the coefficients $a_0, \ldots, a_{N-1}$ of the Lagrange polynomial g_N. An example on how to do so, is presented in Section 4.9.

4.4.2 Option prices

Analytic expressions for call and put prices can be derived when using a Lagrange polynomial as an approximation g_N for the mapping m. This will be done for a general polynomial; the Lagrange polynomial is special case. Lemmas 4.4, 4.5 and Corollary 4.6 are used when X is chosen to be a normal distribution, see also Grzelak et al. [25]. Lemmas 4.4, 4.7 and Corollary 4.8 are used when X is chosen to be a gamma distribution. Call and put prices can usually be expressed as

$$C(t,T,K) = \mathcal{D}(t)\mathbb{E}\left[(S_T - K)^+\right],\ P(t,T,K) = \mathcal{D}(t)\mathbb{E}\left[(K - S_T)^+\right],$$

for some function $\mathcal{D}(t)$. For swaptions $\mathcal{D}(t)$ is the notional times the annuity. The focus will be on the expectation, since $\mathcal{D}(t)$ can be determined at time t.

Lemma 4.4. *Let p be a strictly monotonic polynomial on $[\bar{x}, \infty)$ and $x^* \geq \bar{x}$ with $p(\bar{x}) = 0$. Express p as*

$$p(x) = a_0 + \dots a_{N-1}x^{N-1}.$$

Furthermore, let x^* be such that $p(x^*) = K$ with $K \geq 0$. Define $h(x) = p(x)1_{\{p(x)\geq 0\}} = (p(x))^+$ and define the process $Y := h(X)$. Assume that at time t the distribution of a financial quantity, like the forward swap rate, for time T is given by the process Y. Then the price of a call option (C) and put option (P) on the financial quantity with strike $K \geq 0$ under the process Y are given by:

$$\begin{aligned}
&\mathbb{E}\left[(h(X) - K)^+\right] = \mathbb{E}\left[(h(X) - K)\, 1_{X\geq x^*}\right] = \sum_{i=0}^{N-1} a_i \mathbb{E}\left[X 1_{X\geq x^*}\right] - K(1 - F_X(x^*)),\\
&\mathbb{E}\left[(K - h(X))^+\right] = (\mathbb{E}\left[h(X)\right] - K) + \mathbb{E}\left[(h(X) - K)^+\right].
\end{aligned}$$

Lemma 4.5 and Corollary 4.6 are used to compute the expectations in Lemma 4.4 in the case that X is chosen to be a normal random variable.

Lemma 4.5. *Let Z be a standard normal distributed random variable. Let $a, b \in \mathbb{R}$, then it holds that:*

$$\begin{aligned}
&II_0(a,b) := \mathbb{E}\left[1_{\{a\leq Z<b\}}\right] = F_{\mathcal{N}}(b) - F_{\mathcal{N}}(a),\\
&II_1(a,b) := \mathbb{E}\left[1_{\{a\leq Z<b\}} Z\right] = f_{\mathcal{N}}(a) - f_{\mathcal{N}}(b),\\
&II_i(a,b) := \mathbb{E}\left[1_{\{a\leq Z<b\}} Z^i\right] = a^{i-1} f_{\mathcal{N}}(a) - b^{i-1} f_{\mathcal{N}}(b) + (i-1) I_{i-2}(a,b), \text{ for } i \geq 2.^4
\end{aligned}$$

where $F_{\mathcal{N}}(\cdot)$ is the cumulative density function and $f_{\mathcal{N}}(\cdot)$ is the probability density function of a standard normal random variable. It holds that $f_{\mathcal{N}}(x) \in \mathcal{S}$, the Swartz-space, therefore:

$$\lim_{x\to\pm\infty} x^\alpha f_{\mathcal{N}}(x) = 0,$$

for any $\alpha \in \mathbb{R}$.

Proof. The case $m = 0$ follows directly from direct integration and the case $m \geq 1$ follows from integration by parts. □

Corollary 4.6. *Let $X \sim \text{Norm}(0, \sigma^2)$ with $\sigma \in \mathbb{R}^+$. Let $a, b \in \mathbb{R}$ and $II_i(a,b)$ be defined as in Lemma 4.5, it holds that:*

$$\mathbb{E}\left[1_{\{a\leq X<b\}} X^i\right] = \sigma^i II_i\left(\frac{a}{\sigma}, \frac{b}{\sigma}\right).$$

Proof. The proof directly follows from substituting $X = \sigma Z$, where $Z \sim \text{Norm}(0, 1)$. □

Lemma 4.7 and Corollary 4.7 are used to compute the expectations in Lemma 4.4 in the case that X is chosen to be a random variable distributed according to a gamma distribution.

Lemma 4.7. *Let $a, b, \beta_\Gamma \in \mathbb{R}^+$ and $n \in \mathbb{N}$, it holds that:*

$$\int_a^b e^{-\beta_\Gamma x}\,\mathrm{d}x = -\beta_\Gamma^{-1} e^{-\beta_\Gamma x}\Big|_{x=a}^{b},$$
$$\int_a^b x^n e^{-\beta_\Gamma x}\,\mathrm{d}x = -\beta_\Gamma^{-1} x^n e^{-\beta_\Gamma x}\Big|_{x=a}^{b} + n\int_a^b x^{n-1}\beta_\Gamma^{-1} e^{-\beta_\Gamma x}\,\mathrm{d}x.$$

Note that $e^{-\beta_\Gamma |x|} \in \mathcal{S}$, the Swartz-space, therefore:

$$\lim_{x\to+\infty} x^\alpha e^{-\beta_\Gamma x} = 0,$$

for $\alpha \in \mathbb{R}$.

Proof. The case $n = 0$ follows directly from integration and the case $n \geq 1$ follows from integration by parts. □

Corollary 4.8. *Let X be a gamma distributed random variable, i.e. $X \sim Gam(\alpha_\Gamma, \beta_\Gamma)$ with $\alpha_\Gamma \in \mathbb{N}_{\geq 1}$, probability density function $f_X(x) = \frac{\beta_\Gamma^{\alpha_\Gamma}}{\Gamma(\alpha_\Gamma)} x^{\alpha_\Gamma - 1} e^{-\beta_\Gamma x}$ and Γ is the Gamma function. Let $a, b, \beta_\Gamma \in \mathbb{R}^+$, it holds that:*

$$\mathbb{E}\left[1_{\{a\leq X<b\}} X^n\right] = -\frac{\beta_\Gamma^{\alpha_\Gamma}}{\Gamma(\alpha_\Gamma)}\left(\sum_{i=0}^{n+\alpha_\Gamma-1} \frac{(n+\alpha_\Gamma-1)!}{(n+\alpha_\Gamma-1-i)!} x^{n+\alpha_\Gamma-1-i}\beta_\Gamma^{-(i+1)}\right) e^{-\beta_\Gamma x}\Bigg|_{x=a}^{b} \quad \textit{for } n \geq 0.$$

Proof. The proof follows directly from Lemma 4.7. □

Remark 4.9. *The optimal collocation points depend entirely on the moments of X. If $X \sim Gam(\alpha_\Gamma, \beta_\Gamma)$, then $\mathbb{E}[X^n] = \frac{\Gamma(\alpha_\Gamma+n)}{\Gamma(\alpha_\Gamma)\beta_\Gamma^n}$ and $X \sim \beta_\Gamma^{-1} Z$ with $Z \sim Gam(\alpha_\Gamma, 1)$. From the latter relation, it follows that the optimal collocation points of X are equal to $\{x_i\} = \{\beta_\Gamma^{-1}\tilde{x}_i\}$ where $\{\tilde{x}_i\}$ are the optimal collocation points of Z. To determine the location of the optimal collocation points by the procedure of Grzelak et al. [26] from the moments, this can be done accurately if one uses a $\beta_\Gamma \gg 1$ to compute the optimal collocation points. The moments of X with a large β_Γ are smaller compared to a X with a small β_Γ. As a consequence, smaller numerical errors are being produced. The relation $X \sim \beta_\Gamma^{-1} Z$ provides the optimal collocation points for any gamma distribution with the same α_Γ.*

4.5 Assessing the monotonicity of polynomials

As mentioned in Section 4.4, it is required that the Lagrange polynomial g_N satisfies the property $\frac{\mathrm{d}g_N}{\mathrm{d}x}(x) > 0$, $\forall\, x \in \mathcal{I}(X) \subseteq \mathcal{R}(X)$, to have an arbitrage-free approach with the SCM. The interval $\mathcal{I}(X) \subseteq R(X)$ on which the Lagrange polynomial must be monotonic depends on the variables X and Y. If X is chosen to be a gamma distribution, then $\mathcal{I}(X) = \mathcal{R}(X) = \mathbb{R}_{\geq 0}$. In the case that Y has absorption at some point y^*, this may decrease the size of the interval $\mathcal{I}(X)$. For example, if $y^* = 0$ and $g_N(x^*) = 0$ for some $x^* > 0$, then it must hold that $\frac{\mathrm{d}g_N}{\mathrm{d}x}(x) > 0\ \forall\, x \in [x^*, \infty)$ and therefore $\mathcal{I}(X) = [x^*, \infty)$.

A strictly monotonic Lagrange polynomial is not directly guaranteed by the approach of Grzelak et al. In fact, if N is odd, then g_N is a polynomial of order $N-1$ and its derivative is

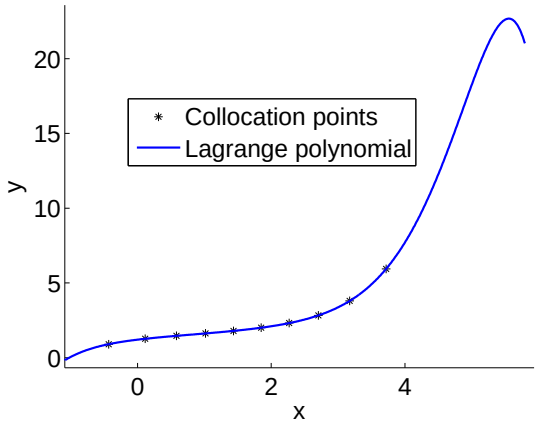

Figure 4.5: Mapping in the SCM for Hagan's Black formula and a seventh order Lagrange polynomial (eight collocation points). The parameters are taken from Table 4.4 with $\zeta_{\min} = \max(G_X(x_N), 0.0001)$, and $\zeta_{\max} = 0.95 \cdot \max_y G_Y(y)$.

a polynomial of order $N-2$ and therefore odd. In that case it is certain that $\frac{\mathrm{d}g_N}{\mathrm{d}x}(x) < 0$, for some $x \in \mathbb{R}$. In the case N is even, it is also not guaranteed that the Lagrange polynomial is monotonic. Figure 4.5 presents the resulting collocation points and Lagrange polynomial, where the Lagrange polynomial is not monotonic.

The collocation points imply that the mapping is monotonic. The collocation points and grid-stretching are chosen such that the Lagrange polynomial does not suffer from Runge oscillation. This results for most practical problems in a monotonic Lagrange polynomial. Sturm's theorem will be used to verify that a polynomial is monotonic. To introduce Sturm's theorem, the definition of a Sturm chain and an algorithm to obtain a Sturm chain will be introduced. These are taken from Akritas [2].

Definition 4.10 (Sturm chain)**.** A Sturm chain or Sturm sequence is a finite sequence of polynomials $p_0, \ldots, p_n$ of decreasing degree with the following properties:

- $p_0 = p$ is square free, i.e. no repeated roots,
- if $p(x) = 0$, then $\operatorname{sign}(p_1(x)) = \operatorname{sign}(p'(x))$,
- if $p_i(x) = 0$ for some $0 < i < n$, then $\operatorname{sign}(p_{i-1}(x)) = -\operatorname{sign}(p_{i+1}(x))$,
- $p_n(x)$ does not change sign.

Algorithm 1 (Obtaining a Sturm chain)**.** Let p_0 be square-free, then

$$\begin{aligned} p_0(x) &:= p(x), \\ p_1(x) &:= p'(x) \\ p_i(x) &:= -\operatorname{rem}(p_{i-2}, p_{i-1}), \\ &\vdots \\ 0 &:= -\operatorname{rem}(p_{n-1}, p_n), \end{aligned}$$

where $\operatorname{rem}(p_i, p_j)$ is the remainder of polynomial long division. Polynomial long division can be expressed as $p_i = p_j q + \operatorname{rem}(p_i, p_j)$, where q is quotient of the polynomial long division.

For example, let

$$p_1(x) = 3x^2 - 12x + 11,\ p_2(x) = -\frac{2}{3}x + \frac{4}{3}.$$

Then $p_1(x) = p_2(x)\left(\frac{-2}{9}x + 9\right) - 1$, i.e. $\mathrm{rem}(p_1, p_2) = -1$ and $q(x) = \frac{-2}{9}x + 9$, which followed from the polynomial long division.

$$\begin{array}{r} -\frac{2}{3}x + \frac{4}{3} \,/\, 3x^2 - 12x + 11 \,\backslash\, \frac{-2}{9}x + 9 \\ \underline{3x^2 - \ 6x + \ 0\ } \\ -\ 6x + 11 \\ \underline{-\ 6x + 12\ } \\ -\ 1 \end{array}$$

Theorem 4.11 (Sturm's Theorem)**.** *Let p be a square-free polynomial and let $p_0, \ldots, p_n$ be the Sturm chain constructed by Algorithm 1. Let* $\mathrm{sign}(x)$ *denote the number of sign changes (ignoring zeroes) in the sequence*

$$p_0(x), \ldots, p_n(x).$$

For each two real numbers $a < b$, the number of distinct roots of p in the half-open interval $(a, b]$ is equal to $\mathrm{sign}(a) - \mathrm{sign}(b)$*. If p is a non-square-free polynomial, then $p_0, \ldots, p_n$ is the canonical Sturm chain constructed by Algorithm 1. The number of distinct roots of p in the half-open interval $(a, b]$ is equal to* $\mathrm{sign}(a) - \mathrm{sign}(b)$*, given that neither a nor b is a multiple root of p.*

Proof. A proof can be found in Sturm [40]. □

Here, an application of Sturm's Theorem will be given. The following polynomial will be considered:

$$p(x) = (x-1)(x-2)(x-3) = x^3 - 6x^2 + 11x - 6.$$

Hence, the following Sturm chain is obtained:

$$\begin{aligned} p_0(x) &= x^3 - 6x^2 + 11x - 6, \\ p_1(x) &= 3x^2 - 12x + 11, \\ p_2(x) &= \frac{2}{3}x - \frac{4}{3}, \\ p_3(x) &= 1 \end{aligned}$$

So p_1 is the derivative of p_0. p_2 and p_3 follow from polynomial long division.

It is desired to determine the number of zeros in the interval $[0, 4]$. To do so, one computes

$$\begin{aligned} p_0(0) = -6,\ p_1(0) = 11,\ p_2(0) = -\frac{4}{3},\ p_3(0) = 1, \\ p_0(4) = 6,\ p_1(4) = 11,\ p_2(4) = \frac{4}{3},\ p_3(4) = 1. \end{aligned}$$

Hence,

$$\begin{aligned} &\mathrm{sign}(p_0(0)) = -,\ \mathrm{sign}(p_1(0)) = +,\ \mathrm{sign}(p_2(0)) = -,\ \mathrm{sign}(p_3(0)) = +, \\ &\mathrm{sign}(p_0(4)) = +,\ \mathrm{sign}(p_1(4)) = +,\ \mathrm{sign}(p_2(4)) = +,\ \mathrm{sign}(p_3(4)) = +. \end{aligned}$$

Thus number of sign changes at 0 and 4 is 3 and 0 respectively. Thus Sturm's Theorem implies $3 - 0 = 3$ zeros, which is indeed the number of zeros on $[0, 4]$.

It will be explained how Sturm's Theorem can be used to verify that a polynomial is strictly monotonic on the real line. For a bounded interval or half-bounded interval the algorithm works similarly to this example on the real line. For example, the polynomial $p(x) = \frac{1}{3}x^3 + x$ is used. This is a strictly monotonic polynomial on the entire real line.[5] Sturm's Theorem is applied to verify this. In the construction of a Sturm chain one sets $p_0(x) = p^{'}(x)$ and computes that:

$$\begin{aligned} p_0(x) &= p^{'}(x) = x^2 + 1, \\ p_1(x) &= p_0^{'}(x) = 2x, \\ p_2(x) &= -1. \end{aligned}$$

In the limits for $x \to \pm\infty$ it can be proven that the sign of a polynomial $p(x) = a_n x^n + \ldots + a_0$ is determined by the highest order coefficient a_n of the polynomial. For example, this can be done for $x \to \infty$ and $a_n > 0$ by proving that there exists a number b such that $p(x) > 0$ for all $x > b$. It can be proven that $p(x) > 0$ for all $x > b$ provided that $b \geq \max\left\{1, \frac{\sum_{i=1}^{n-1} |a_i|}{a_n}\right\}$. This follows from the fact that $a_n x^n > a_{n-1}x^{n-1} + \ldots a_0 x^{n-1} > a_{n-1}x^{n-1} + \ldots a_0$ for $x > b$. This implies that $p(x)$ has no zeros for $x > b$. Thus checking the number of zeros of a polynomial is completely determined by the highest order coefficients of the polynomials in the Sturm chain.

This gives the following result for this example:

$$\begin{aligned} &\text{sign}(\lim_{x\to\infty} p_0(x)) = +,\ \text{sign}(\lim_{x\to\infty} p_1(x)) = +,\ \text{sign}(\lim_{x\to\infty} p_2(x)) = -, \\ &\text{sign}(\lim_{x\to-\infty} p_0(x)) = +,\ \text{sign}(\lim_{x\to-\infty} p_1(x)) = -,\ \text{sign}(\lim_{x\to-\infty} p_2(x)) = -. \end{aligned}$$

The sign changes in the limits are both 1, so $p^{'}(x)$ has $1 - 1 = 0$ zeros. Thus $p(x)$ is monotonic on the real line. Sturm's Theorem 4.11 is a computationally rapid method of verifying the monotonicity of a polynomial a posteriori.

The algorithm can be summarized as follows:

- Input a polynomial and the interval (a,b) on which the monotonicity of the polynomial needs to be verified.
- Compute the Sturm chain for the derivative of the polynomial.
- Compute the signs changes of the Sturm chain for a and b.
- If the difference between the sign changes is zero, the polynomial is strictly monotonic. Otherwise, it is not strictly monotonic.

Remark 4.12. *Since the Lagrange coefficients can be computed by solving the VanDerMonde matrix equation $\mathcal{V}(\mathbf{x})\mathbf{a} = \mathbf{y}$ and the inverse of $\mathcal{V}(\mathbf{x})$ is known from Turner [24], in theory one could find under which condition of $\{x_i\}$ and $\{y_i\}$ imply a strictly monotonic polynomial. This however will be a tough exercise to work out for the general case. For practical purposes it is checked with the above construction. Finding the conditions under which a Lagrange polynomial is strictly monotonic does not give a priori knowledge in which fashion the points x_i have to be chosen, since the monotonicity will also depend on y_i. Thus, knowledge on y_i is required too.*

[5] This can be shown to be true if one looks at its derivative, since the derivative has no zeros.

4.6 Convergence properties and error estimates

This section starts with an error expression for the Lagrange polynomial for a general function. This error expression will be used to derive an error bound for the expectation of the process implied by the SCM. These error bounds indicate convergence for call prices.

Lemma 4.13 (Error Expression For A Lagrange Polynomial)**.** *Let g_N be the Lagrange polynomial that interpolates a $N+1$ differentiable function h on the points $\{x_1, \ldots, x_N\}$. Then, there exists a κ_x for each x such that:*

$$h(x) - g_N(x) = \frac{h^{(N)}(\kappa_x)}{N!}\Pi_{i=1}^{N}(x - x_i).$$

Furthermore, κ_x is continuous.

Proof. The proof can be found in Stewart [39]. □

Lemma 4.14 (Error Bound On The Expectation By A Lagrange Polynomial)**.** *Let X be a random variable with probability density function $f_X(x)$ and assume $Y := h(X)$ is a well-defined variable with h a strictly monotonic function. Let $g_N(x)$ be the Lagrange polynomial that interpolates $h(x) \in \mathcal{C}^{n+1}$ on the set of points $\{x_1, \ldots, x_n\}$. Then*

$$\left| \int_a^b (h(x) - g_N(x)) f_x(x)\,\mathrm{d}x \right| \leq \frac{1}{N!} \max_{\kappa\in[a,b]} |h^{(N)}(\kappa)| \max_{\bar{x}\in[a,b]} \Pi_{i=1}^{N} |\bar{x} - x_i|.$$

Proof. By Lemma 4.13, it follows that:

$$\begin{aligned}
\left| \int_a^b (h(x) - g_N(x)) f_x(x)\,\mathrm{d}x \right| &= \frac{1}{N!} \left| \int_a^b h^{(N)}(\kappa_x)\Pi_{i=1}^{N}(x - x_i) f_x(x)\,\mathrm{d}x \right| \\
&\leq \frac{1}{N!} \int_a^b \left| h^{(N)}(\kappa_x)\Pi_{i=1}^{N}(x - x_i) \right| f_x(x)\,\mathrm{d}x \\
&\leq \frac{1}{N!} \max_{\kappa\in[a,b]} h^{(N)}(\kappa) \max_{\bar{x}\in[a,b]} \Pi_{i=1}^{N} |\bar{x} - x_i| \int_a^b f_x(x)\,\mathrm{d}x \\
&\leq \frac{1}{N!} \max_{\kappa\in[a,b]} h^{(N)}(\kappa) \max_{\bar{x}\in[a,b]} \Pi_{i=1}^{N} |\bar{x} - x_i|.
\end{aligned}$$

□

Remark 4.15. *It must be noted that the Chebyshev nodes minimize the condition*

$$\max_{\bar{x}\in[-1,1]} \Pi_{i=1}^{N} |\bar{x} - x_i| = 2^{1-N},$$

such that [39]:

$$\min_{x_i\in[-1,1],\ i=1,\ldots,N} \max_{\bar{x}\in[-1,1]} \Pi_{i=1}^{N} |\bar{x} - x_i| = 2^{1-N}.$$

Therefore, these will be investigated in Section 4.8 and compared to the optimal collocation points.

Similar to the expectation of the process, analytical expressions for error estimations for a call price is derived. The mapping between X and S is dependent on the derivatives of call prices. Thus it is important to investigate the convergence of call prices.

Lemma 4.16. *For convenience, the call price at maturity is written as $C(x) = (x - K)^+$ where K is the strike of the option. It satisfies the following relation:*

$$|C(x) - C(y)| \leq |x - y|.$$

Proof. A proof can be found in Appendix C.2. □

Corollary 4.17. *Let the call price at maturity be written as $C(x) = (x - K)^+$, where K is the strike of the option. Let X be a random variable with probability density function $f_X(x)$. Assume that g_N is the Lagrange polynomial that approximates $h(x)$ on the interval $[a, b]$. Then:*

$$\left| \int_a^b \left(C(h(x)) - C(g_N(x)) \right) f_x(x) \, \mathrm{d}x \right| \leq \frac{1}{N!} \max_{\kappa \in [a,b]} |h^{(N)}(\zeta)| \max_{\bar{x} \in [a,b]} \Pi_{i=1}^N |\bar{x} - x_i|.$$

Proof. It follows that

$$\begin{aligned} \left| \int_a^b \left(C(h(x)) - C(g_N(x)) \right) f_x(x) \, \mathrm{d}x \right| &\leq \int_a^b |C(h(x)) - C(g_N(x))| \, f_x(x) \, \mathrm{d}x \\ &\leq \int_a^b |h(x) - g_N(x)| \, f_x(x) \, \mathrm{d}x. \end{aligned}$$

The rest of the proof is analogous to the proof of Lemma 4.14. □

By using Lemmas 4.17 and 4.16, a bound on the error of a call option is derived. The error for expectations in the extrapolation interval for the Lagrange polynomial will be investigated too. This is based on the choice of grid-stretching by setting a $\zeta_{\min}$. First, Lemmas 4.18 and 4.19 are given, which will give a bound if $G_X(x_N) = \epsilon$ is chosen for the Lagrange polynomial.

Lemma 4.18. *Let X be a random variable and $x^* \in \mathbb{R}$ and $h(x) \in \mathcal{C}$. Then:*

$$\mathbb{E}\left[h(X) 1_{X > x^*} \right] = \mathbb{E}\left[h(X) | \, X > x^* \right] G_X(x^*).$$

Proof.

$$\begin{aligned} \mathbb{E}\left[h(X) 1_{X > x^*} \right] &= \mathbb{E}\left[\mathbb{E}\left[h(X) 1_{X > x^*} | \, X \right] \right] \\ &= \mathbb{E}\left[\mathbb{E}\left[h(X) 1_{X > x^*} | \, X > x^* \right] \mathbb{P}(X > x^*) + \mathbb{E}\left[h(X) 1_{X > x^*} | \, X \leq x^* \right] \mathbb{P}(X \leq x^*) \right] \\ &= \mathbb{E}\left[h(X) | \, X > x^* \right] G_X(x^*). \end{aligned}$$

□

Lemma 4.19. *Let X be a random variable and Y be a random variable satisfying $Y := h(X)$. Let $g_N(x)$ be the Lagrange polynomial that interpolates $h(x)$ on the set of points $\{x_1, \ldots, x_N\}$ and let $\{y_1, \ldots, y_n\} = \{h(x_1), \ldots, h(x_n)\}$. Let $G_Y(y_n) = G_X(x_n) \leq \epsilon$. Then:*

$$\left| \int_{x_N}^{+\infty} \left(h(x) - g_N(x) \right) f_x(x) \, \mathrm{d}x \right| \leq \epsilon \mathbb{E}\left[|h(x) - g_N(X)| | \, X > x_n \right].$$

Proof.

$$\begin{aligned} \left| \int_{x_N}^{+\infty} \left(h(x) - g_N(x) \right) f_x(x) \, \mathrm{d}x \right| &\leq \int_{x_N}^{+\infty} |h(x) - g_N(X)| f_X(x) \, \mathrm{d}x \\ &\leq G_X(x_n) \mathbb{E}\left[|h(x) - g_N(X)| | \, X > x_n \right] \\ &\leq \epsilon \mathbb{E}\left[|h(x) - g_N(X)| | \, X > x_n \right]. \end{aligned}$$

□

In general it can be expected that the expectation $\mathbb{E}[\tilde{h}(X)|X > x_N]$ goes to zero when x_N goes to infinity for some function $\tilde{h}$. Combining Lemmas 4.18 and 4.19 indicates that choosing $\zeta_{\min} = G_X(x_n) \ll 1$ gives a good bound on the error made in the expectations. Thus applying the SCM on a process will have a minimal impact on option prices if $\zeta_{\max}$ is chosen to be small. This will be investigated by applying the SCM to Hagan's formulas.

4.7 Results by a direct application of Grzelak et al.

Direct applications of Grzelak et al. [25] for Hagan's Black formula will be shown. For the simpler variable X in the mapping a normal distribution will be compared against a gamma distribution. The parameters are given by Table 4.5. It can be computed that $\max_s G_S(s) \approx 0.8167$. The parameters for the gamma distribution were chosen for this example such that they gave the most accurate results.

General parameters		SABR parameters				Normal distribution		Gamma distribution	
T	S_0	α	β	ρ	ν	μ	σ	α_Γ	β_Γ
10	1	0.25	0.6	-0.8	0.3	0	1	6	1

Table 4.5: Parameters for Figures 4.6–4.8.

Figure 4.6 presents the result where X is chosen to be a standard normal distribution, whereas Figure 4.7 presents the result where X is chosen to be a gamma distribution. In both cases $\zeta_{\min} = \max(G_X(x_N), 0.0001)$ and $\zeta_{\max} = 0.98 \cdot \max_s G_S(s)$ in the figure on the left and $\zeta_{\max} = 0.9 \cdot \max_s G_S(s)$ in the right on the figure respectively. The probability density functions implied by the SCM are not negative, whereas the probability density function implied by Hagan's Black formula is negative for low values of the underlying process. Absorption was not used in these figures, such that the extrapolation of the probability density function implied by the SCM could be investigated. These figures imply a similar extension of the probability density function for both distributions when at least six collocation points are used and there is not visual a difference between the probability densities functions in these figures when at least eight collocation points are used.

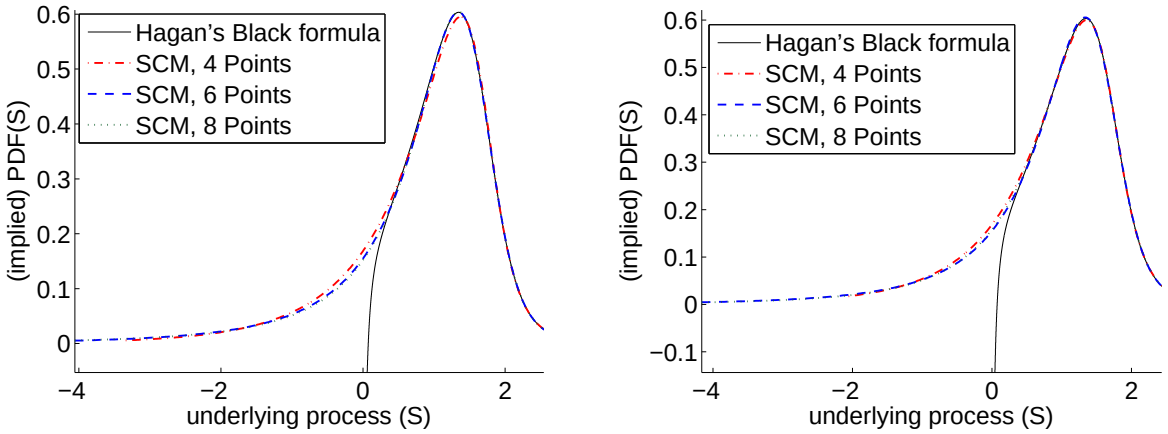

(a) $\zeta_{\max} = 0.98 \cdot \max_s G_S(s)$. (b) $\zeta_{\max} = 0.9 \cdot \max_s G_S(s)$.

Figure 4.6: (Implied) probability density functions for the normal distribution. Parameters are given by Table 4.5.

Figure 4.8 presents the error in the probability density function made by the SCM for the normal distribution in the figure on the left and the gamma distribution in the figure on the right. They are compared on the interval $[s_1, s_N]$. It is chosen to investigate the error in the probability density function and not in the mapping or the SDF. If the probability density function converges on the interval $[s_1, s_N]$, the SDF, the mapping and the option prices implied

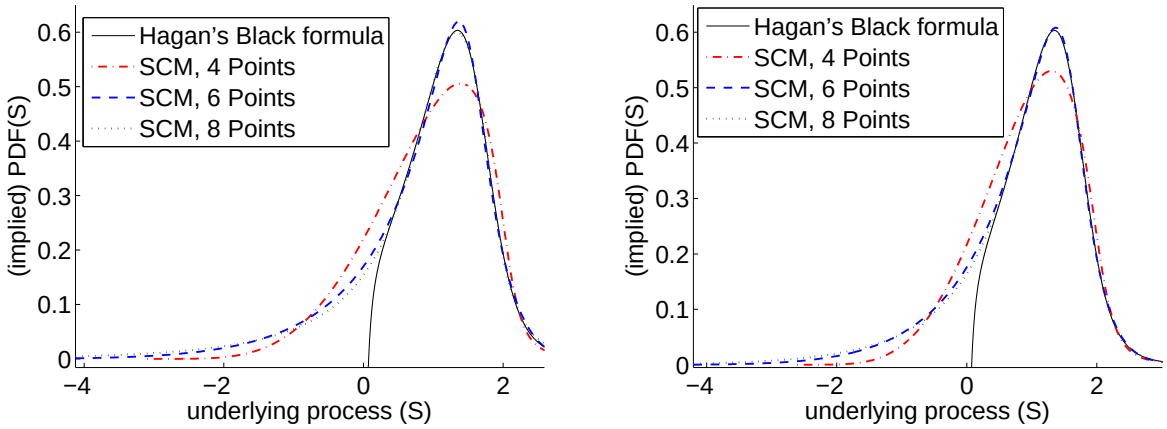

(a) $\zeta_{\max} = 0.98 \cdot \max_s G_S(s)$. (b) $\zeta_{\max} = 0.9 \cdot \max_s G_S(s)$.

Figure 4.7: (Implied) probability density functions for the gamma distribution. Parameters are given by Table 4.5.

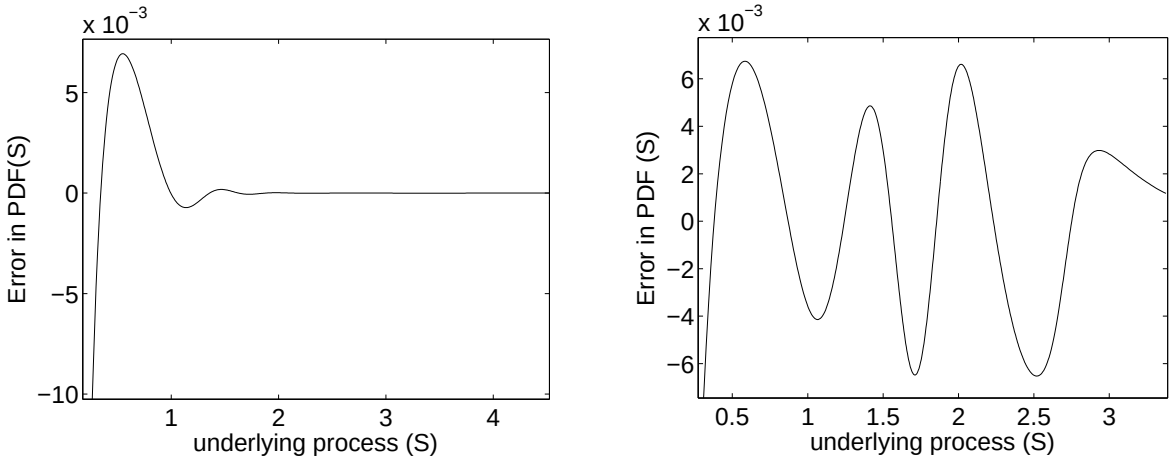

(a) Normal distribution. (b) Gamma distribution.

Figure 4.8: Error in (Implied) probability density functions. Parameters are given by Table 4.5.

by the SCM will converge. For each distribution eight collocation points were used. Using the normal distribution leads to the fastest convergence of the probability density function on the interval $[s_1, s_N]$ compared to the gamma distribution for this example.

If Hagan's Black formula implies a process which has a distribution that is more skewed, it makes more sense to map the process to a Gamma distribution. Figure 4.6 presents such an example.

General parameters		SABR parameters				Normal distribution		Gamma distribution	
T	S_0	α	β	ρ	ν	μ	σ	α_Γ	β_Γ
10	1	0.3	0.6	-0.4	0.37	0	1	6	1

Table 4.6: Parameter for Figure 4.9.

The distribution implied by Hagan's Black formula is now more skewed than in the previous

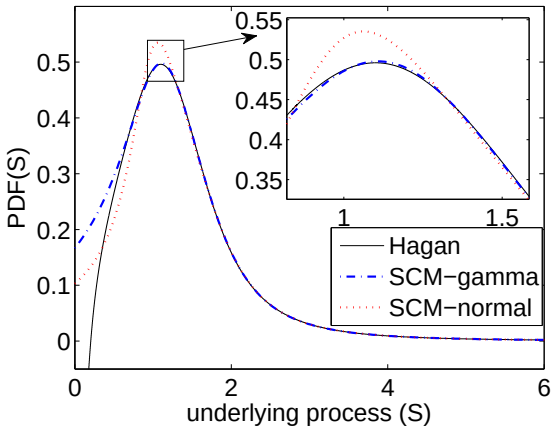

(a) probability densities compared.

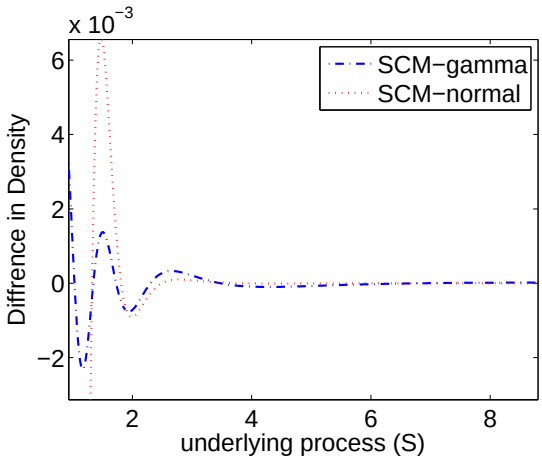

(b) Error in probability densities functions compared to the probability density function implied by Hagan's Black formula.

Figure 4.9: SCM: normal distribution compared to gamma distribution. Parameters are in Table 4.6.

example. Eight collocation points are used and $\zeta_{\max} = 0.90 \cdot \max_y G_Y(y)$ for both distributions. In this figure it can be observed that the gamma distribution can capture the distribution implied by Hagan's Black formula more accurately. Besides the random variable X in the mapping, the interpolation technique for the mapping must be investigated too.

4.8 Different types of interpolation

This section compares two different interpolation techniques to the standard approach. These are a first order Hermite interpolation and a Lagrange polynomial implied by the Chebyshev nodes. Other interpolation techniques like (monotonic) splines, second order Hermite interpolation and linear interpolation were investigated too, however those interpolation techniques did not gave satisfactory results compared to the standard approach.

For the Lagrange polynomial implied by the Chebyshev nodes, the standard approach is used. The difference is that the location of the collocation points is different. Like the standard approach, a $\zeta_{\min}$ and $\zeta_{\max}$ are found such that the collocation points are chosen by the Chebyshev nodes on a interval for $[a, b] = [G_X^{-1}(\zeta_{\min}), G_X^{-1}(\zeta_{\max})]$:

$$x_k = \frac{1}{2}(a+b) + \frac{1}{2}(b-a)\cos\left(\frac{2k-1}{N}\pi\right), \ k = 1, \ldots, N. \tag{4.4}$$

For the Hermite interpolation the following set of mapping points is used:

$$\begin{aligned} &\text{Set I}: \ \{y_i\} = S_0 \cdot [0.4, 0.6, 0.8, 1, 1.1, 1.4, 1.8, 3, 5, 8, 13], \\ &\text{Set II}: \{y_i\} = S_0 \cdot [0.5, 0.65, 0.8, 1, 1.1, 1.2, 1.4, 1.6, 2, 2.5, 4, 10]. \end{aligned}$$

These sets are chosen for the Hermite polynomial since they give satisfactory results. For example, for the Lagrange polynomials 8 and 10 collocation points are used for Set I and II respectively, where the SABR parameters are taken from Table 4.7.

General parameters		SABR parameters			
T	S_0	α	β	ρ	ν
10	1	0.25	0.6	-0.8	0.3

Table 4.7: Parameter for Figures 4.10–4.11.

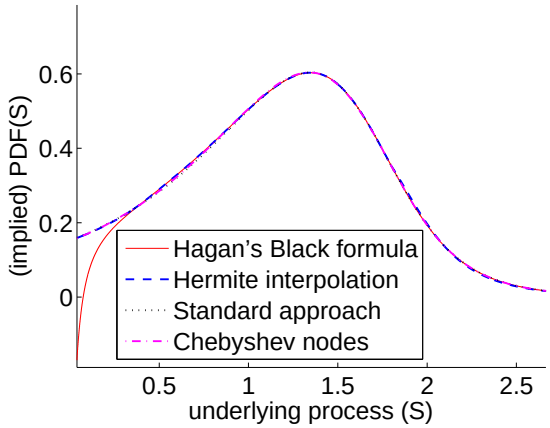

Figure 4.10: (Implied) probability density function.

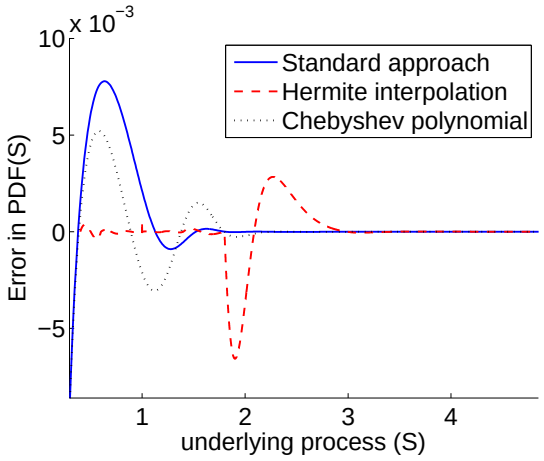

(a) Set I for Hermite interpolation.

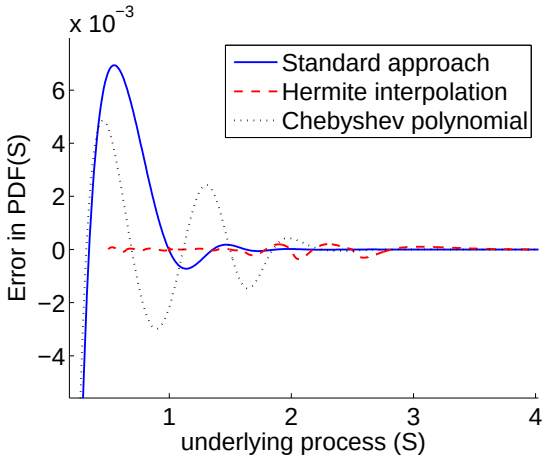

(b) Set II for Hermite interpolation.

Figure 4.11: Error of the probability density functions compared to the one implied by Hagan's Black formula. Parameters are taken from Table 4.7. For the Lagrange polynomials eight and ten collocation points are used in the figures on the left and right respectively. $\zeta_{\max} = 0.98 \cdot \max_y G_Y(y)$.

Figure 4.10 presents the resulting PDFs. Figure 4.11a and 4.11b presents the convergence of the three different types of interpolation. The standard approach converges fastest for high values of the underlying process, but has the largest mismatch in the probability density function for low values of the underlying process. The Chebyshev nodes do not give a faster convergence than the standard approach and do not provide a more accurate result for high values of the underlying process. Lastly, the Hermite interpolation is more accurate for low values of the

underlying process, but the relative error is larger for high values of the underlying process compared to the other two interpolation techniques. Furthermore, the computation of option prices and the inversion are computationally more expensive for the Hermite interpolation. Lastly, there is no general set of collocation points that directly imply a stable interpolation for the Hermite interpolation, whereas this is usually the case for the standard approach and the Chebyshev nodes.

The focus for the convergence of the probability density function should be on the high values for the underlying process. In the application of the SCM for Hagan's formulas, one uses Hagan's implied random variable. Hagan's implied random variable is derived from call prices. The expectation in a call price can be computed by

$$\int_K^\infty (s-K) f_S(s)\,\mathrm{d}s.$$

A large error in the approximation of the probability density function by the SCM for high values of the underlying process, can give larger mismatches in the call prices. Thus the approximation is less accurate if there are large mismatches in the probability density function for high values of the underlying process. Therefore, the standard approach seems to be the most promising interpolation technique for the SCM. However, the standard approach does not directly imply the martingale property, which is needed to exclude arbitrage. It will be investigated in the next section in which manner the martingale property can be obtained.

4.9 The martingale property using a virtual collocation point

It will be described how one can obtain the martingale property by using virtual collocation points. In the approach by Grzelak et al, this is needed to make this approach arbitrage-free. If the martingale property does not hold, put-call-parity does not hold and this implies arbitrage. For this approach, the original approach of Grzelak et al. was followed as closely as possible, since it gave satisfactory results. It is investigated whether in general one can obtain the martingale property using only a Lagrange polynomial. This section describes the approach, presents some results where this approach works satisfactorily and presents some extreme cases of Hagan's formulas. In this section, cases where Hagan's formulas imply no arbitrage, or imply a wildly behaving probability density function will be considered too.

4.9.1 Description of the approach

As in Section 4.3 it is assumed that S is well-defined for some $s^* \geq 0$. Like the standard approach, the optimal collocation points $\tilde{x}_1, \ldots, \tilde{x}_N$ and$\zeta_{\max}$ are determined first. The optimal collocation points $\tilde{x}_1, \ldots, \tilde{x}_N$ are then mapped linearly to an equivalent set of collocation points $x_1, \ldots, x_N$. Unlike the standard approach, this linear map is obtained by setting $G_X(x_2) = \zeta_{\max}$ and not $G_X(x_1) = \zeta_{\max}$ for the grid-stretching.[6] As a consequence, when applying the grid-stretching, the collocation points for X, $\{x_i\}_{i=1}^N$ are obtained and for S only $\{s_i\}_{i=2}^N$. The collocation point s_1 is a now virtual collocation point. This virtual collocation s_1 will be used to ensure the martingale property.

In this approach y_1 is calibrated such that the martingale property is obtained, i.e. $\mathbb{E}\left[(g_N(X))^+\right] = S_0$. During calibration g_N is constrained such that $\frac{\mathrm{d}g_N}{\mathrm{d}x} > 0 \;\forall\; x \in \mathbb{R}$ and only

[6] For $\zeta_{\max}$ a heuristic rule was developed for Hagan's formulas. This rule has been tested in many calibration results in Chapter 5 and produced satisfactory results.

even N are considered. The results will be limited where X is chosen to be a standard normal distribution and the approach will only be used for Hagan's Black formula. This is to illustrate the approach and similar results can be obtained for other distributions.

This approach can also be reformulated as an optimization problem for which a polynomial p_N has to be fitted, which fits the points $\{(x_i, y_i)\}_{i=2}^{N}$ under the condition $\frac{\mathrm{d}p_N}{\mathrm{d}x} > 0,\ \forall\ x \in \mathbb{R}$, and $\mathbb{E}\left[(p_N)^+(X)\right] = S_0$.

The idea of this approach is that one controls the polynomial and therefore the mapping for $x < x_2$. By controlling the polynomial, the martingale property can be obtained and arbitrage can be removed in the strike dimension.

Since for the exact mapping m and the constrained p_N, it holds that

$$\int_{-\infty}^{\infty} (m(x))^+ f_X(x)\,\mathrm{d}x = S_0 = \int_{-\infty}^{\infty} (p_N(x))^+ f_X(x)\,\mathrm{d}x,$$

convergence can be expected on the interval $[x_2, x_N]$. This is also the reason why absorption at zero comes as a natural extension for Hagan's Black formula. Hagan's Black formula originates from the SABR model and therefore implies a point mass at zero as discussed in Section 2.5.[7] Furthermore, Hagan's Black formula directly implies the martingale property for the implied underlying process. The result of the point mass is omitted, since it will have no effect on the call and put prices. Due to the constraint of $\frac{\mathrm{d}g_N}{\mathrm{d}x}(x) > 0\ \forall\ x \in \mathbb{R}$ one obtains a well-defined variable compared to Y, i.e. it has a nonnegative probability density function and implies the martingale property. In the case that one wants to use more virtual collocation points (e.g. one wants to ensure an accurate fit for some option price), one might get issues due to a less stable polynomial. If more constraints are available, then more virtual collocation points can be used, but it might be that less virtual points are needed than the number of constraints. This approach shall be referred to as the M-SCM, where M comes from martingale.

The algorithm can be summarized as:

- Input the SABR parameters and the number of collocation points.
- Determine an appropriate $\zeta_{\max}$ and compute $\{x_i\}_{i=1}^{N}$, $\{s_i\}_{i=2}^{N}$.
- Optimize s_1 such that the Lagrange polynomial implies the martingale property, while constraining it to be strictly monotonic.

4.9.2 Accurate results

Cases for which this approach works accurately are presented. Table 4.8 provides the parameter sets that are investigated. For each set 8, 10 and 12 collocation points are used.

The first three sets represent cases where Hagan's formulas give an unsatisfactory probability density function. For Set I, Hagan's formulas imply a process where the probability density function is negative around zero for the underlying process. For Set II, Hagan's formulas imply a process where the probability density function goes negative and then blows up around zero for the underlying process. For Set III, Hagan's formulas imply a process where the probability

[7] The case $\beta = 0$ is not considered here. The SABR model allows the financial quantity to become negative for $\beta = 0$, whereas the financial quantity cannot become negative for Black's model. It is therefore not natural to use Hagan's Black formula with $\beta = 0$.

density function stays positive, but goes to infinity around zero for the underlying process. For cases similar to Set III, it can happen that the probability density function integrates to some number larger than one. For Set IV, Hagan's formulas imply a well-defined process. In this case, it is investigated whether this virtual collocation approach remains stable.

	S_0	α	β	ρ	ν	T
Set I	1	0.25	0.6	-0.8	0.3	10
Set II	0.5	0.04	0.05	-0.2	0.3	10
Set III	0.5	0.2	0.2	-0.2	0.4	1
Set IV	0.5	0.6	0.9	-0.2	0.2	1

Table 4.8: SABR parameter sets for investigation.

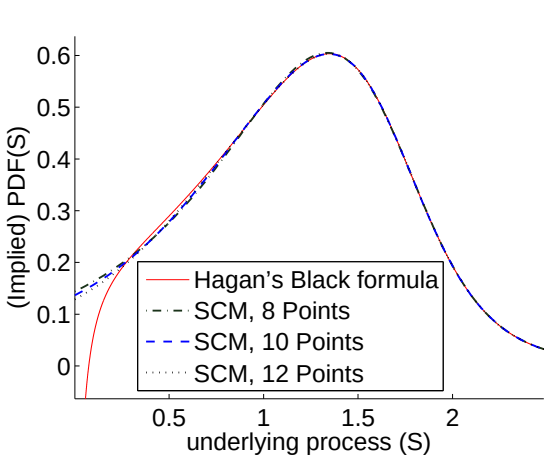

(a) (Implied) probability density functions.

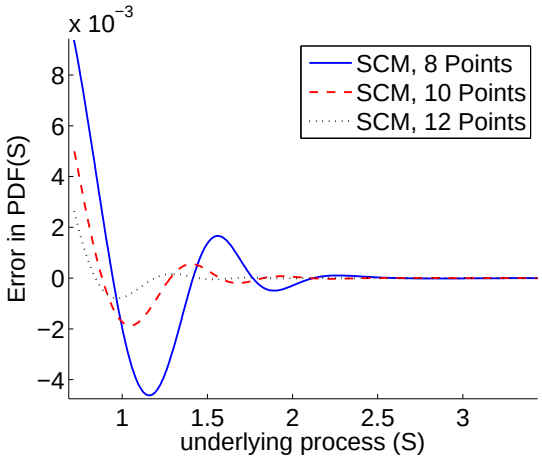

(b) Errors made in new probability density functions.

Figure 4.12: Set I of Table 4.8.

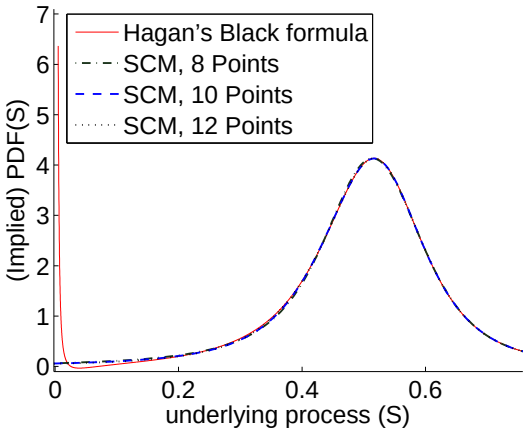

(a) (Implied) probability density functions.

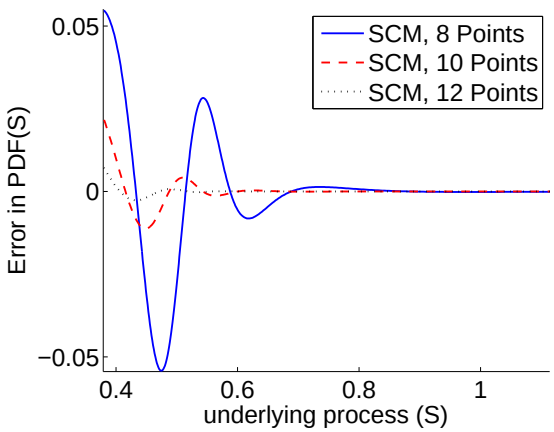

(b) Errors made in new probability density functions.

Figure 4.13: Set II of Table 4.8.

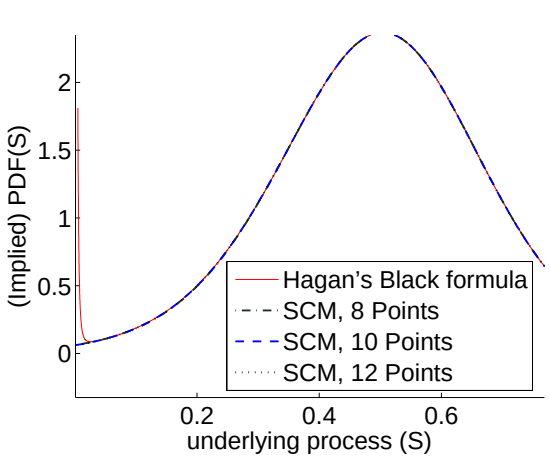

(a) (Implied) probability density functions.

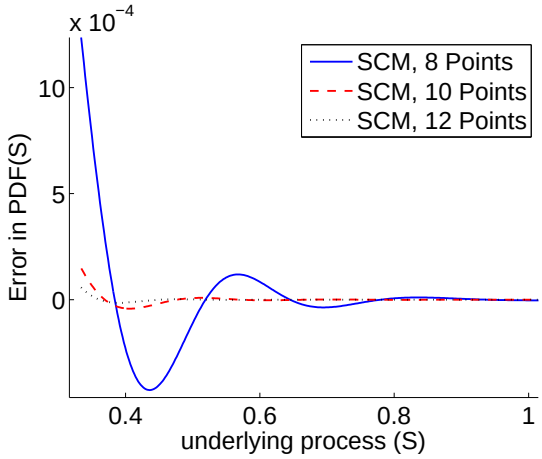

(b) Errors made in new probability density functions.

Figure 4.14: Set III of Table 4.8.

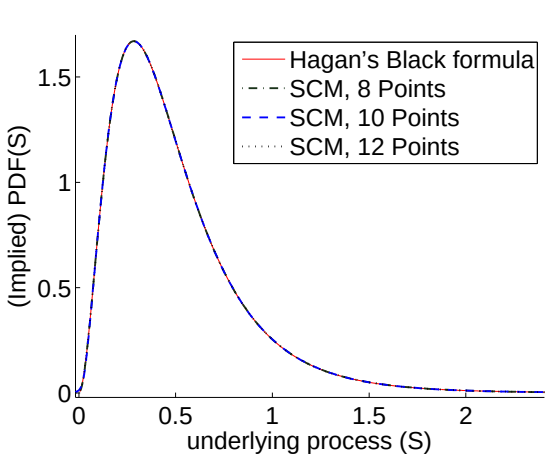

(a) (Implied) probability density functions.

.

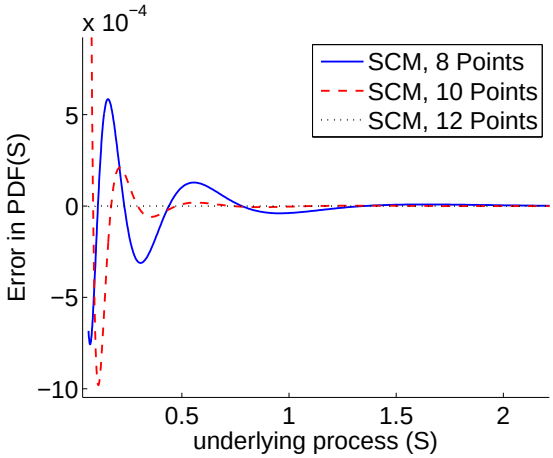

(b) Errors made in new probability density functions.

Figure 4.15: Set IV of Table 4.8.

Figures 4.12-4.15 present the probability density functions implied by Hagan's Black formula and the SCM in the figures on the left. In the figures on the right, the errors in the probability density functions made by using the SCM on the interval $[s_2, s_N]$ are presented. As can be observed from the figures, there is convergence for each set on $[s_2, s_N]$. Furthermore, for each set the martingale property is obtained.

Figure 4.16 presents the volatility curves for Hagan's formulas and the SCM. As can be observed, the difference is small between the volatility curves of Hagan's Black formula and the SCM. Table 4.9 summarizes the error and difference in the volatility for the interpolation and extrapolation respectively. It can be concluded that the M-SCM is accurate on the interpolation and decreases the value of the volatility for a low strike with a relative small difference. It removes the discontinuity in Hagan's formulas in a sophisticated manner for strikes near zero.

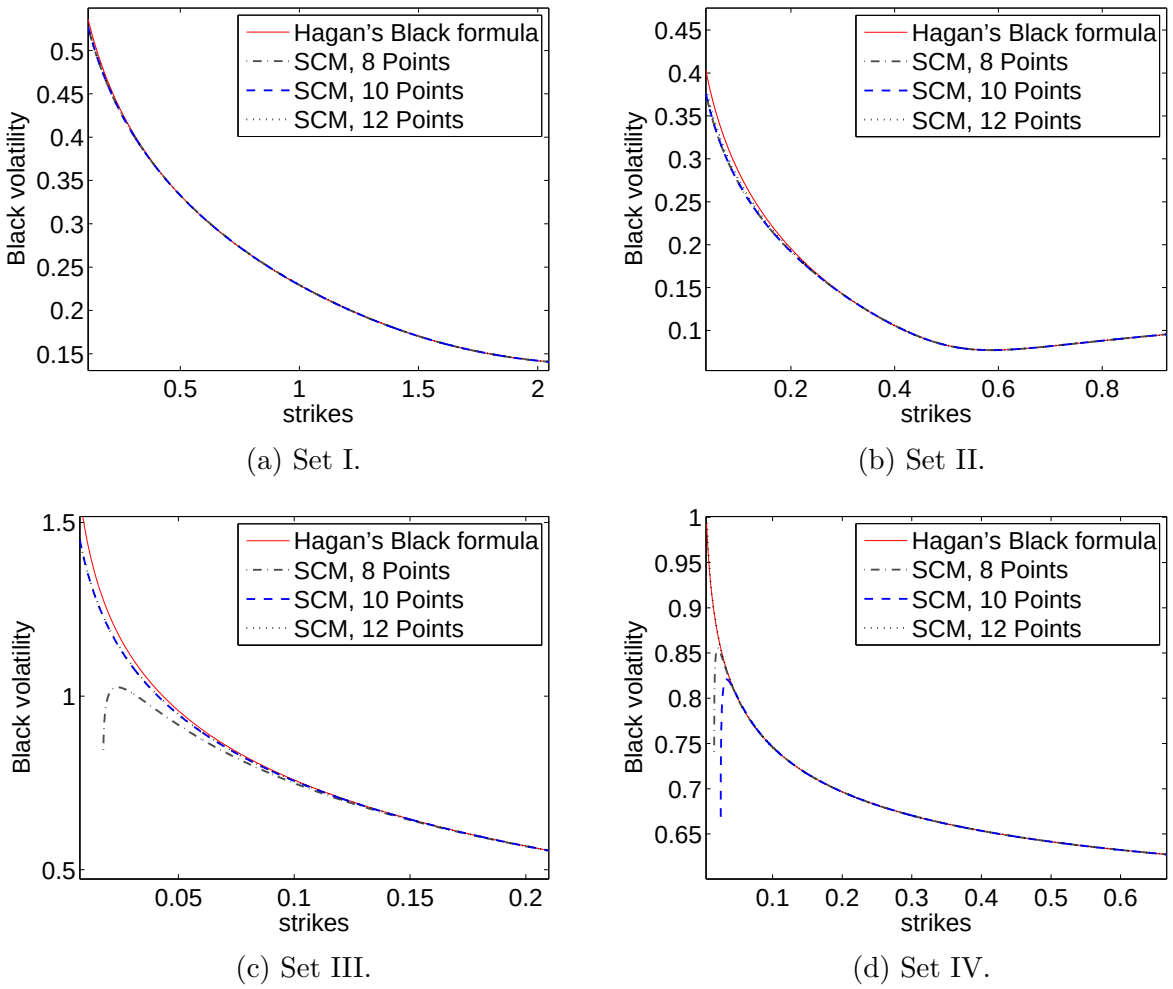

(a) Set I.

(b) Set II.

(c) Set III.

(d) Set IV.

Figure 4.16: Volatility curve for the parameter sets from Table 4.8.

Set	Interpolation (bp)	Extrapolation (%)[8]
I	5	2
II	2	3
III	0.2	20
IV	0.5	2

Table 4.9: Maximum difference between the volatility implied by Hagan's formulas and SCM-Hagan on the inter- and extrapolation of the Lagrange polynomial.

These four sets either imply only a small problem or no problem with Hagan's formulas. Therefore, this approach worked satisfactorily. Now, some investigation is done on some parameter sets where Hagan's formulas imply a more "extreme" probability density function. These will be cases in which Hagan's formulas imply arbitrage on a wider set of strikes, not only for strikes near zero.

[8]With the exceptions when the volatility curves implied by SCM-Hagan are down sloping.

4.9.3 Some extreme cases

Table 4.10 gives sets for which the behavior of Hagan's formulas can be considered extreme for the implied probability density function. Again 8, 10 or 12 collocation points are used, where the first one is a virtual one. Figures 4.17a-4.18c present the probability density functions and the errors made by the M-SCM on the interval $[s_2, s_N]$ respectively. Figures 4.18e - 4.18d present the resulting volatilities.

	S_0	α	β	ρ	ν	T
Set V	0.5	0.8	0.8	-0.2	0.5	1
Set VI	0.5	0.04	0.2	-0.2	0.4	10
Set VII	1	0.5	0.6	-0.4	0.3	10

Table 4.10: Parameter set under investigation.

These three sets give rise to undesired results with Hagan's formulas. In the cases of Set V and VII one may argue that the probability density function was changed too much by the M-SCM to directly apply it to Hagan's formulas, but this comes mainly from the fact that for these cases Hagan's formulas are behaving wildly. Therefore, one can observe differences up to 15% in the volatility. In the interpolation, a similar inaccuracy is observed as for Sets I-IV for 12 collocation points. This could be up to an error of 3bp in the volatility.

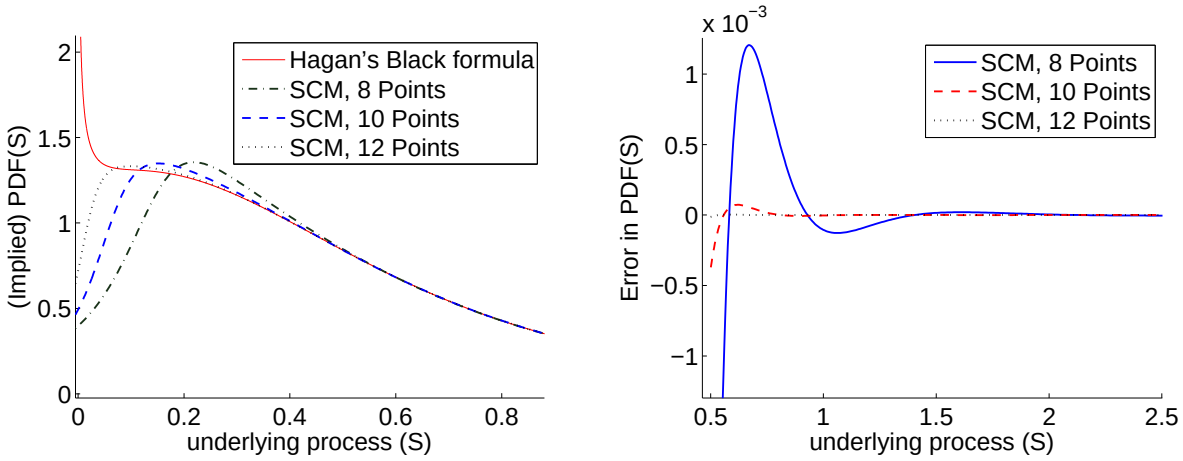

(a) (Implied) probability density functions.

(b) Errors made in new probability density functions.

Figure 4.17: Set V of Table 4.10.

In the case of Set VI, the approach was not able to guarantee a martingale process for 8 and 10 collocation points. This mostly has to do with the fact that where the Hagan's formulas generate arbitrage a probability density function was needed that was almost equal to zero. Since the probability density function implied by the SCM is equal to $f_x(x)\left(\frac{\mathrm{d}g_N}{\mathrm{d}x}(x)\right)^{-1}$, it is required that $\frac{\mathrm{d}g_N}{\mathrm{d}x}(x) \gg 1$ in this area. This could be obtained in this case with a higher order polynomial. Setting a higher $\zeta_{\max}$ could provide the martingale property too for 8 and 10 collocation points, but then the M-SCM still gives an unsatisfactory result for the probability density function, i.e. the probability density function was altered too much.

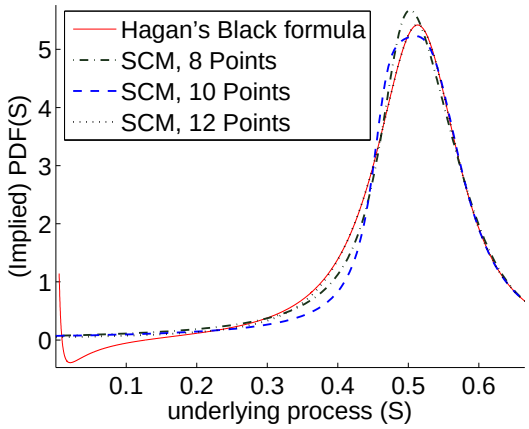

(a) (Implied) probability density functions for Set VI.

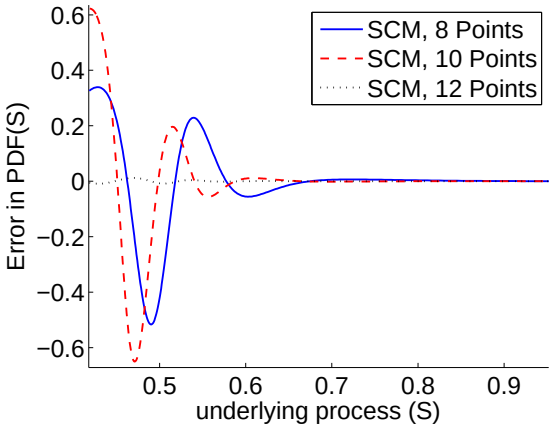

(b) Errors made in new probability density functions for Set VI.

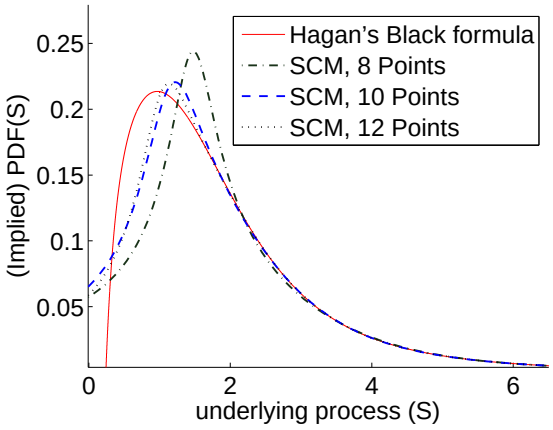

(c) (Implied) probability density functions for Set VI.

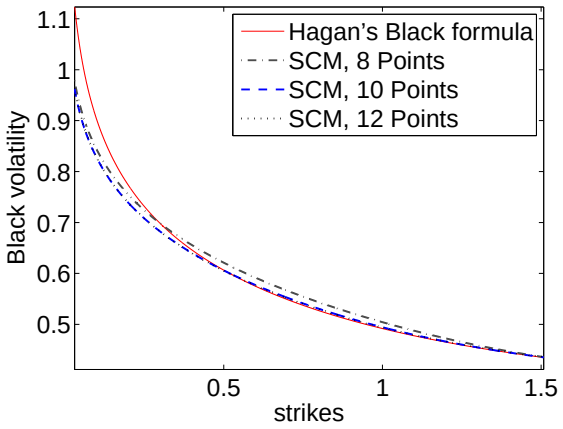

(d) Volsurfaces for Set VII.

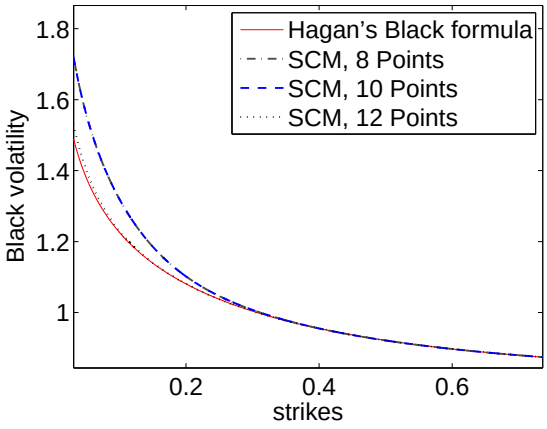

(e) Volsurfaces for Set V.

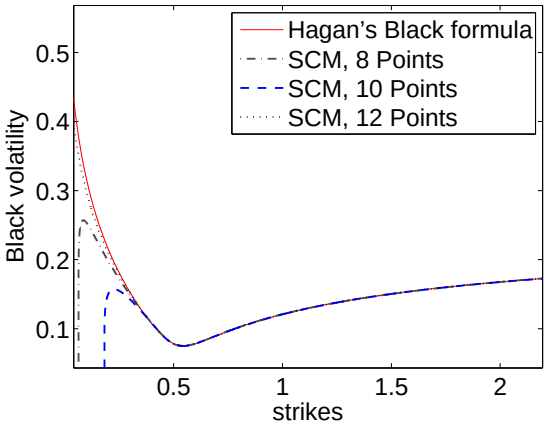

(f) Volsurfaces for Set VI.

Figure 4.18: Sets are taken from Table 4.10.

4.10 Discussion of the approach

The SCM maps an expensive distribution to a simpler distribution and it works accurately for processes that are well-defined [26]. As can be observed from this chapter, this mapping can be used to give satisfactory results for a process that is not well-defined like those arising from Hagan's formulas by correcting its probability density function. This mapping is approximated by a Lagrange polynomial, which was compared to other standard interpolation techniques. This showed that the Lagrange polynomial was the most accurate interpolation technique. For the simpler distribution in the mapping, a normal distribution has been compared to a gamma distribution. It has been shown the gamma distribution can provide more accurate results if the distribution of the process implied by Hagan's formulas is strongly skewed.

The approximation technique should be monotonic to guarantee that this approach is arbitrage-free. Therefore, a computationally rapid algorithm was developed to verify the monotonicity of a polynomial. With this algorithm an extension of this approach was developed to include the martingale property to make this approach completely arbitrage-free. With an explicit analytical expression and practical problems, the convergence and stability of this approach has been shown.

Furthermore, the M-SCM is computationally rapid[9], does not become more expensive for longer maturities, Hagan's formulas can still be used and for most practical problems with Hagan's formulas, the M-SCM seems suitable to remove the arbitrage. This will be verified by calibrating all the approaches discussed in this thesis in the next chapter.

[9]In matlab, the average CPU time was 100 ms. for 12 collocation points.

Chapter 5

Calibration to market data

This chapter compares the approaches discussed in this thesis by calibrating them to a set of market data. These are the approaches of Hagan et al. [29], Antonov et al. [3], Grzelak et al. [25] and Hagan et al. [30]. These approaches will be abbreviated as Hagan's Black formula, uncorrelated Antonov, SCM-Hagan and Hagan's AF SABR respectively. The SCM will be used to remove the arbitrage in Hagan's Black formula. Therefore, it will be abbreviated as SCM-Hagan.

It is chosen to focus on 1Y1Y, 2Y2Y, 5Y5Y and 10Y10Y swaptions in the months April, July and December 2014 with the EURIBOR (euro interbank offered rate) as the underlying floating rate. The standard conventions will be used for the swaptions in the euro market. The focus will be on the stability and the extrapolation of the Black volatility curve of the approaches. Only Black volatilities are considered in this chapter, since only positive rates are considered. Section 5.1 describes the market data, Section 5.2 describes the calibration procedure, Section 5.3 presents results and Section 5.4 gives a conclusion on the results.

5.1 Description of the market data

For the construction of volatility curves the forward swap rates and at-the-money (swaptions where the strike is equal to the forward swap rate) volatilities are used from market data. From the first day of the month the curvature of the volatility curve is extracted from a volatility representation of ING. To produce a volatility curve for the remaining days of the month, it is assumed that the shape of the volatility curve is preserved over time. This means that the absolute difference between the volatility at a strike and the at-the-money volatility remain the same on a grid of strikes relative to the forward swap rate. See Figure 5.1 as an example for a 10Y10Y swaption from April 2014. It is assumed that the right figure remains constant over time. The strikes relative to the forward swap rate will be referred to as the relative strikes. The volatilities relative to the at-the-money volatility will be referred to as the volatility add-ons.

To be more precise, the volatility add-ons for the Black volatilities are computed on the first day of the month. The following grid of relative strikes (%) is used:

$$\bar{K} = \{\bar{K}_i\}_{i=1}^{19} = \{-5, -4, -3, -2.5, -2, -1.5, -1, -0.5, -0.25, 0, 0.25, 0.5, 1, 1.5, 2, 2.5, 3, 4, 5\} \tag{5.1}$$

If S_0 is the swap rate, the quoted market volatilities are given on the strikes $S_0 + \bar{K}$. For calibration, only positive strikes and rates are used. Thus a subset of $\bar{K}$ is used, such that

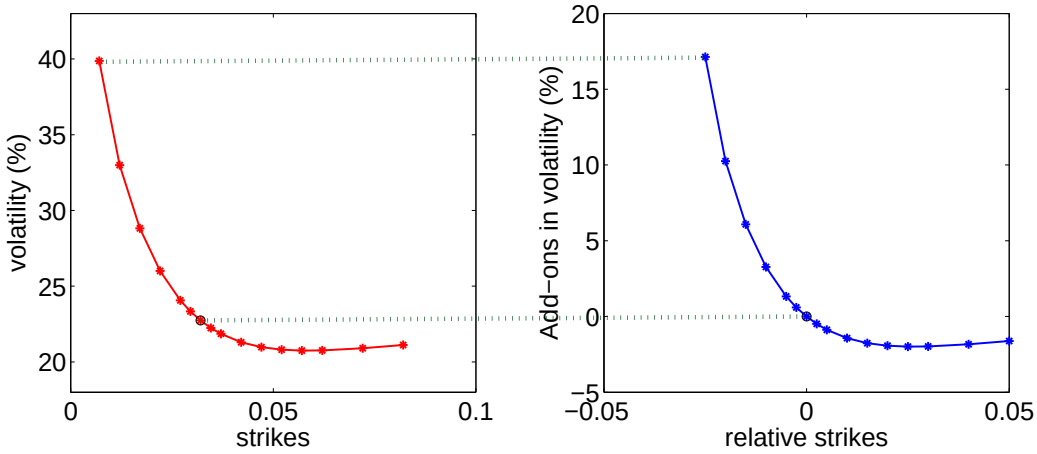

Figure 5.1: Volatility curve (left) and relative volatility curve (right).

$S_0 + \bar{K} > 0$. The strikes for which the market quotes are given, are defined by $K_i := S_0 + \bar{K}_i$. The relative volatility add-ons for the Black volatility are computed by:

$$\bar{\sigma} \;=\; \{\bar{\sigma}_i\}_{i=1}^{N} \;=\; \left\{\sigma_1^1 - \sigma_*^1, \ldots, \sigma_n^1 - \sigma_*^1\right\}, \tag{5.2}$$

where σ_*^m is the at-the-money volatility on the m-th day of the month, σ_i^m is the volatility corresponding to strike K_i and N is the number of elements in the set $\{\bar{K}_i \in \bar{K} : S_0 + \bar{K}_i > 0\}$, i.e. the relative strikes which give an absolute positive strike. The market volatilities for the remaining days of the month are computed by:

$$\sigma_i^m = \sigma_*^m + \bar{\sigma}_i.$$

5.2 Calibration procedure

For each approach, the SABR model parameters α, β, ρ and ν have to be chosen such that they closely match the market data. The difference in the volatilities implied by the market and the approaches will be minimized, which has the advantage that the volatility curve is captured best compared to fitting it to the option prices. This will be done by solving a minimization problem, where function Tar is minimized:

$$\min_{\alpha,\beta,\rho,\nu} \mathrm{Tar}(\alpha,\beta,\rho,\nu) = \frac{1}{n}\sqrt{\sum_{i=1}^{n}\left(\omega_i\left\{\sigma^{\mathrm{Market}}(K_i) - \sigma^{\mathrm{Model}}(K_i)\right\}\right)^2}, \tag{5.3}$$

where α, β, ρ, ν are the model parameters of the SABR model, K_i are the strikes for which a market volatility is given, $\sigma^{\mathrm{Market}}(K_i)$ is the market volatility corresponding to strike K_i, $\sigma^{\mathrm{Model}}(K_i)$ is the volatility implied by the model corresponding to strike K_i and ω_i are weights. Function Tar will be referred to as the target function. The weights ω_i are given by

$$\omega_i = \frac{\sigma^{\mathrm{Market}}(K_1)}{\sigma^{\mathrm{Market}}(K_i)}.$$

The weight ω_i ensures that the relative error for each volatility is compared equally. Therefore, the shape of the volatility curve will be fitted accurately. As can be observed from Figure 5.1, the volatilities can differ up to double the value for a different strike. Minimizing a two norm

($\omega_i = 1$ for each i) would value the volatility that is the largest as the most important and captures therefore the market quotes less accurately. After α, β, ρ and ν are fitted for each model, α is re-calibrated to fit the at-the-money volatility with an error of less than 1bp.[1] This strike is traded the most and therefore important to match exactly.

5.3 Results

Hagan's Black formula, uncorrelated Antonov, SCM-Hagan and Hagan's AF SABR are compared by fitting the approaches to the market data by solving the minimization problem described in the previous section.

For SCM-Hagan, the virtual collocation technique will be used, i.e. M-SCM as discussed in Section 4.9. Furthermore, twelve collocation points will be used in this approach. For Hagan's AF SABR it is chosen to set $\frac{z^+}{\sqrt{T}} = 6$, i.e. $S_{\max} = S(z^+ = 6)$.[2] Setting $\frac{z^+}{\sqrt{T}} = 4$ could undervalue call prices for high strikes due to a the fact $S_{\max}$ is chosen too small.[3]. This could affect the calibration. Furthermore, 200 points are used for the discretization in the spatial direction and a time step of $\Delta t = 0.1$, i.e. one-tenth of a year, is used. Due to the analysis of Section 3.1, this is sufficiently accurate and computationally rapid for calibration. Table 5.1 gives an overview of the main ideas behind the approaches and the settings of the approaches.

Method	Main idea	Specific sections
Hagan's Black formula	Map the SABR model to the volatility in Black's model.	-
Hagan's AF SABR	Reduction of dimensionality in the dynamics in the SABR process.	$\frac{z^+}{\sqrt{T}} = 6,\ J = 200,\ \Delta t = 0.1$
Uncorrelated Antonov	Exact solution of the SABR model for $\rho = 0$.	-
SCM-Hagan	Removes arbitrage in Hagan's formulas by altering the underlying probability density function.	12 collocation points, M-SCM.

Table 5.1: Settings for the approaches.

5.3.1 Stability and interpolation

Figure 5.2 presents the calibrated parameters of β and ρ for Hagan's AF SABR during the month of April for the 5Y5Y swaptions. As can be observed, these parameters do not remain stable over time. Therefore, the day-to-day change in β is constrained to 0.05 in the remainder of this chapter, i.e. if β_n is the calibrated value of the parameter β on the nth day, the calibration of

[1] Hagan's Black formula can match the at-the-money exactly by solving a polynomial equation of maximum order three. To equally compare the approaches it is chosen not to use this benefit of Hagan's Black formula. Each approach is re-calibrated to minimize the target function by only calibrating α and using the at-the-money volatility.

[2] For the definition of z and S := S(z) see Equation (3.4).

[3] If $S_{\max}$ is chosen to be too small, this impacts the extrapolation of the volatility curve for high strikes. It can undervalue the volatility curve implied by Hagan's AF SABR model, since $\mathbb{E}\left[(S_T - K)^+\right] = \int_K^\infty (s-K) f(s)\,\mathrm{d}s \approx \int_K^{S_{\max}} (s-K)\,\mathrm{d}s$.

β on the $(n+1)$th day is limited to the domain $[\max\{\beta_n - 0.05, 0\}, \min\{\beta_n + 0.05, 1\}]$. This constraint is based on a heuristic rule which is fair compared to the other approaches. For the other approaches, this was not needed.

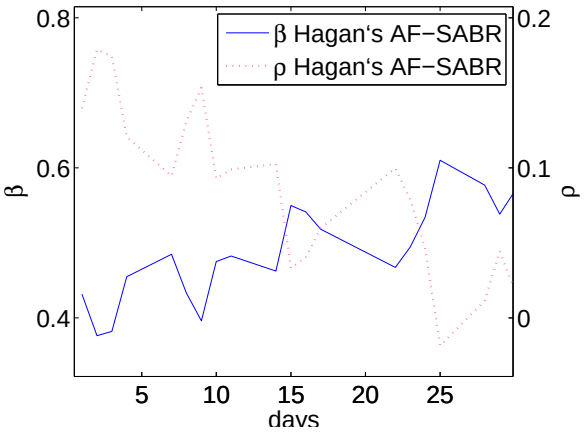

Figure 5.2: Calibration of Hagan's AF-SABR: time series of β and ρ.

Figures 5.3a - 5.3d present the calibrated parameters α, β, ρ and ν respectively for a 5Y5Y swaption in April 2014 for all approaches. There are no calibrated parameters for SCM-Hagan, since it will only be applied to Hagan's Black formula to remove the arbitrage. For all approaches the parameters remain stable over time. For the other test periods and swaptions in scope, similar behavior was observed for the stability of the parameters. The results are therefore limited to April in the remainder of the thesis. The time series for the parameters α, β and ν are similar for each approach. For example, if β increases from day n to day $n+1$ for one approach, all approaches show this behavior for the calibrated parameter. The parameters β and ρ are more stable over time in Hagan's AF SABR due to the constraint for β. This holds especially for β. It did not change significantly compared to the other approaches for every type of swaption. It was almost constant over time as can be observed from Figure 5.3b. For other test periods in scope there was not a change of more than 0.05 in the overall change of β, i.e. the absolute difference between the highest and lowest calibrated value for β for Hagan's AF SABR was 0.05 for a fixed month and swaption. This is due to the effect that β and ρ have a similar impact on the volatility curve.

Figures 5.4a and 5.4b display the value of the target function for the 5Y5Y and 10Y10Y swaption in April. Hagan's Black formula and SCM-Hagan give similar fit errors when fitting the market data for the 5Y5Y swaption. For the 10Y10Y swaption the value of the target function of SCM-Hagan is up to double the value of the target value of Hagan's Black formula. For most days, the value of the target function of SCM-Hagan gives a similar or lower value than uncorrelated Antonov and Hagan's AF SABR.

In the special case that Hagan's Black formula fits a ρ close to zero, uncorrelated Antonov gives a similar accuracy in fit. On the other hand, if Hagan's Black formula calibrates ρ not near zero, uncorrelated Antonov could not fit the shape of the volatility curve as accurately as Hagan's Black formula. Due to the constraint in the variation of β for Hagan's AF SABR, this approach fits the market data less accurately. The value for the target function is up to ten times higher than the one implid by Hagan's Black formula and five times than the one implied by

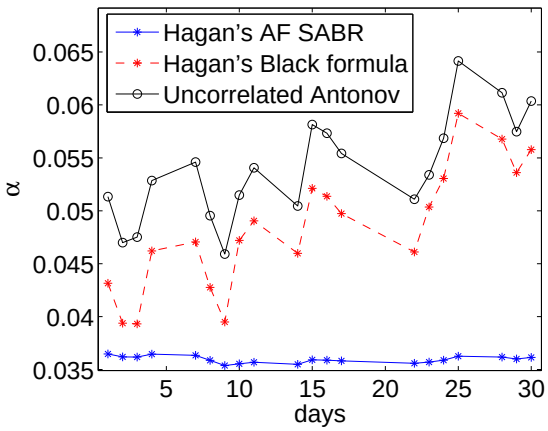

(a) α.

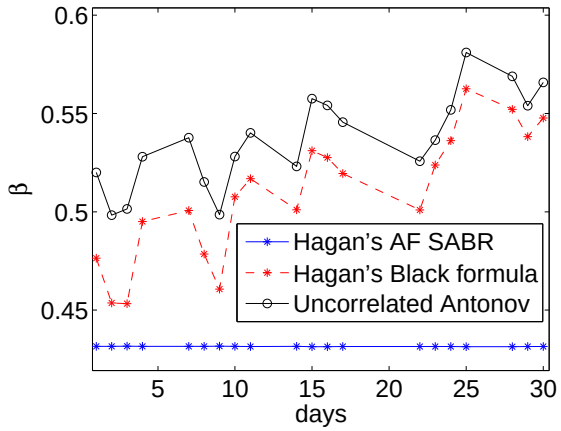

(b) β.

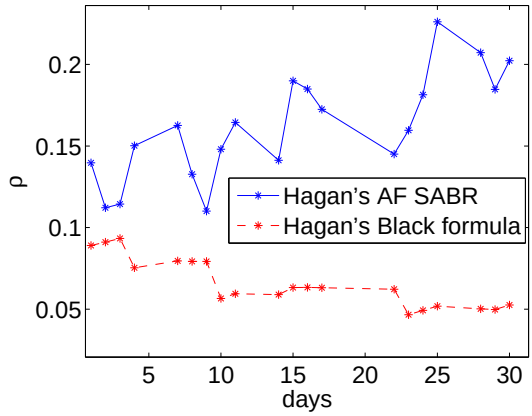

(c) ρ.

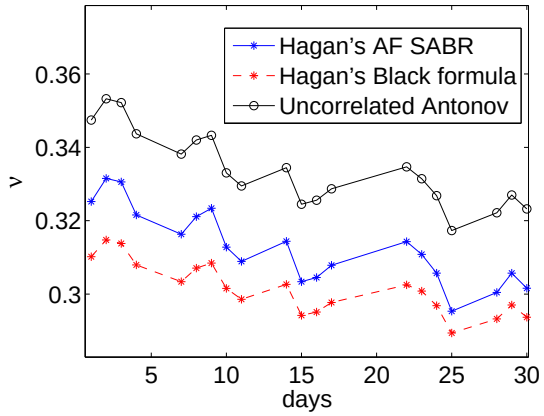

(d) ν.

Figure 5.3: Times series of model parameters.

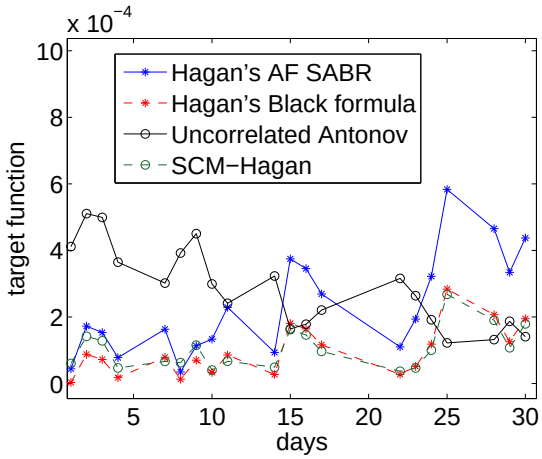

(a) 5Y5Y swaption, April.

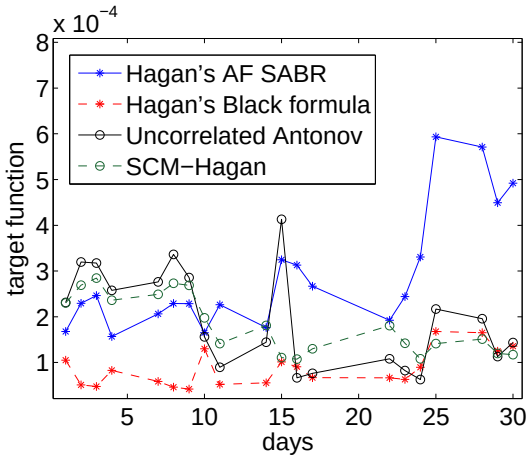

(b) 10Y10Y swaption, April.

Figure 5.4: Times series of the target function.

SCM-Hagan. Without this constraint, it could be fitted as accurately as Hagan's Black formula and the SCM-Hagan.

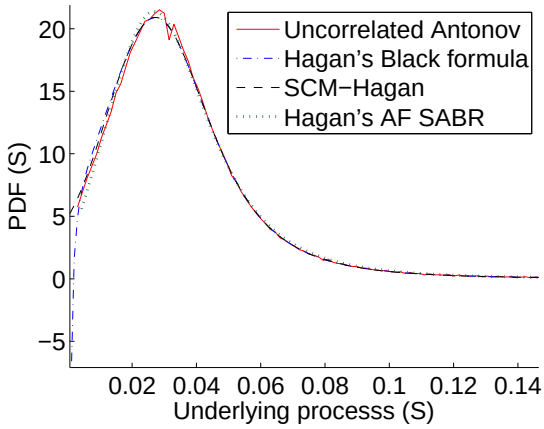

(a) Fitted underlying probability density function.

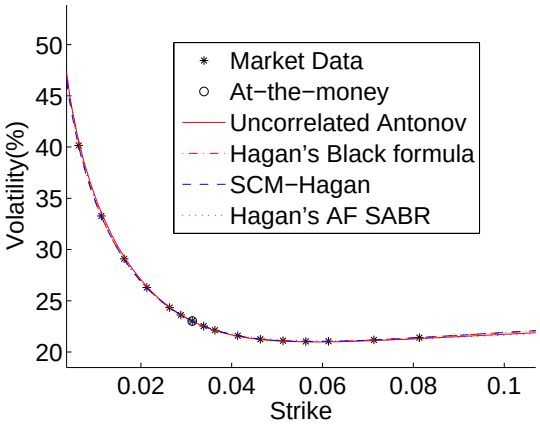

(b) Volatility curve.

Figure 5.5: 10Y10Y swaptions, April 15th.

If all approaches calibrate with a similar precision, they imply approximately the same underlying probability density function and volatility curve.[4] No general conclusion can be made regarding in which manner they differ in the interpolation of the market data. Figure 5.5a presents the underlying probability density functions of the approaches when fitted to the market data with a different value of the target function. The underlying probability density functions of the approaches are presented when they were fitted to a 10Y10Y swaption for the 15th of April. For this example, Hagan's AF-SABR and uncorrelated Antonov could not fit the market quotes as well as the other approaches. The underlying probability density functions implied by the approaches and the volatility curve match closely, just like the volatility curve, see Figure 5.5b. This can be explained, as each approach originate from the SABR model. Furthermore, Hagan's Black formula generates arbitrage in this example.

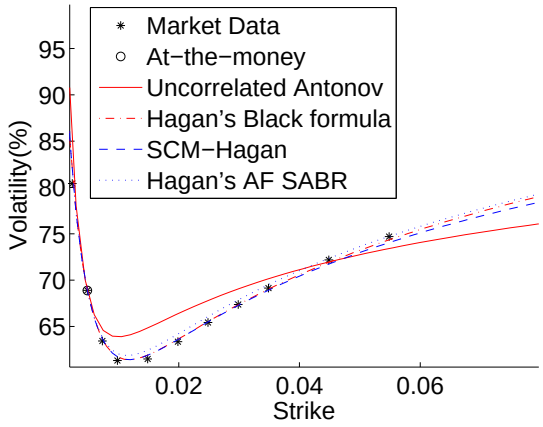

(a) 1Y1Y swaption.

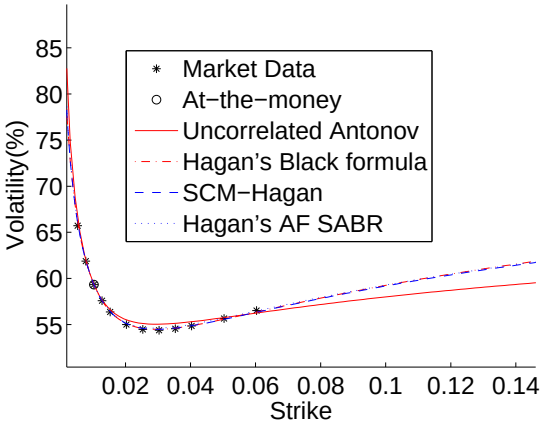

(b) 2Y2Y swaption.

Figure 5.6: Volatility curve for swaptions, April 15th.

[4]Uncorrelated Antonov has an inaccurate approximation for butterfly options near at-the-money due to the one-dimensional approximation. This results in an inaccurate approximation of the probability density function.

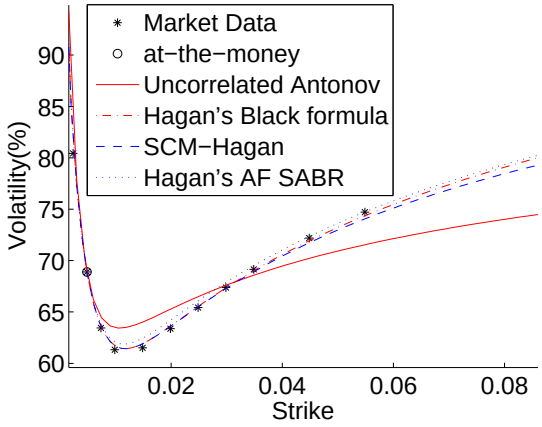

Figure 5.7: Volatility curve for 1Y1Y swaptions, April 15th.

Uncorrelated Antonov could not fit swaptions with short maturities accurately compared to the other approaches. See Figure 5.6b and 5.6a for the 15th of April as an example. For short maturities, uncorrelated Antonov needs the effect of the correlation parameter ρ to fit the volatility curve accurately.

It is investigated whether uncorrelated Antonov could produce a better fit where the at-the-money volatility is still closely matched for the short maturities. Therefore, β and ν are calibrated in the target function. Within this loop of calibrating β and ν, α is calibrated for a given β and ν to match the at-the-money volatility. Figure 5.7 gives the resulting volatility curve of uncorrelated Antonov compared to the other approaches. This procedure did not give a more accurate result compared the original calibration procedure and it led to unstable time series of the parameters. Therefore, it can be concluded that uncorrelated Antonov cannot be fitted accurately to the market quotes for short maturities due to the missing effect of the correlation. For the remainder of the thesis, the calibration procedure is therefore limited to the procedure as described in Section 5.2.

To investigate the errors of each approach in the volatility and the prices on the market quotes, Tables 5.2 and 5.3 present the errors in the volatilities and prices for the 1Y1Y payer swaption on the 30th of April and the 10Y10Y swaption on the 15th of April respectively. By prices the values of a payer-swaption are meant.

For the 1Y1Y swaption, Hagan's Black formula and SCM-Hagan are the most accurate for swaptions with strikes near at-the-money (near the swap rate). Uncorrelated Antonov has the largest mismatch for the market quotes for all strikes. This can be up to 335bp in the volatility. Hagan's Black formula and SCM-Hagan perform the best on average. In the prices of the 1Y1Y payer swaptions there is at most a mismatch of 0.35bp in price for uncorrelated SABR and 0.05bp in price for the other approaches.

For the 10Y10Y swaption Hagan's Black formula and SCM-Hagan are again most accurate for swaptions with strikes at-the-money (near the swap rate). Uncorrelated Antonov could fit the market quotes reasonably, for relative strikes higher than -1%. Threre it has a maximum error of 10bp in the volatility and 2.5bp in price. Hagan's Black formula and SCM-Hagan perform the best on average, but each aproach gave satisfactory results. Only Hagan's Black formula gave an unsatisfactory result by implying arbitrage for low strikes in the form of an implied negatively

valued probability density function. In the prices for the 10Y10Y payer swaptions a mismatch is observed of at most 3.5 bp in price for uncorrelated SABR, 3 bp in price for Hagan's AF SABR and 1 bp in price for the Hagan's Black formula and SCM-Hagan.

Relative strikes (%)	Market volatility (%)	Hagan's Black formula (bp)	SCM-Hagan (bp)	Hagan's AF SABR (bp)	Uncorrelated Antonov (bp)
0.00	68.90	-0.8	-1.3	-0.5	0.2
0.25	63.44	17.8	17.4	36.5	124.0
0.50	61.33	39.9	39.2	75.9	256.0
1.00	61.50	41.1	39.7	93.9	335.0
1.50	63.37	24.9	22.3	81.0	300.0
2.00	65.43	9.8	5.2	64.4	237.0
2.50	67.38	-2.37	-9.46	49.5	168.0
3.00	69.14	-12.0	-22.3	36.7	101.0
4.00	72.19	-26.2	-45.0	16.5	-22.0
5.00	74.72	-36.0	-65.7	1.3	-130.0
Average of absolute difference		21.1	26.8	45.6	167.2

(a) 1Y1Y swaption, April 30th, 2014.

Relative strikes (%)	Market volatility (%)	Hagan's Black formula (bp)	SCM-Hagan (bp)	Hagan's AF SABR (bp)	Uncorrelated Antonov (bp)
-2.50	40.15	10.8	-11.9	29.2	42.0
-2.00	33.28	-6.3	-7.8	6.7	31.4
-1.50	29.10	-5.6	-5.4	-4.7	20.1
-1.00	26.29	-2.8	-2.7	-7.5	10.1
-0.50	24.34	-0.5	-0.5	-4.8	3.0
-0.25	23.61	0.2	0.2	-2.4	0.6
0.00	23.02	0.4	0.4	0.1	-0.7
0.25	22.53	0.8	0.9	2.8	-2.5
0.50	22.13	0.9	0.9	5.1	-3.4
1.00	21.58	0.6	0.6	8.3	-4.0
1.50	21.26	0.1	0.1	9.4	-4.1
2.00	21.09	-0.3	-0.3	8.8	-4.2
2.50	21.03	-0.6	-0.6	6.9	-4.4
3.00	21.04	-0.6	-0.6	4.2	-5.0
4.00	21.18	-0.2	-0.1	-2.5	-6.8
5.00	21.40	0.9	0.9	-9.6	-9.1
Average of absolute difference		2.0	2.1	7.0	9.5

(b) 10Y10Y swaption, April 15th, 2014.

Table 5.2: Difference in volatility compared to the market quotes for each approach.

General comments

For some days, Hagan's AF SABR fitted with $\beta \approx 1$. This was the case for the 1Y1Y swaptions in particular. The singularity in the PDE in the approach by Le Floch et al. [15] is more pronounced in this case, especially for strikes near zero which can give numerical issues. It might be better to cap β when fitting to market data, e.g. by constraining β to be smaller than

Relative strikes (%)	Market price (bp)	Hagan's Black formula (bp)	SCM-Hagan (bp)	Hagan's AF SABR (bp)	Uncorrelated Antonov (bp)
0.00	0.1306	-0.0015	-0.0023	-0.0009	0.0004
0.25	0.0567	0.0326	0.0317	0.0667	0.2280
0.50	0.0253	0.0540	0.0532	0.1030	0.3540
1.00	0.0069	0.0256	0.0248	0.0594	0.2250
1.50	0.0027	0.0079	0.0071	0.0263	0.1060
2.00	0.0014	0.0018	0.0010	0.0122	0.0486
2.50	0.0008	-0.0003	-0.0011	0.0061	0.0219
3.00	0.0005	-0.0010	-0.0019	0.0031	0.0090
4.00	0.0003	-0.0012	-0.0021	0.0008	-0.0010
5.00	0.0002	-0.0011	-0.0020	0.0000	-0.0037
Average of absolute difference		0.012	0.012	0.0279	0.0996

(a) 1Y1Y swaption, April 30th, 2014.

Relative strikes (%)	Market price (bp)	Hagan's Black formula (bp)	SCM-Hagan (bp)	Hagan's AF SABR (bp)	Uncorrelated Antonov (bp)
-2.50	21.91	0.60	-0.66	1.63	2.35
-2.00	18.37	-0.69	-0.85	0.73	3.47
-1.50	15.10	-0.95	-0.91	-0.79	3.41
-1.00	12.17	-0.63	-0.62	-1.71	2.32
-0.50	9.65	-0.14	-0.14	-1.33	0.84
-0.25	8.55	0.06	0.06	-0.70	0.18
0.00	7.56	0.13	0.14	0.02	-0.22
0.25	6.69	0.28	0.28	0.96	-0.81
0.50	5.91	0.29	0.30	1.70	-1.12
1.00	4.63	0.19	0.20	2.77	-1.35
1.50	3.67	0.03	0.04	3.07	-1.35
2.00	2.94	0.10	-0.09	2.73	-1.29
2.50	2.38	-0.17	-0.16	2.00	-1.27
3.00	1.96	-0.17	-0.16	1.12	-1.32
4.00	1.37	-0.03	-0.03	-0.56	-1.53
5.00	1.00	0.17	0.17	-1.80	-1.71
Average of absolute difference		0.29	0.30	1.47	1.53

(b) 10Y10Y swaption, April 15th, 2014.

Table 5.3: Difference in price for payer swaptions compared to the market quotes for each approach.

0.95.

The prices of swaptions with a short maturity can be fitted best by Hagan's formulas. Only in a few exceptions did Hagan's Black formula resulted in a process with an underlying negatively valued probability density function. In these cases, the negatively valued probability density function was fixed with SCM-Hagan in a satisfactory fashion without decreasing the value of target function significantly. This can be explained by the fact that Hagan's formulas were originally derived only for options with short maturities [29]. Therefore, the underlying process is almost equal to the SABR process and the SCM can be applied to the well-defined part to

get a naturally well-defined extension based on an accurate approximation of the SABR model.

Swaptions with a long maturity could most often be almost fitted equally by all approaches. In general, Hagan's formulas generated arbitrage by an implied underlying process with a negatively valued probability density function. Applying SCM-Hagan generally resulted in a new underlying arbitrage-free probability density function with only a small impact on the volatility curve. In general, the volatility curve implied by SCM-Hagan had a lower value of the target function than the other two approaches.

5.3.2 Extrapolation

In the previous section it was observed that all the considered approaches gave similar results in the interpolation of the strike interval, with the exception of uncorrelated Antonov for the short maturities. It is investigated how the approaches perform in the extrapolation of the strike interval. To do so, for each approach the volatility add-ons for relative strikes in the extrapolation are computed. With volatility add-on the difference between the volatility and the at-the-money volatility is meant. For example, see Figures 5.8a and 5.8b for the volatility add-ons for 10Y10Y swaptions in April with strikes near zero and relatively high strikes. S_0 denotes the value of the swap rate. As a low strike $S_0 - 3\%$ is taken, as a high strike $S_0 + 10\%$, where $S_0 \approx 3.2\%$ for April 2014. As a reference, the volatility for $K = S_0$ on the first day of the month was 22.7%.

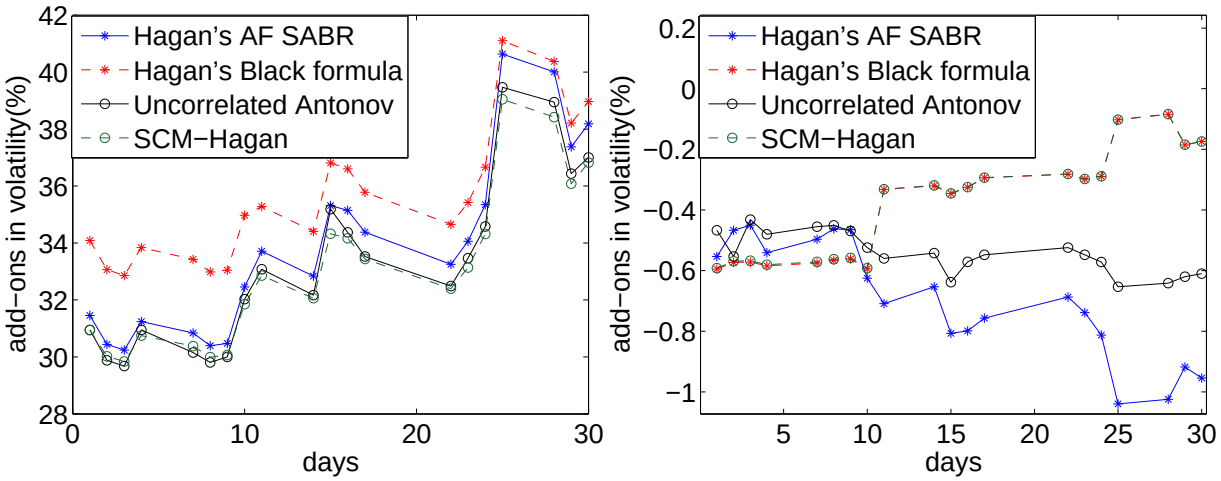

(a) Low strikes, $K = S_0 - 3\%$.

(b) High strikes, $K = S_0 + 10\%$.

Figure 5.8: Volatility add-on, 10Y10 swaption April.

The approaches gave a similar volatility add-on for low strikes. Only Hagan's formulas gave a higher volatility add-on for long maturities for low strikes. It was not arbitrage-free in these cases. In Figure 5.8a this difference is approximately 2%. For high strikes the volatility curves were very similar in most cases. The differences are within 1%, which is small for such a high strike. Uncorrelated Antonov could suffer for short maturities and therefore gives a high or low extrapolation of the volatility curve compared to the other approaches, but in these cases it could also not fit the market data accurately. This is mainly due to the constraint $\rho = 0$ which guarantees that the approach is arbitrage-free.

day	Payer swaption price with a strike equal to zero (bp)	Hagan's Black formula (bp)	SCM-Hagan (bp)	Hagan's AF SABR (bp)	Uncorrelated Antonov (bp)
1	222.7	2.87	2.86	2.85	3.65
2	230.6	3.34	3.34	3.37	4.27
3	222.2	2.61	2.61	2.65	3.37
4	208.4	1.49	1.49	1.53	1.99
7	206.5	1.32	1.32	1.36	1.79
8	212.4	1.63	1.62	1.68	2.20
9	219.4	2.09	2.09	2.15	2.78
10	208.7	1.38	1.37	1.42	1.87
11	204.4	1.13	1.12	1.17	1.55
14	208.1	1.36	1.36	1.41	1.85
15	196.9	0.66	0.66	0.69	0.96

(a) Prices 2Y2Y receiver swaptions for low strikes, $K = S_0 - 0.9\%$.

day	Payer swaption price with a strike equal to zero (bp)	Hagan's Black formula (bp)	SCM-Hagan (bp)	Hagan's AF SABR (bp)	Uncorrelated Antonov (bp)
1	222.7	0.415	0.408	0.416	0.291
2	230.6	0.295	0.289	0.286	0.192
3	222.2	0.328	0.322	0.318	0.224
4	208.4	0.396	0.390	0.392	0.294
7	206.5	0.387	0.382	0.384	0.290
8	212.4	0.281	0.277	0.276	0.198
9	219.4	0.232	0.228	0.224	0.155
10	208.7	0.302	0.297	0.297	0.217
11	204.4	0.362	0.357	0.359	0.271
14	208.1	0.324	0.320	0.321	0.237
15	196.9	0.408	0.402	0.411	0.320

(b) Prices 2Y2Y payer swaptions for high strikes, $K = S_0 + 10\%$.

Table 5.4: Prices payer and receiver 2Y2Y swaptions.

To investigate the price impact on a swaption on these strikes, Tables 5.4 and 5.5 present the prices of payer and receiver swaptions for the low and high strikes respectively for 2Y2Y and 10Y10Y swaptions from 1st until 15th of April. The remaining days gave similar results. The second column presents the price of a payer swaption with strike 0 as a reference value. The value of the payer swaption is presented for the relatively high strike and the receiver swaption for the relative low strike, such that the differences are more pronounced. The value of the other swaptiontype can be determined by put-call-parity.

For the 2Y2Y swaption, this was done at relative strikes $S_0 - 0.9\%$ and $S_0 + 10\%$, since the swap rate was around 1%. The difference in price was at most 1bp for low strikes and 0.1bp for high strikes for the 2Y2Y swaptions. For the 10Y10Y swaptions Hagan's Black formula was up to 6 bp higher than the other approaches for low strikes. The other approaches did not differ more than 1.5 bp. For the high strikes, Hagan's Black formula and SCM-Hagan could be up to 4 bp higher than the other approaches, but in general with a difference less than 1bp.

day	Payer swaption price with a strike equal to zero (bp)	Hagan's Black formula (bp)	SCM-Hagan (bp)	Hagan's AF SABR (bp)	Uncorrelated Antonov (bp)
1	2715	26.0	20.5	21.3	20.7
2	2734	29.7	23.5	24.4	23.6
3	2740	30.2	24.0	24.8	24.1
4	2722	26.4	20.8	21.7	21.2
7	2730	27.5	21.8	22.6	21.8
8	2738	28.8	22.8	23.6	22.7
9	2735	28.2	22.4	23.2	22.6
10	2700	21.9	17.2	18.1	17.5
11	2683	17.5	14.4	15.4	14.7
14	2695	19.5	16.2	17.2	16.6
15	2662	14.2	11.7	12.7	12.5

(a) Prices 10Y10Y receiver swaptions for low strikes, $K = S_0 - 3\%$.

day	Payer swaption price with a strike equal to zero (bp)	Hagan's Black formula (bp)	SCM-Hagan (bp)	Hagan's AF SABR (bp)	Uncorrelated Antonov (bp)
1	2715	29.5	29.5	29.8	30.6
2	2734	28.8	28.8	29.7	29.1
3	2740	28.1	28.1	29.1	29.3
4	2722	28.6	28.6	29.0	29.5
7	2730	27.3	27.3	27.9	28.3
8	2738	26.2	26.2	27.0	27.2
9	2735	25.8	25.8	26.5	26.6
10	2700	27.5	27.5	27.3	28.1
11	2683	30.5	30.5	27.4	28.6
14	2695	30.0	30.1	27.3	28.3
15	2662	31.6	31.6	27.7	29.1

(b) Prices 10Y10Y payer swaptions for high strikes, $K = S_0 + 10\%$.

Table 5.5: Prices payer and receiver 10Y10Y swaptions.

The difference in the volatility add-ons is further investigated by computing vega, i.e. $\frac{\partial V}{\partial \sigma}$ (V denotes the option price). Vega is used in finance to get an indication of the impact on the price by a parallel shift in the volatility curve. Vega is approximated here by

$$\text{Vega}(0, T, K_i, \sigma^{\text{Approach}}) \approx A(0) \frac{C_{\text{Black}}(0, T, K_i, \sigma^{\text{Approach}} + \Delta\sigma) - C_{\text{Black}}(0, T, K_i, \sigma^{\text{Approach}})}{\Delta\sigma},$$

where $A(0)$ is the annuity, $\Delta\sigma = 1\%$, K_i is the strike, T is the maturity of the swaption and C is computed by Black's formula.

Figures 5.9a - 5.10b present the results of the volatility sensitivity of the 2Y2Y and 10Y10Y swaption in April. The focus is on relatively high and low strikes again. This is done for the same relatively high and low strike as for the volatility add-ons.

For comparison, the following value for vega can be computed for $K = S_0$ of the first day at the month in April for the 2Y2Y and 10Y10Y swaption respectively: 1.16% and 320.2%. For

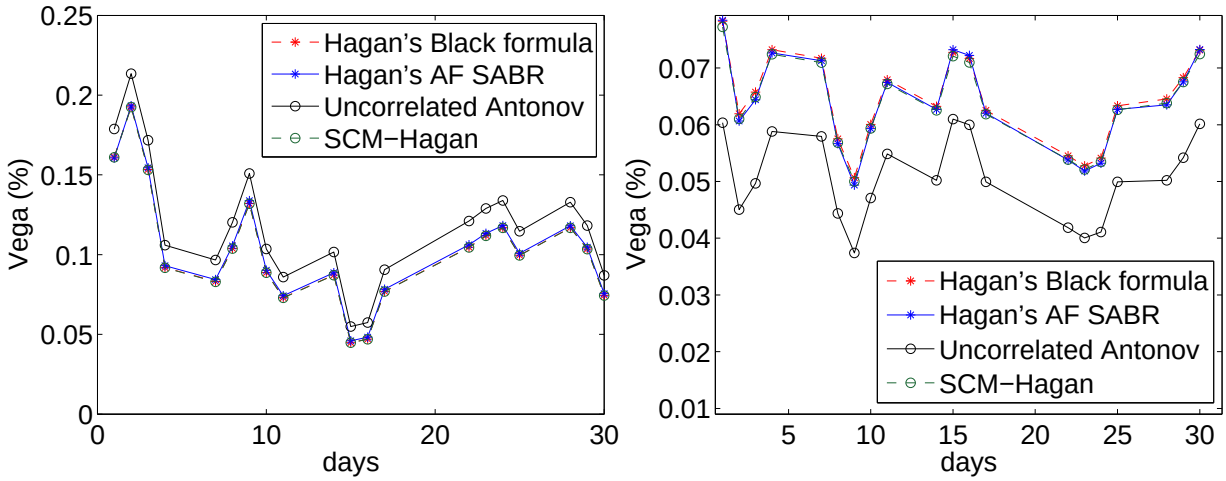

(a) Low strikes, $K = S_0 - 0.9\%$. (b) High strikes, $K = S_0 + 10\%$.

Figure 5.9: Vega, 2Y2Y swaptions, April.

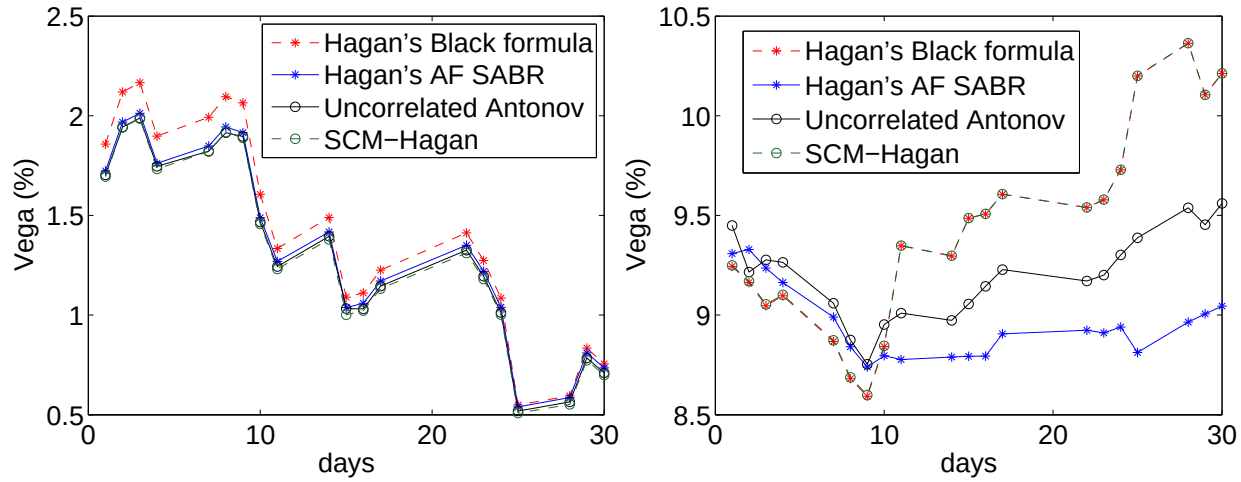

(a) Low strikes, $K = S_0 - 3\%$. (b) High strikes, $K = S_0 + 10\%$.

Figure 5.10: Vega, 10Y10Y swaptions, April.

the short maturity it is observed that each approach gives a similar value to vega and that the differences are relatively small. Only for the approach of uncorrelated Antonov vega is inaccurate for the 2Y2Y swaption compared to the other approaches, since it could not be fitted accurately to the market quotes as discussed. For the long maturities and low strikes Hagan's Black formula gives higher values to vega compared to the other approaches, just like the volatility implied by Hagan's Black formula as investigated earlier. This difference was up to 0.15% higher compared to an average value of 1.5% for the other approaches. For high strikes, Hagan's AF SABR gives lower sensitivities for some days, since it could not fit the market quotes accurately for high strikes. This is only due to the constraint in the model parameters.[5]

[5]The day-to-day change for β is constrained in Hagan's AF SABR such that a stable time series of parameters is obtained. Without this constraint, the approach gave more accurate results, such that the values for vega were more in alignment compared to the other approaches.

To express the impact of the difference in vega in terms of volatilities, the difference in prices between the approaches and Hagan's Black formula are expressed in terms of vega implied by Hagan's Black formula, i.e. the following quantity will be computed:

$$A(0)\frac{C_{\text{Black}}(0,T,K_i,\sigma^{\text{Approach}})-C_{\text{Black}}(0,T,K_i,\sigma^{\text{Hagan's Black formula}})}{\text{Vega}(0,T,K_i,\sigma^{\text{Hagan's Black formula}})},$$

where $A(0)$ is the annuity. This is done for uncorrelated Antonov, Hagan's AF SABR and SCM-Hagan. The quantity will be referred to as the price difference in vega. Vega was approximated by:

$$\frac{\partial C}{\partial \sigma}(0,T,K_i,\sigma^{\text{Approach}}) \approx A(0)\frac{C_{\text{Black}}(0,T,K_i,\sigma^{\text{Approach}}+\Delta\sigma)-C_{\text{Black}}(0,T,K_i,\sigma^{\text{Approach}})}{\Delta\sigma},$$

with $\Delta\sigma = 1\%$ This gives that the price difference in vega is expressed as:

$$\Delta\sigma\frac{C_{\text{Black}}(0,T,K_i,\sigma^{\text{Approach}})-C_{\text{Black}}(0,T,K_i,\sigma^{\text{Hagan's Black formula}})}{C_{\text{Black}}(0,T,K_i,\sigma^{\text{Hagan's Black formula}}+\Delta\sigma)-C_{\text{Black}}(0,T,K_i,\sigma^{\text{Hagan's Black formula}})}.$$

Thus the impact of the difference in vega is expressed in volatilities by this sensitivity.

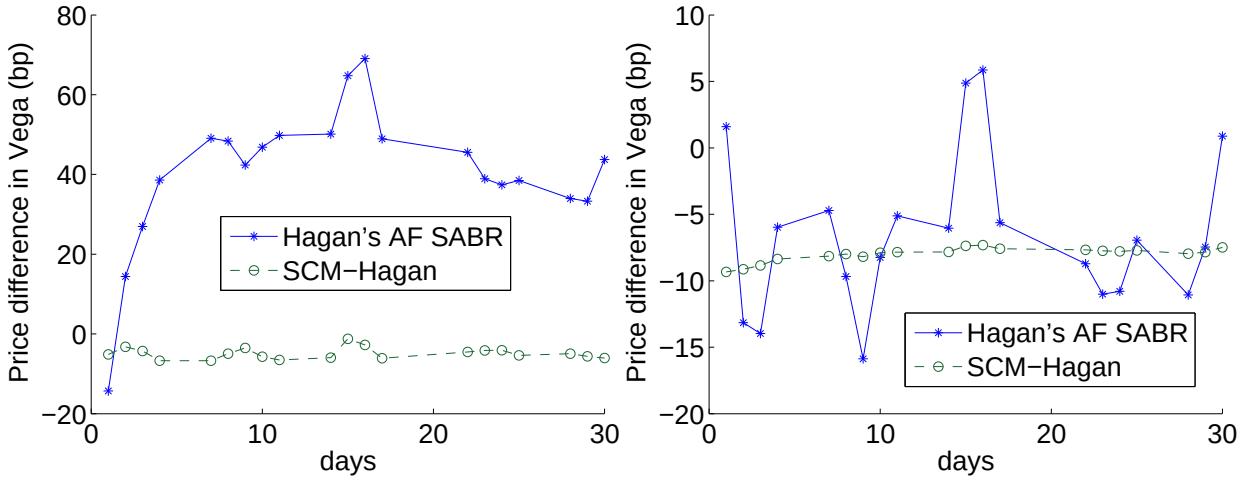

(a) Low strikes, $K = S_0 - 0.9\%$.

(b) High strikes, $K = S_0 + 10\%$.

Figure 5.11: Price difference in vega with Hagan's Black formula, 2Y2Y swaptions, April.

This is done for strikes in the extrapolation region of the market quotes for the 2Y2Y and 10Y10Y swaptions, with the exception of uncorrelated Antonov for the 2Y2Y swaptions, since it could not be fitted accurately to the market volatility curve. The results are presented in Figure 5.11b–5.12b. From these figures, it can be observed that for the 2Y2Y swaptions there is approximately a difference of 0.15% for the high strikes and 0.5% for the low strikes.[6] For the 10Y10Y swaptions there is a difference of 0.5% approximately for the high strikes. These differences are small and can be considered to be in the model risk as all methods fit the market quotes accurately and the arbitrage impact is negligible. The difference for the 10Y10Y swaptions is approximately 2% on average for the low strikes. Hagan's Black formula consistently gives a higher sensitivity (price difference in vega) compared to the other approaches.

[6]Uncorrelated Antonov could give a difference of up to 7% compared to the other approaches for the 2Y2Y swaptions.

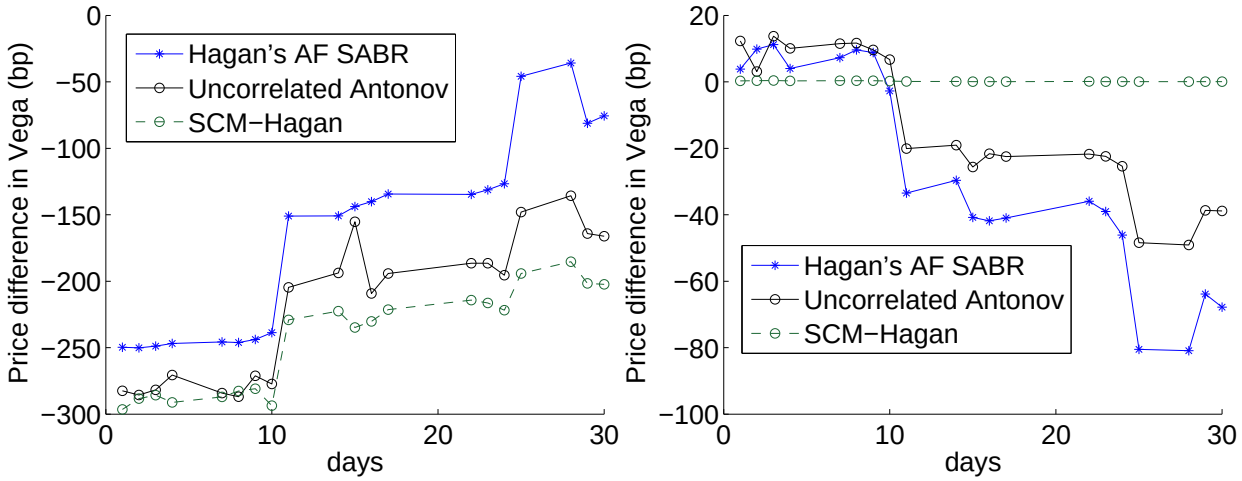

(a) Low strikes, $K = S_0 - 3\%$. (b) High strikes, $K = S_0 + 10\%$.

Figure 5.12: Price difference in vega with Hagan's Black formula, 10Y10Y swaptions, April.

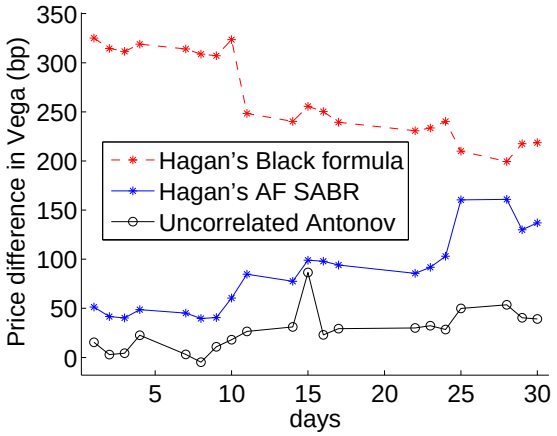

Figure 5.13: Price difference in vega with SCM-Hagan, Low strikes, $K = S_0 - 3\%$.

As a benchmark, the price difference in vega is computed with SCM-Hagan too, i.e.

$$\frac{C_{\text{Black}}(0,T,K_i,\sigma^{\text{Approach}}) - C_{\text{Black}}(0,T,K_i,\sigma^{\text{SCM-Hagan}})}{\text{Vega}(0,T,K_i,\sigma^{\text{SCM-Hagan}})},$$

for Antonov, Hagan's AF SABR and Hagan's Black formula. This is presented only for the 10Y10Y swaption, with low strikes, since there Hagan's Black formula generated arbitrage and gave a higher value to vega. This gives a better indication for the impact of the arbitrage in Hagan's Black formula. As can be observed, the price difference in vega for Hagan's Black formula is approximately 2% higher on average than the arbitrage-free approaches. These differences in volatilities can be used by risk management to estimate uncertainties in the valuation of pricing methods.

5.4 Conclusion

This chapter compared Hagan's formulas, Hagan's AF SABR, uncorrelated Antonov and SCM-Hagan by calibrating them to market data. This gives insights on how they inter- and extrapolate

the market quotes. The approaches are compared on stability of the parameters, accuracy of the fit and the impact of the extrapolation in the prices and sensitivities.

Hagan's AF SABR has shown that if the model parameter β is not fixed or limited in its day-to-day change, the time series of the SABR parameters do not remain stable compared to the other approaches. It has been shown that restricting the model parameter β, gives a stable time series of the SABR parameters. Hagan's AF SABR could still be fitted accurately to the market volatility curve with this constraint, but less accurate compared to Hagan's formulas and SCM-Hagan. For uncorrelated Antonov, it has been shown that the approach did not fit the market volatility accurately due to the limitation of the SABR to the uncorrelated case.

For short maturities, Hagan's Black formula and SCM-Hagan could be fitted best to the market data and was arbitrage-free in almost every case. It was not needed in most cases to apply SCM-Hagan, since for the short maturities Hagan's Black formula was often already arbitrage-free. For the long maturities, Hagan's formulas often generated an excessively high volatility near zero and therefore arbitrage. This could be fixed with the SCM in a satisfactory fashion. Hagan's AF SABR produced similar results as the SCM for low strikes.

SCM-Hagan has shown to be very stable during calibration. Choosing twelve collocation points gave satisfactory results in the sense of an arbitrage-free approach and with a minimal impact on the volatility curve of Hagan's Black formula. The corrected probability density function was very similar to the probability density function of the SABR model and Hagan's AF SABR. It looks like a very natural extension and proved to be stable in market examples. Furthermore, SCM-Hagan is computationally less expensive to calibrate compared to Hagan's AF SABR and uncorrelated Antonov, since it only has to be applied to Hagan's formulas.

Applying uncorrelated Antonov gave the insight that the SABR model seems to have the same stability as Hagan's formulas and SCM-Hagan. This holds also for long maturities. Unfortunately, it still has no fast approach that is stable.[7]

It seems therefore that SCM-Hagan performs better than Hagan's formulas, uncorrelated Antonov and Hagan's AF-SABR. On the other hand, it is dependent on Hagan's formulas and therefore one has to check the probability density function implied by Hagan's formulas and apply the SCM in a clever way. By doing so, it produces satisfactory results (no arbitrage and an accurate fit) for most practical problems.

On the extrapolation of the market quotes, the impact of the arbitrage in Hagan's formulas was investigated and mainly contributed to a higher volatility and option price for options with a long maturity and a low strike compared to the arbitrage-free approaches. In the extrapolation of high strikes, Hagan's formulas and SCM-Hagan gave higher prices to swaptions compared to uncorrelated Antonov and Hagan's AF SABR. All approaches were arbitrage-free in this region and no general conclusion could be made based on arbitrage.

In the extrapolation vega, and the difference in vega have been investigated too. For the swaptions with a long maturity and a low strike, Hagan's formulas generated higher sensitivities, which was larger than the average model risk of an approach. No general conclusion could be

[7]The one-dimensional integral in the approach of Antonov et al. [3] is unstable around $K = S_0$. The two-dimensional integral is expensive to approximate, especially when an entire volatility curve has to be constructed. No fast approaches that produce prices implied by the SABR model are known for the general case, i.e. $\rho \neq 0$ and a long maturity. By fast, comparable in computational cost of Hagan's Black formula, Hagan's AF SABR or SCM-Hagan is meant.

made for other extrapolation regions, since the difference for the other extrapolation regions between the sensitivities was small.

In this chapter, swaptions have been used to compare the approaches. To further investigate how the approaches inter- and extrapolate the market quotes, more complex products will be priced in the next chapter. This gives more insights into the impact of each approach on the inter- and extrapolation.

Chapter 6

Pricing of exotic interest rate derivatives

In this thesis, the approaches by Hagan et al. [29], Hagan et al. [30], Antonov et al. [3] and Grzelak et al. [25] have been considered, which are abbreviated by Hagan's formulas, Hagan's AF SABR, uncorrelated Antonov and SCM-Hagan respectively. This chapter compares the approaches by pricing products that depend on the inter- and extrapolation of the market quotes. By pricing these products, the impact of the inter- and extrapolation on the volatility curve of the approach will be investigated further. This section will price constant maturity swap (CMS) derivatives. The focus will be on CMS swaplets, floorlets and caplets priced with a convexity adjustment method [17]. With this method, it will be shown how the pricing of these products depends on the inter- and extrapolation of the market quotes. The difference in these prices will be compared to measure the impact of the inter- and extrapolation of the market quotes and the impact of the arbitrage in Hagan's formulas. For the pricing of these products, the calibrated volatility curves of the 10Y10Y swaptions of April 2014 from Chapter 5 will be used. This chapter ends with a summary and a conclusion.

6.1 CMS products

The main difference between a CMS swap and a swap as defined in Section 2.2.2 is that the floating rate is chosen to be a swap rate and not LIBOR or EURIBOR. The swap rate has a fixed underlying tenor structure[1], which is the origin of the term constant maturity and it is therefore referred to as a CMS rate in a CMS swap. Compared to a swap, a CMS swap has more exposure to the curvature of the yield curve. The yield curve is a representation of the interest rates implied by the market quotes, often referred to as the zero-coupon curve. Furthermore, a CMS swap is less exposed to a change in the absolute level of the interest rate [41]. A CMS swap can be used to profit from the shape of the yield curve.

A CMS swaplet is one coupon of the floating rate of the CMS swap, i.e. one payment based on the swap rate. A CMS swap consists of M of these payments, where they are exchanged to a fixed rate.[2] The fixed rate can have its own tenor structure as with the swap. If the underlying fixed tenor structure of the swap rate is known and the payments of the floating rate and fixed rate are assumed to be on the same days, a CMS swap could be defined by:

[1] By which it is meant that it has a fixed tenor structure for the floating rate and a fixed tenor structure for the fixed rate.

[2] For simplicity, a fixed rate is assumed, but a floating rate or even a combination could also be used.

Definition 6.1 (CMS Swap)**.** Let a tenor structure $T_0, \dots T_M$, $\tau_n = T_{n+1} - T_n$ for $n = 0, \dots, M-1$, a fixed rate K and a CMS rate S be given. One party pays simple compounded interest based on the fixed rate K in return for simple interest payments based on the CMS rate fixed on date T_n, for each period $[T_n, T_{n+1}]$. The payments are exchanged at the end of each period, i.e. T_{n+1}. The payments are assumed to have the same tenor structure, day count convention and business day convention. The net cash flow from the perspective of the fixed rate payer is at time T_{n+1}:

$$N\tau_n(S(T_n) - K).$$

It can be shown that the value of a CMS swap at $T_{k-1} \leq t \leq T_k$ is:

$$V_{\text{CMS swap}}(t) = N \sum_{n=k}^{M-1} \tau_n D(t, T_{n+1}) \mathbb{E}^{T_{n+1}} \left[S(T_n) - K \right],$$

where N is the notional of the CMS swap. For the remainder of this chapter, the notional is set equal to one. $D(t,T)$ is the price of a zero-coupon bond and $\mathbb{E}^T$ is the expectation under the T-forward measure.

One must be aware that $S(T_n)$ is usually not a martingale under the T_{n+1} forward measure. Therefore, it holds in general that $\mathbb{E}^{T_{n+1}} [S(T_n)] \neq S(0)$. This is the main problem in pricing a CMS swap. Therefore, the focus lies on pricing a CMS swaplet. The CMS swaplet price is given by $V_{swaplet}(0, T_n, T_{n+1}) = D(0, T_{n+1}) \mathbb{E}^{T_{n+1}} [S(T_n)]$ for which the focus will be on computing $\mathbb{E}^{T_{n+1}} [S(T_n)]$.

It can be shown that the expectation $\mathbb{E}^{T_{n+1}} [S(T_n)]$ at $t = 0$ is given by [17]:

$$\mathbb{E}^{T_{n+1}} [S(T_n)] = S(0) + \frac{1}{A(0)} \left(\int_{S(0)}^{+\infty} C(x) v''(x) \, \mathrm{d}x + \int_{-\infty}^{S(0)} P(x) v''(x) \, \mathrm{d}x \right), \tag{6.1}$$

where

$$v(x) := (x - K) \left(\frac{w(x)}{w(S(0))} - 1 \right)$$

$$w(S(T_n)) := S(T_n) \frac{\left(1 + \frac{S(T_n)}{q}\right)^{M-\Delta}}{\left(1 + \frac{S(T_n)}{q}\right)^{M} - 1} \approx \frac{D(T_n, T_{n+1})}{A(T_n)},$$

and where q is the frequency of the swap (thus $q = 1$ for annual, $q = 2$ for semi-annual, etc.), $\Delta = qT_{n+1}$, A is the annuity corresponding to the swap rate $S(T_n)$, and $C(x)$ and $P(x)$ denote the price of a payer and receiver swaption respectively, with strike x and corresponding to the tenor structure of the swap rate $S(T_n)$. For the CMS swaplet one sets $K = S(0)$ in $v(x)$. This derivation is based on switching between the T-forward measure and the annuity measure. After this switch, the expectation is cleverly split into multiple parts.

The part

$$\frac{1}{A(0)} \left(\int_{S(0)}^{+\infty} C(x) v''(x) \, \mathrm{d}x + \int_{-\infty}^{S(0)} P(x) v''(x) \, \mathrm{d}x \right),$$

is called the convexity adjustment in Equation (6.1). It is the part for which the expectation $\mathbb{E}^{T_{n+1}} [S(T_n)]$ differs from the forward swap rate. This accounts for the drift of the swap rate under the T-forward measure.

Equation (6.1) shows that the pay-off of a CMS swaplet can be replicated by a continuous set of payer and receiver swaptions. The expectation $\mathbb{E}^{T_{n+1}}[S(T_n)]$ (and thus a CMS swaplet too) therefore depends on the entire volatility surface in the strike and maturity direction, since the convexity adjustment is given by two integrals of weighted prices of payer and receiver swaptions in the strike dimension. It is also dependent on the maturity direction for the CMS swap, since the swap rates is exchanged on multiple times in the future for which there might be no market quotes given. The focus will be on the strike dimension since there it has been shown that Hagan's formulas imply arbitrage. Computing $\mathbb{E}^{T_{n+1}}[S(T_n)] - S(0)$ gives the impact of the inter- and extrapolation of the market quotes of each approach in the strike dimension.

To further investigate the impact of the inter- and extrapolation of the market quotes, CMS caplets and floorlets will be priced too. These are a call and put option on the swap rate respectively.

Definition 6.2 (CMS Caplet)**.** A *CMS caplet* gives the holder the right, but not the obligation, to pay a fixed rate in exchange for receiving a swap rate fixed at T_n at a pre-defined future time T_{n+1}.

Definition 6.3 (CMS Floorlet)**.** A *CMS floorlet* gives the holder the right, but not the obligation, to pay a swap rate fixed at T_n in exchange for receiving a fixed rate at a pre-defined future time T_{n+1}.

A CMS caplet and floorlet give protection to the holder of the option if the swap rate becomes too high or too low respectively. For example, suppose that one goes into a CMS swap, where one agrees to pay a swap rate in exchange for a fixed rate K_1. Buying a CMS caplet with a strike $K_2 \geq K_1$ ensures that one never has to pay more that K_2. One can limit the loss with this option if the swap rate becomes large.

The price of a CMS caplet and floorlet at time $t = 0$ with fixing date T_n for the swap rate, paying date T_{n+1} and strike K are given by:

$$V_{\text{caplet}}(0, T_n, T_{n+1}, K) = D(0, T_{n+1})\mathbb{E}^{T_{n+1}}\left[(S(T_n) - K)^+\right],$$
$$V_{\text{floorlet}}(0, T_n, T_{n+1}, K)) = D(0, T_{n+1})\mathbb{E}^{T_{n+1}}\left[(K - S(T_n))^+\right].$$

In a similar fashion as for the CMS swaplet, this can be reduced to [17]:

$$V_{\text{caplet}}(0, T_n, T_{n+1}, K) = \frac{D(0, T_{n+1})}{A(0)}\left(C(K) + v'(K)C(K) + \int_K^{+\infty} C(x)v''(x)\,\mathrm{d}x\right), \tag{6.2}$$
$$V_{\text{floorlet}}(0, T_n, T_{n+1}, K)) = \frac{D(0, T_{n+1})}{A(0)}\left(P(K) + v'(K)P(K) - \int_{-\infty}^{K} P(x)v''(x)\,\mathrm{d}x\right). \tag{6.3}$$

where A, C, P and v are as defined in Equation (6.1).

Like the CMS swaplet, the CMS caplet and floorlet prices depend on the volatility curve. In this case, the expressions

$$C(K) + v'(K)C(K) + \int_K^{+\infty} C(x)v''(x)\,\mathrm{d}x,$$
$$P(K) + v'(K)P(K) - \int_{-\infty}^{K} P(x)v''(x)\,\mathrm{d}x,$$

depend on the inter- and extrapolation of the market quotes. These expressions will therefore be replicated with the calibrated volatility curves in Chapter 5.

Furthermore, like a call and a put option, if there exists no arbitrage, there exists a put-call parity for a CMS swaplet, floorlet and caplet:

$$V_{\text{caplet}}(t, T_n, T_{n+1}, K) - V_{\text{floorlet}}(t, T_n, T_{n+1}, K) = (V_{\text{swaplet}}(t, T_n, T_{n+1}) - D(0, T_{n+1})K)\,. \quad (6.4)$$

6.2 Pricing results

The decision was made to focus on CMS swaplets, floorlets and caplets where the underlying CMS rate has a tenor of 10 years. This is one of the more frequently traded swap rates in CMS derivatives (thus CMS rate with a swap tenor of 10 years). The fixing date is set equal to 10 years, i.e. $T_n = 10$ years in Equations (6.1-6.3). For the other specifications of the CMS swap the standard euro conventions are used. Test in this section are done with the data from April, 2014. For each day the calibrated volatility curve implied by Hagan's Black formula generated arbitrage. To price the CMS swaplets, caplets and floorlets the integrals in Equations (6.1-6.3) are approximated by a discrete variant.

day	swap rate (%)	Hagan's Black formula (bp)	SCM-Hagan (bp)	Hagan's AF SABR (bp)	Uncorrelated Antonov (bp)	Max difference w.r.t. Hagan's Black formulas (bp)
1	3.209	31.9	31.8	32.0	32.1	0.2
2	3.236	31.8	31.7	32.0	31.8	0.2
3	3.241	31.5	31.5	31.8	31.8	0.3
4	3.213	31.6	31.5	31.7	31.7	0.1
7	3.224	31.0	31.0	31.2	31.2	0.2
8	3.236	30.6	30.6	30.8	30.8	0.2
9	3.233	30.4	30.4	30.6	30.6	0.1
10	3.183	30.9	30.9	30.9	31.0	0.4
11	3.158	31.4	31.4	31.0	31.1	0.3
14	3.175	31.3	31.3	30.9	31.0	0.4
15	3.131	31.7	31.7	31.1	31.3	0.6
16	3.133	31.7	31.7	31.1	31.4	0.6
17	3.146	31.9	31.9	31.3	31.6	0.6
22	3.167	31.8	31.8	31.3	31.4	0.5
23	3.152	31.9	31.8	31.3	31.5	0.6
24	3.130	32.1	32.1	31.5	31.7	0.6
25	3.070	32.7	32.7	31.4	31.9	1.3
28	3.076	33.1	33.1	31.7	32.2	1.4
29	3.103	32.7	32.7	31.7	32.1	1.0
30	3.093	33.0	33.0	31.9	32.4	1.1

Table 6.1: The forward swap rate and the convexity adjustment implied by each approach for April, 2014.

First, CMS swaplet prices are investigated to compare the impact of inter- and extrapolation of the market quotes in the strike dimension for each approach. As discussed in the previous

section, the focus is on the convexity adjustment part since this part of the CMS swaplet price is affected by the inter- and extrapolation of the market quotes. Thus for each approach the followed expression is computed:

$$\frac{1}{A(0)}\left(\int_{S(0)}^{+\infty} C(x)f''(x)\,\mathrm{d}x + \int_{-\infty}^{S(0)} P(x)f''(x)\,\mathrm{d}x\right).$$

Table 6.1 presents the convexity adjustment of the CMS swaplets for each approach. For a fixed day in the month, there is a deviation in the convexity adjustment varying from 0.2bp up to 1.1bp in the approaches. Between SCM-Hagan and Hagan's Black formula, there is a maximum difference of 0.04bp. The relative difference of 0.04bp in the convexity adjustment compared to a swap rate of 3% is approximately 0.013% and thus small. The relative difference of 1.1bp in the convexity adjustment compared to a swap rate of 3% is approximately 0.37%, which is considered small too here. Furthermore, there is no bias between the approaches, i.e. no approach gives a consistently higher price compared to the other approaches.

Prices of CMS floorlets and caplets with a strike equal to the swap rate are now compared. These will be called at-the-money CMS floorlets and caplets respectively.[3] Like the CMS swaplet, the focus of the CMS caplet and floorlet prices will be on the part that depends on the volatility surface. For the CMS caplet and floorlet, these are respectively:

$$C(K) + v'(K)C(K) + \int_{K}^{+\infty} C(x)v''(x)\,\mathrm{d}x,$$
$$P(K) + v'(K)P(K) - \int_{-\infty}^{K} P(x)v''(x)\,\mathrm{d}x.$$

These expressions are referred to as prices.[4] Due to the put-call parity between a CMS swaplet, caplet and floorlet, the results of CMS swaplets are omitted. These do not give complementary insights.

Table 6.2 presents the results. For a fixed day in the month, there is a deviation in the CMS floorlet prices up to 0.8bp in the approaches. For fixed day in the month, there is there is a deviation in the CMS caplet price of up to 1.1bp for the approaches . Between SCM-Hagan and Hagan's Black formula, there is a maximum difference of 0.04bp difference in the floorlets. The relative difference of 0.04bp in price compared to an at-the-money floorlet price of 80bp is 0.05%. The relative difference of 0.8bp in price compared to an at-the-money floorlet price of 80bp is 1%. These differences are considered to be small too. Furthermore, there is no bias between the approaches.

[3] An at-the-money option is usually an option for which the forward is equal to the strike. It would be more correct to set the strike equal to $\mathbb{E}^{T_{n+1}}[S(T_n)]$, however the value of this expectation depends on the approach.

[4] Effectively these are prices of CMS floorlets and caplets with a notional equal to $\frac{A(0)}{D(0,T_{n+1})}$.

day	Hagan's Black formula (bp)	SCM-Hagan (bp)	Hagan's AF SABR (bp)	Uncorrelated Antonov (bp)
1	80.43	80.47	80.43	80.39
2	80.36	80.41	80.38	80.49
3	80.19	80.24	80.21	80.20
4	80.18	80.22	80.15	80.15
7	79.70	79.74	79.72	79.70
8	79.34	79.39	79.33	79.36
9	79.10	79.14	79.10	79.09
10	79.53	79.56	79.52	79.49
11	79.60	79.62	79.60	79.59
14	79.51	79.53	79.50	79.51
15	79.76	79.78	79.75	79.65
16	79.79	79.81	79.78	79.77
17	79.97	79.99	79.94	79.92
22	79.86	79.88	79.83	79.82
23	79.92	79.94	79.89	79.88
24	80.07	80.09	80.07	80.05
25	80.14	80.15	80.15	80.13
28	80.40	80.41	80.41	80.40
29	80.41	80.42	80.41	80.39
30	80.60	80.60	80.59	80.57

Table 6.2: At-the-money CMS floorlet price for each approach for April, 2014.

In the results of 16th of April, 2014, there is one of the largest differences between the approaches in the CMS swaplet price.[5] The focus will therefore be on pricing out-of-the-money CMS caplets and floorlets, where CMS caplets are taken with the strikes higher than the swap rate and CMS floorlets with the strikes lower than the swap rate. The strikes are chosen to vary relative to the swap rate up to 10%, i.e. for CMS floorlet strikes in the regions 0 to S_0, for the CMS caplets strikes in the region S_0 to $S_0 + 10\%$. A difference of 1% between the strikes was taken.

Table 6.3 presents the results. For a fixed day in the month, there is between the approaches a deviation in price up to 1.5bp for the caplets and up to 0.3bp for the floorlets. Between Hagan's Black formula and SCM-Hagan, there is a maximum difference of 0.04bp overall, except for the CMS floorlet with a strike of $S_0 - 3\%$, for which the difference is 0.3bp. The CMS floorlet price for this strike was between 1.2 and 1.5bp for all the approaches. Hagan's Black formula was at least 0.2bp higher compared to the other approaches in this case. The arbitrage in Hagan's Black formula resulted in a higher price compared to the other approaches which were arbitrage-free in this relatively low strike for a floorlet. For the caplet, Hagan's Black formula and SCM-Hagan gave higher prices for high strikes compared to Hagan's AF SABR and uncorrelated Antonov. This difference was up to 1.5bp compared to the lowest price of 7bp for Hagan's AF SABR of a caplet with strike $S_0 + 10\%$. In this case there is a bias between the approaches for the more "extreme" strikes. The absolute difference between the approaches for these extreme strikes is

[5]There are larger differences for later dates, but for these dates Hagan's AF SABR could not fit the market quotes accurately for high strikes compared to the other approaches due to a limitation in the SABR parameter β as disccused in Section 5.3.

considered to be small. These are options not actively traded and therefore the difference is considered to be in the bid-offer spread[6] (the difference in the price for which an option can be sold and bought).

Relative strike (%)	Hagan's Black formula (bp)	SCM-Hagan (bp)	Hagan's AF SABR (bp)	Uncorrelated Antonov (bp)
0	111.50	111.50	110.90	111.20
1	73.07	73.07	72.75	72.76
2	49.66	49.67	49.33	49.42
3	35.50	35.50	34.92	35.20
4	26.59	26.59	25.73	26.17
5	20.70	20.70	19.62	20.17
6	16.62	16.63	15.39	16.00
7	13.68	13.68	12.35	13.00
8	11.48	11.48	10.10	10.76
9	9.79	9.80	8.40	9.05
10	8.47	8.47	7.09	7.72

(a) CMS caplet.

Relative strike (%)	Hagan's Black formula (bp)	SCM-Hagan (bp)	Hagan's AF SABR (bp)	Uncorrelated Antonov (bp)
0	79.79	79.81	79.78	79.77
-1	37.82	37.83	37.68	37.87
-2	13.86	13.86	14.00	13.96
-3	1.46	1.20	1.30	1.22

(b) CMS floorlet.

Table 6.3: Out-of-the-money CMS floorlets and caplets, 16th of April, 2014.

6.3 Conclusion

All approaches have been compared by pricing CMS swaplet, caplets and floorlets with a convexity adjustment by using the calibrated volatility curves for the 10Y10Y swaptions in April, 2014 of Chapter 5. For the caplets and floorlets the strikes were varied in a wide range for the 16th of April, 2014.

Between the approaches, there was a difference of at most of 1.1bp for CMS swaplets, and at-the-money CMS floorlets and caplets. This difference was relatively small compared to the CMS swaplet, caplet and floorlet prices. No approach was biased compared to the other approaches. The arbitrage in Hagan's formulas did not have an impact on these prices.

Between the approaches, there was a difference of at most 1.5bp for the prices of out-of-the-money CMS floorlets and caplets. The absolute differences between the approaches was in an acceptable region; they were in the bid-offer spread region. CMS floorlets with a low strike were priced the highest by Hagan's Black formula. The arbitrage in Hagan's Black formula generated a higher price for these strikes compared to the other approaches which were arbitrage-free. CMS caplets with a high strike were priced the highest by Hagan's Black formula and SCM-Hagan.

[6] In these options the bid-offer spread are around 2.5bp for a CMS swaplet, caplet or floorlet.

The extrapolation for high strikes of Hagan's Black formula and therefore also of SCM-Hagan gave higher prices for these relatively high strikes. In this region Hagan's Black formula was arbitrage-free too.

Hence, the general conclusion is that the arbitrage in Hagan's formulas leads to an overpricing of options in the low strike region compared to other approaches that are arbitrage-free. For the other regions no general conclusion could be made whether one approach is biased or not.

Chapter 7

Conclusion

Hagan's formulas [29] are widely used in the interest rate market to parametrize the volatility curve of swaptions to inter- and extrapolate market quotes in the strike dimension. They are an approximation of the Black and Bachelier volatilities implied by the Stochastic Alpha Beta Rho (SABR) model. It is known that these approximations are not arbitrage-free. They can imply negative values for butterfly options or equivalently a negatively valued probability density function as has been shown in this thesis. It is undesired to have arbitrage in the approach, since this does not give the fair price and can impact the sensitivities to market movements of these products. This results in an incorrect computation of the sensitivities and the risk of the products, although reasonably describing the implied Black volatility curve.

Several approaches in the literature have been addressed the issue of arbitrage in Hagan's formulas, by either proposing a new method to price under the SABR model or altering Hagan's formulas. In this thesis, the approaches are chosen such that these are arbitrage-free and computationally rapid. The goal of the thesis was to investigate the impacts of an arbitrage-free approach on the inter- and extrapolation of market quotes compared to Hagan's formulas. In this thesis the approaches by Hagan et al. [30], Antonov et al. [3] and Grzelak et al. [25] were investigated and are referred to as Hagan's AF SABR, uncorrelated Antonov and SCM-Hagan in the thesis.

For Hagan's AF SABR model, the approach by Le Floch et al. [15] has been followed to ensure a sufficiently efficient implementation. In this approach a one-dimensional PDE has to be solved, which gives the probability density function of the underlying process. The discretization of the PDE has been analyzed to derive sufficient conditions to ensure that the numerical solution of the PDE is arbitrage-free. An alternative integration technique is suggested, which leads to more stable butterfly option prices compared to the one proposed by Le Floch et al. The convergence of this integration technique has been tested and gave accurate results. In Chapter 5 it has also been shown that during calibration, the SABR parameter β must be limited in Hagan's AF SABR to ensure a sufficiently stable time series of the model parameters.

Uncorrelated Antonov gives the exact call price under the SABR model for the uncorrelated case. In order to speed up the approach, Antonov et al. derived an approximation of this two-dimensional integral in the form of a one-dimensional integral. The drawback of this one-dimensional integral is that it can lead to inaccuracies in the butterfly option prices and in the implied probability density function, although reasonably describing the implied Black volatility curve. In Chapter 5 it has been shown that uncorrelated Antonov could not fit the market quotes accurately for options with a short maturity.

The SCM maps a computationally expensive distribution to a simpler distribution. The mapping has been used to transform the negative part of the probability density function implied by Hagan's formulas to a positively valued probability density function, following the approach by Grzelak et al, which led to an approach fast enough for market practice. This mapping is approximated by a Lagrange polynomial and should be strictly monotonic to have an arbitrage-free approach. Therefore, a computationally rapid algorithm has been developed to check if a polynomial is strictly monotonic, based on some classical results in mathematics. This provides the knowledge that the Lagrange polynomial is usually strictly monotonic in the SCM. Different interpolation techniques compared to a Lagrange polynomial have been compared as well, showing that the Lagrange polynomial gives the most accurate results. For the simpler distribution in the mapping, a normal distribution has been compared to a gamma distribution. It has been shown the gamma distribution can provide even more accurate results if the distribution of the process implied by Hagan's formulas is strongly skewed. Furthermore, the approach has been extended by a virtual collocation technique to incorporate the martingale property to make this approach completely arbitrage-free. It has been shown that this approach is stable too. This approach is referred to as the M-SCM and applying this approach for Hagan's formulas is referred to as SCM-Hagan.

Each approach has been tested to a realistic market setting and compared to Hagan's formulas for the volatility curves, option prices and sensitivities in the inter- and extrapolation of market quotes. During calibration it has been shown that Hagan's formulas did not generate arbitrage in general for options with short maturities and thus are suitable for market practice. For these cases, Hagan's formulas and SCM-Hagan performed best to fit the market volatility curve. For long maturities, Hagan's formulas generated butterfly arbitrage for low strikes. SCM-Hagan has shown that it could remove this arbitrage in a satisfactory fashion, it was stable during calibration for practical problems and gave similar results for options with low strikes as Hagan's AF-SABR and uncorrelated Antonov.

The impact of the arbitrage in Hagan's formulas was investigated and mainly contributed to a higher volatility and option price for options with a long maturity and a low strikes compared to the arbitrage-free approaches. In the extrapolation of high strikes, Hagan's formulas and SCM-Hagan gave higher prices to swaptions compared to uncorrelated Antonov and Hagan's AF SABR. Since all approaches were arbitrage-free in this region and, no general conclusion could be made based on arbitrage. Lastly, vega was approximated to investigate the sensitivities implied by the approaches. Vega is used in finance to get an indication of the impact on the price by a parallel shift in the volatility curve. The vega sensitivities seemed to be stable and did not differ significantly, except for the cases with long maturities and low strikes, for which Hagan's formulas implied higher sensitivities.

To further investigate the impact of the inter- and extrapolation of market quotes for all approaches, each approach was compared in pricing more complex products that depend on the inter- and extrapolation of market quotes. The focus was on CMS swaplets, caplets and floorlets as the prices of these products can be expressed as an integral of swaptions in the strike dimension. For the CMS swaplets, the difference in price was insignificantly as with the at-the-money options CMS floorlets and caplets. As with the swaptions, the impact of the arbitrage in Hagan's formulas was yet again overpricing options with low strikes compared to the arbitrage-free approaches. In the extrapolation of high strikes, Hagan's formulas and SCM-Hagan gave higher prices to CMS caplets compared to uncorrelated Antonov and Hagan's AF SABR. Since all approaches were arbitrage-free in this region and, no general conclusion could be made based on arbitrage.

Further research

The following issues are recommended for future research.

- **Negative rates.**
  Currently, negative rates are observed in the market and a therefore extensions to negative rates must also be investigated. Antonov et al. [6] propose the free-boundary SABR model and suggest an extension of this model by setting $\mathrm{d}S_t = \alpha_t \left(S_t^2 + \epsilon^2\right)^{\frac{\beta}{2}} \mathrm{d}W_t$ in the dynamics for the forward swap rate. The suggestion removes a discontinuity in the probability density function implied by the free-boundary SABR model. For this model no analytical expressions for prices are yet derived. The approaches by Hagan et al. [29, 30] are still applicable. For Hagan et al. [29], it can be investigated if arbitrage can be removed by the SCM yet again.

- **Arbitrage in the maturity and tenor direction?**
  This thesis investigates the impact of arbitrage in the strike dimension. Arbitrage in the maturity and tenor directions should be investigated too, since this impacts prices and sensitivities too. For the equity market, arbitrage in the maturity direction can be defined as negative values to calendar spread options. For the interest rate market, this is less trivially achieved. It could be investigated if interpolation in the probability density functions of processes for different annuities can be used to interpolate in time and how this compares to other approaches. In particular, the SCM can be used for this interpolation in the probability density functions.

- **Enhancements to the SCM.**
  In this thesis, the SCM has been used to map the implied random variable by Hagan's formulas to a normal and a gamma distribution. Ideally, there should be a close relation between the processes in the SCM. Hagan's formulas originate from the SABR model, which is a stochastic CEV process. It could thus be investigated if the implied distribution of the CEV process would result in less collocation points and thus a faster approach.[1]
  Further research should also be done on the interpolation technique used in the SCM. The interpolation technique should imply directly a monotonic function independent of the location of the collocation points.[2]

[1] As an alternative when one cannot determine analytical expressions under the CEV process, one can choose to use the SCM to map the CEV process once again to a normal distribution as discussed in Section 4.2.

[2] An interpolation technique by Witteveen et al [23] can be used as a starting point.

Appendix A

Background and proofs for Chapter 2

A.1 Bessel processes

To investigate the CEV process, Bessel processes are used in Section 2.4.1. This section presents a more detailed discussion on Bessel processes, where Bessel processes will be related to the Euclidean norm of a n-dimensional Brownian motion. All definitions are taken from Jeanblanc [13].

Definition A.1 (Euclidean Norm Of The n-Dimensional Brownion Motion)**.** Let $\mathbf{W}_t = (W_1, \ldots, W_n)$ be a n-dimensional Brownian motion where $n \in \mathbb{N}$ and define the process X as $X_t := ||\mathbf{W}_t||$, i.e. $X_t^2 = \sum_{i=1}^n W_i^2(t)$. Itô's Lemma gives $\mathrm{d}X_t^2 = \sum_{i=1}^n 2W_i(t)\,\mathrm{d}W_i(t) + n\,\mathrm{d}t$.

It can be proven that

$$\mathrm{d}W_t := \frac{1}{X_t}\sum_{i=1}^{n} W_i(t)\,\mathrm{d}W_i(t),$$

is a Brownian motion [13]. Introducing $Y_t = X_t^2$, it follows that:

$$\mathrm{d}Y_t = 2X_t\,\mathrm{d}W_t + n\,\mathrm{d}t = 2\sqrt{Y_t}\,\mathrm{d}W_t + n\,\mathrm{d}t. \tag{A.1}$$

Using Itô's formula, it follows that:

$$\mathrm{d}X_t = \mathrm{d}W_t + \frac{n-1}{2X_t}\,\mathrm{d}t$$

These two SDEs of X_t and Y_t describe the dynamics of the norm and the squared norm of the n-dimensional Brownian respectively. To define such a process for a general positive dimension, the definition of a squared Bessel process is given, which relates to the process Y_t.

Definition A.2 (w-Dimensional Squared Bessel Process (With Positive Dimension))**.** For every $w \geq 0$ and $y \geq 0$, the unique strong solution to the equation

$$Y_t = y + wt + 2\int_0^t \sqrt{Y_s}\,\mathrm{d}W_s,\ Y_t \geq 0$$

is called a squared Bessel process with dimension w, starting at y and is denoted by BESQ_y^w.

The quantity w corresponds to the dimensionality of the n-dimensional Brownian motion. The Bessel process will be introduced by the squared Bessel process. As the name suggests, the squared Bessel process is the square of a Bessel process and relates to the process X_t.

Definition A.3 (w-Dimensional Bessel Process (With Positive Dimension w))**.** Let Y be a BESQ_x^w. The process $X = \sqrt{Y}$ is called a Bessel process of dimension w, starting at $x = \sqrt{y}$ and is denoted by BES_x^w. The family of Bessel processes with the index η is given by $\eta = \frac{w}{2} - 1$. It will be written as $\mathrm{BESQ}^{(\eta)}$

To elaborate on the (squared) Bessel processes further, several of its properties are presented[13]:

- If $w > 2$, the process BES_x^w will never reach zero and is a transient process.
- If $w = 2$, the process BES_x^2 will never reach zero.
- If $0 < w < 2$, the processes BES_x^w and X reach zero in finite time and is stopped naturally at zero.
- The probability density function from x at time 0 to y at time t is given by:

$$f_t^{(\eta)}(x, y) = \frac{y}{t}\left(\frac{y}{x}\right)^{\eta} e^{-\frac{x^2+y^2}{2t}} I_\eta\left(\frac{xy}{t}\right),$$

  where I_η is the modified Bessel function with index η.

- The modified Bessel function can be written as

$$I_\eta(u) = \left(\frac{u}{2}\right)^{\eta} \sum_{k=0}^{\infty} \frac{\left(\frac{u^2}{4}\right)^k}{k!\Gamma(\eta + k + 1)} = \frac{1}{\pi}\int_0^{\pi} e^{u\cos(x)}\cos(\mu x)\,\mathrm{d}x - \frac{\sin(\mu\pi)}{\pi}\int_0^{\infty} e^{-u\cosh(y)-\mu y}\,\mathrm{d}y, \tag{A.2}$$

  where Γ is the Gamma function.

A more general definition of a squared Bessel process will be presented, such that it can be extended for all $w \in \mathbb{R}$. Thus (squared) Bessel processes with a negative dimensionality will be included.

Definition A.4 (w-Dimensional Squared Bessel Process)**.** The solution to the equation

$$\mathrm{d}Y_t = w\,\mathrm{d}t + 2\sqrt{|Y_t|}\,\mathrm{d}W_t,\ X_0 = x.$$

where $w,\ x \in \mathbb{R}$, is called the square of a w-dimensional Bessel process starting from x.

The process $X_t = \sqrt{Y_t}$ is the general w-dimensional Bessel process. It satisfies the SDE

$$\mathrm{d}X_t = \mathrm{d}W_t + \frac{w-1}{2X_t}\,\mathrm{d}t.$$

A.2 Proof of Lemma 2.19

Proof. For a call option, it holds[1]:

$$\begin{aligned} C(t, T, K, t) &= \mathcal{D}(t)\mathbb{E}\left[(S_T - K)^+ \middle| \mathcal{F}_t\right], \\ &= \mathcal{D}(t)\int_K^{\infty} (S_T - K) f(S_T|S_t)\,\mathrm{d}S_T, \end{aligned}$$

[1]The expectation is to be assumed under the appropriate measure, under which the process S_t is a martingale.

where $f(S_T|S_t) = f(T, S_T|S_t)$ is the probability density function. Setting $\mathcal{D}(t) = 1$ and rewriting the integral as:

$$\int_x^\infty (y - x) f(y)\,\mathrm{d}y,$$

simplifies the expression. For convenience the Leibniz rule is stated [1][2]:

$$\frac{\partial}{\partial\theta}\left(\int_{a(\theta)}^{b(\theta)} g(x,\theta)\,\mathrm{d}x\right) = \int_{a(\theta)}^{b(\theta)} \frac{\partial g(x,\theta)}{\partial\theta}\,\mathrm{d}x + g(b(\theta),\theta)b'(\theta) - g(a(\theta),\theta)a'(\theta).$$

For a martingale process, it holds that $\mathbb{E}\left[|S_t|\right] < \infty$ $t > 0$, and $\int_{-\infty}^{\infty} |f(y)|\,\mathrm{d}y = 1 < \infty$. This justifies taking the limit out of the integral below:

$$\begin{aligned}
\frac{\partial}{\partial x}\int_x^\infty (y-x)f(y)\,\mathrm{d}y &= \frac{\partial}{\partial x}\lim_{c\to\infty}\int_x^c (y-x)f(y)\,\mathrm{d}y \\
&= \lim_{c\to\infty}\frac{\partial}{\partial x}\int_x^c (y-x)f(y)\,\mathrm{d}y \\
&= \lim_{c\to\infty}\int_x^c -f(y)\,\mathrm{d}y + (c-x)f(c)\cdot 0 - (x-x)f(x)\cdot 1 \\
&= \int_x^\infty -f(y)\,\mathrm{d}y = -G(x) = -(1-F(x)),
\end{aligned}$$

where G and F are the survival density function and cumulative density function respectively. By justifying that $\int_{-\infty}^{\infty} |f(y)|\,\mathrm{d}y = 1 < \infty$, it can be computed that:

$$\begin{aligned}
&\frac{\partial}{\partial x}\int_x^\infty -f(y)\,\mathrm{d}y = \frac{\partial}{\partial x}\lim_{c\to\infty}\int_x^c -f(y)\,\mathrm{d}y, \\
&= \lim_{c\to\infty}\frac{\partial}{\partial x}\int_x^c -f(y)\,\mathrm{d}y \;= \lim_{c\to\infty}\int_x^c 0\,\mathrm{d}y + f(c)\cdot 0 - -f(x)\cdot 1 \;= f(x),
\end{aligned}$$

Hence, it has been shown that

$$\begin{aligned}
\frac{\partial C}{\partial K}(t,T,K) &= \mathcal{D}(t)(F(K)-1), \\
\frac{\partial^2 C}{\partial K^2}(t,T,K) &= \mathcal{D}(t)f(K).
\end{aligned}$$

By put-call-parity, it follows that:

$$\begin{aligned}
\frac{\partial P}{\partial K}(t,T,K) &= \mathcal{D}(t)F(K), \\
\frac{\partial^2 P}{\partial K^2}(t,T,K) &= \mathcal{D}(t)f(K).
\end{aligned}$$

□

[2]The function g is in this section only used to indicate a differentiable function and should not be confused with other notation in the thesis.

Appendix B

Derivations and proofs for Chapter 3

B.1 Derivations for Hagan's AF SABR

B.1.1 Derivations of the untransformed PDE

Following Hagan et al. [29], the SABR dynamics are investigated by using a singular perturbation technique, i.e. the SDE is investigated in the form[1]:

$$\begin{cases} \mathrm{d}\tilde{S} = \epsilon\tilde{A}C(\tilde{S})\,\mathrm{d}\tilde{W}^1, \\ \mathrm{d}\tilde{A} = \epsilon\nu\tilde{A}\,\mathrm{d}\tilde{W}^2, \\ \mathrm{d}\tilde{W}_1\,\mathrm{d}\tilde{W}_2 = \rho\,\mathrm{d}t, \end{cases}$$

in the limit $\epsilon \ll 1$, where $C(S) = S^\beta$ in the SABR model. Thus only a small change in the dynamics of the SABR model is assumed and therefore the time indication is omitted in the dynamics. Let $f(t, S_t, \alpha, T, S, A)$ be the probabiliy density function such that $\tilde{S}(T) = S$ and $\tilde{A}(T) = A$, given that $\tilde{S}(t) = S_t$ and $\tilde{A}(t) = \alpha$. For convenience, f denotes $f(t, S_t, \alpha, T, S, A)$. Furthermore, the following moments are defined by:

$$Q^{(k)}(t, S_t, \alpha, T, S) := \int_0^\infty A^k f(t, S_t, \alpha, T, S, A)\,\mathrm{d}A,$$

where δ is the Dirac function. Hence

$$\begin{aligned} Q^{(k)}(t, S_t, \alpha, T, S) &= \int_0^\infty A^k f(t, S_t, \alpha, T, S, A)\,\mathrm{d}A \\ &= \int_0^\infty \int_0^\infty A^k \delta(\tilde{S} - S) f(t, S_t, \alpha, T, \tilde{S}, A)\,\mathrm{d}\tilde{S}\,\mathrm{d}A \\ &= \mathbb{E}\left[A^k \delta(\tilde{S} - S) \middle| \tilde{S}(t) = S_t, \tilde{A}(t) = \alpha \right]. \end{aligned}$$

Thus, the zeroth moment Q^0 is the probability density function at time T and $Q(T, S)$ will be defined as:

$$Q(T, S) := Q^0(t, S_t, \alpha, T, S).$$

This is the variable for which a PDE will be derived. Applying the Fokker-Planck equation, it is follows that the probability density function f satisfies the PDE:

$$\begin{cases} \frac{\partial f}{\partial T} = \frac{1}{2}\epsilon^2 \frac{\partial}{\partial S^2}\left[C^2(S)A^2 f\right] + \epsilon^2\rho\nu\frac{\partial 2}{\partial S \partial A}\left[C(S)A^2 f\right] + \frac{1}{2}\epsilon^2\nu^2\frac{\partial^2}{\partial A^2}\left[A^2 f\right] & \text{for } T > t, \\ f = \delta(S - S_t)\delta(A - \alpha) & \text{for } T = t. \end{cases}$$

[1] C is in this section defined as a function, and should not be confused with the call price as used throughout the thesis. Furthermore, α is replaced by A in the dynamics of the SABR model.

Integrating over A gives:

$$\int_0^\infty \frac{\partial^2}{\partial S \partial A}\left[C(S)A^2 f\right] \mathrm{d}A = \frac{\partial}{\partial S}\left[C(S)A^2 f\right]\Big|_{A=0}^{A=+\infty} = 0.$$

This is justified since $C(S)$ is finite and positive for $S \in \mathbb{R}_{\geq 0}$ and it can be proven that $f < \mathcal{O}(A^{-2})$ as $A \to \infty$. This can be deducted from the fact that A is a martingale and thus using the tower property $\alpha = \mathbb{E}[A(T)] = \mathbb{E}[\mathbb{E}[A(T)|\, S]] = \int_0^\infty \int_{-\infty}^{+\infty} Af \,\mathrm{d}S \,\mathrm{d}A$. Note the double integral can only converge if $f < \mathcal{O}(A^{-2})$ if $A \to \infty$. Furthermore, it holds

$$\int_0^\infty \frac{\partial^2}{\partial A^2}\left[A^2 f\right] \mathrm{d}A = \left[A^2 f\right]_A\Big|_{A=0}^{+\infty} = 0,$$

which is justified by the similar argument as above. Hence integrating the Fokker-Planck equation over$A$ gives:

$$\int_0^\infty \frac{\partial}{\partial T} f \,\mathrm{d}A = \int_0^\infty \frac{1}{2}\epsilon^2 \frac{\partial^2}{\partial A^2}\left[C^2(S)A^2 f\right] \mathrm{d}A.$$

This implies

$$Q_T^{(0)} = \frac{1}{2}\epsilon^2 \frac{\partial^2}{\partial S^2}\left[C^2(S)Q^{(2)}\right].$$

Switching differentiation and integration is justified due to the convergence of the integrals and positiveness of the integration kernel. Also by using a similar argument as above, it can be deduced that $Q^{(k)}$ is finite also for $k \geq 2$, since A has finite moments, which is known from the Black-and-Scholes model.

In a similar way it can be deduced by using the multivariate version of the Feynmac-Kac theorem [13] that the moments $Q^{(k)}$ satisfy the PDE:

$$\begin{cases} \frac{\partial Q^k}{\partial T} + \frac{1}{2}\epsilon^2 A^2 C^2(S)\frac{\partial^2 Q^{(k)}}{\partial S^2} + \epsilon^2 \rho\nu A^2 C(S)\frac{\partial^2 Q^{(k)}}{\partial S \partial A} + \frac{1}{2}\epsilon^2\nu^2 A^2 \frac{\partial^2 Q^{(k)}}{\partial A^2} = 0 & \text{for } t < T, \\ Q^k(t, S_t, \alpha, T, S) = \alpha^k \delta(S - S_t) & \text{for } T = t. \end{cases}$$

In the next part terms of order $\mathcal{O}(\epsilon^2)$ will be neglected. So from here on, the real approximation wil be prepared. First the change to the following variables will be done:

$$\tau = T - t, \;\; z = \frac{1}{\epsilon A}\int_{S_t}^{S} \frac{1}{C(u)} \,\mathrm{d}u,$$

and the following function will be introduced $B(\epsilon A z) := C(S)$.[2] It is then found by basic calculation for the transformation of variable that:

$$\frac{\partial}{\partial S} \equiv \frac{\partial}{\partial z}\frac{\partial z}{\partial S} = \frac{-1}{\epsilon\alpha B(\epsilon A z)}\frac{\partial}{\partial z},$$

$$\frac{\partial}{\partial A} \equiv \frac{\partial}{\partial A} + \frac{\partial}{\partial z}\frac{\partial z}{\partial A} = \frac{\partial}{\partial A} - \frac{z}{A}\frac{\partial}{\partial z},$$

$$\frac{\partial^2}{\partial S^2} = \frac{\partial}{\partial S}\left(\frac{\partial}{\partial S}\right) \equiv \frac{1}{\epsilon^2\alpha^2 B^2(\epsilon A z)}\left(\frac{\partial^2}{\partial z^2} - \epsilon A \frac{\frac{\partial B(\epsilon A z)}{\partial z}}{B(\epsilon A z)}\frac{\partial}{\partial z}\right),$$

$$\frac{\partial^2}{\partial S \partial A} = \frac{\partial}{\partial S}\left(\frac{\partial}{\partial A}\right) \equiv \frac{1}{\epsilon A B(\epsilon A z)}\left(-\frac{\partial^2}{\partial z \partial A} + \frac{z}{A}\frac{\partial^2}{\partial z^2} + \frac{1}{A}\frac{\partial}{\partial z}\right),$$

$$\frac{\partial^2}{\partial A^2} = \frac{\partial}{\partial A}\left(\frac{\partial}{\partial A}\right) \equiv \frac{\partial^2}{\partial A^2} - \frac{2z}{A}\frac{\partial^2}{\partial z \partial A} + \frac{z^2}{\partial A^2}\frac{\partial^2}{\partial z^2} + \frac{2z}{\alpha^2}\frac{\partial}{\partial z}.$$

[2]The variable z in this section is only used in this section and should not be confused with the transformation done in Section 3.1.1. B is in this section defined as a function and should not be confused with the continuously compounded money market account.

Where "≡" means equal to the original partial derivative under the transformation. Following [30], there is a less-straightforward statement:

$$\delta(S - S_t) = \delta(\epsilon A z C(S_t)) = \frac{1}{\epsilon A B(0)}\delta(z).$$

The first statement can be justified by

$$\begin{aligned}\lim_{S\to S_t} \epsilon A z C(S) = \lim_{S\to S_t} C(S_t) \int_{S_t}^{S} \frac{1}{C(u)}\,\mathrm{d}u \\ = C(S_t)\int_{S_t}^{S_t} \frac{1}{C(u)}\,\mathrm{d}u = 0.\end{aligned}$$

So then it follows for $S > 0$ for all time

$$\int_{-\infty}^{+\infty} g(S)\delta(\epsilon A z C(F))\,\mathrm{d}S = g(S_t) = \int_{-\infty}^{+\infty} g(S)\delta(S - S_t)\,\mathrm{d}S,$$

where g is any continuous function. For the second equation the well-known property $\delta(ax) = \frac{\delta(x)}{|a|}$ is used and the fact when $S = S_t$ that $z = 0$ is used. Thus, it follows that $C(S_t) = B(0)$. Let $Q^{(k)}(t, S_t, \alpha, S(z), A)$ be written as $Q^{(k)}(\tau, z, A) := Q^{(k)}(t, S_t, \alpha, S(z), A)$ under this transformation of variable, $Q^{(k)}$ satisfies the PDE:

$$\begin{cases} \frac{\partial Q^{(k)}}{\partial \tau} = & \frac{1}{2}\left(1 + 2\epsilon\rho\nu z + \epsilon^2\nu^2 z^2\right)\frac{\partial^2 Q^{(k)}}{\partial z^2} - \frac{1}{2}\epsilon A \frac{\frac{\partial B(\epsilon A z)}{\partial z}}{B(\epsilon A z)}\frac{\partial Q^{(k)}}{\partial z} \\ & + \left(\epsilon\rho\nu + \epsilon^2\nu^2 z\right)\left(-A\frac{\partial^2 Q^{(k)}}{\partial A \partial z} + \frac{\partial Q^{(k)}}{\partial z}\right) + \frac{1}{2}\epsilon^2\nu^2 A^2 \frac{\partial^2 Q^{(k)}}{\partial A^2}, & \text{for } \tau > 0, \\ Q^{(k)}(0, z, \alpha) = & \alpha^k \delta(S - S_t) = \frac{\alpha^k}{\epsilon\alpha B(0)}\delta(z) = \frac{a^{k-1}}{\epsilon B(0)}\delta(z), & \text{for } \tau = 0. \end{cases}$$

In order to align the initial condition for each $Q^{(k)}$, $\hat{Q}^{(k)}(\tau, z, \alpha)$ is defined by:

$$Q^{(k)}(\tau, z, A) := \frac{A^{k-1}}{\epsilon B(0)}\hat{Q}^{(k)}(\tau, z, A).$$

Then, $\hat{Q}^k(\tau, z, A)$ satisfies the PDE:

$$\begin{aligned}\frac{\partial \hat{Q}^{(k)}}{\partial T} =& \frac{1}{2}\left(1 + 2\epsilon\rho\nu z + \epsilon^2\nu^2 z^2\right)\frac{\partial^2 \hat{Q}^{(k)}}{\partial z^2} - \frac{1}{2}\epsilon A \frac{\frac{\partial B(\epsilon A z)}{\partial z}}{B(\epsilon A z)}\frac{\hat{Q}^{(k)}}{\partial z} \\ & - \left(\epsilon\rho\nu + \epsilon^2\nu^2 z\right)(k-2)\frac{\partial \hat{Q}^{(k)}}{\partial z} - \left(\epsilon\rho\nu + \epsilon^2\nu^2 z\right)A\frac{\partial^2 \hat{Q}^{(k)}}{\partial A \partial z} \\ & + \frac{1}{2}\epsilon^2\nu^2\left(A^2\frac{\partial^2 \hat{Q}^{(k)}}{\partial A^2} + 2(k-1)A\frac{\partial \hat{Q}^{(k)}}{\partial A} + (k-1)(k-2)\hat{Q}^{(k)}\right),\end{aligned}$$

for $\tau > 0$ and the boundary condition $\hat{Q}^{(k)}(0, z, \alpha) = \delta(z)$. Here the true approximation starts and the PDE that will follow, will only be an accurate approximation for the SABR model for small maturities. First, it is noticed that to leading order of ϵ the PDE satisfies

$$\begin{cases} \frac{\partial \hat{Q}^{(k)}}{\partial \tau} \approx \frac{1}{2}\frac{\partial^2 \hat{Q}^{(k)}}{\partial z^2}, & \text{for } \tau > 0, \\ \hat{Q}^{(k)}(0, z, \alpha) = \delta(z). \end{cases}$$

These PDEs are independent of A [30]. So when one expands $\hat{Q}^k$ in ϵ as:

$$\hat{Q}^{(k)}(\tau, z, A) = \hat{Q}_0^{(k)}(\tau, z) + \epsilon\hat{Q}_1^{(k)}(\tau, z, A) + \epsilon^2\hat{Q}_2^{(k)}(\tau, z, A) + \ldots,$$

$\hat{Q}_0^{(k)}$ does not depend on A (however $\hat{Q}_1^{(k)}$ does depend on A). Thus, the derivatives w.r.t. A are already at least of order $\mathcal{O}(\epsilon)$ and therefore the terms

$$\epsilon^2 \frac{\partial^2 \hat{Q}^{(k)}}{\partial A \partial z},\ \epsilon^2 \frac{\partial^2 \hat{Q}^{(k)}}{\partial A^2},\ \epsilon^2 \frac{\partial \hat{Q}^{(k)}}{\partial A},$$

are no larger than $\mathcal{O}(\epsilon^3)$. These will be therefore neglected, since only an expansion up to second order in ϵ is needed. Therefore, the following approximation is done:

$$\begin{aligned}\frac{\partial \hat{Q}^{(k)}}{\partial \tau} \approx & \frac{1}{2}\left(1 + 2\epsilon\rho\nu z + \epsilon^2\nu^2 z^2\right)\frac{\partial^2 \hat{Q}^{(k)}}{\partial z^2} - \frac{1}{2}\epsilon A \frac{\frac{\partial B(\epsilon\alpha z)}{\partial z}}{B(\epsilon\alpha z)}\frac{\partial \hat{Q}^{(k)}}{\partial z} \\ & - \left(\epsilon\rho\nu + \epsilon^2\nu^2 z\right)(k-2)\frac{\partial \hat{Q}^{(k)}}{\partial z} - \epsilon\rho\nu A \frac{\partial^2 \hat{Q}^{(k)}}{\partial A \partial z} + \frac{1}{2}\epsilon^2\nu^2(k-1)(k-2)\hat{Q}^{(k)},\end{aligned}$$

with boundary condition $\hat{Q}^{(k)} = \delta(z)$ for $\tau = 0$. The derivation starting here deviates from Hagan et al. [29]. It is noted that for $k = 0$ and $k = 2$ it gives the following two PDEs:

$$\begin{aligned}\frac{\partial \hat{Q}^{(k)}}{\partial \tau} \approx & \frac{1}{2}\left(1 + 2\epsilon\rho\nu z + \epsilon^2\nu^2 z^2\right)\frac{\partial^2 \hat{Q}^{(0)}}{\partial z^2} - \frac{1}{2}\epsilon A \frac{\frac{\partial B(\epsilon A z)}{\partial z}}{B(\epsilon A z)}\frac{\partial \hat{Q}^{(0)}}{\partial z} - \epsilon\rho\nu A \frac{\partial^2 \hat{Q}^{(0)}}{\partial A \partial z}, \\ \frac{\partial \hat{Q}^{(0)}}{\partial \tau} \approx & \frac{1}{2}\left(1 + 2\epsilon\rho\nu z + \epsilon^2\nu^2 z^2\right)\frac{\partial^2 \hat{Q}^{(0)}}{\partial z^2} - \frac{1}{2}\epsilon A \frac{\frac{\partial B(\epsilon\alpha z)}{\partial z}}{B(\epsilon\alpha z)}\frac{\partial \hat{Q}^{(0)}}{\partial z} \\ & + 2\left(\epsilon\rho\nu + \epsilon^2\nu^2 z\right)\frac{\partial \hat{Q}^{(0)}}{\partial z} - \epsilon\rho\nu A \frac{\partial^2 \hat{Q}^{(k)}}{\partial A \partial z} + \epsilon^2\nu^2 \hat{Q}^{(0)}, \\ = & \frac{1}{2}\frac{\partial^2}{\partial z^2}\left[1 + 2\epsilon\rho\nu z + \epsilon^2\nu^2 z^2 \hat{Q}^{(0)}\right] - \frac{1}{2}\epsilon A \frac{\frac{\partial B(\epsilon A z)}{\partial z}}{B(\epsilon A z)}\frac{\partial \hat{Q}^{(0)}}{\partial z} - \epsilon\rho\nu A \frac{\partial^2 \hat{Q}^{(k)}}{\partial A \partial z}.\end{aligned}$$

Some straightforward details will be left out. The following variable is introduced:

$$U(\tau, z, A) := (1 + 2\epsilon\rho\nu z + \epsilon^2\nu^2 z^2) e^{\epsilon^2\rho\nu A\Theta\tau}\hat{Q}^{(0)}(\tau, z, A),$$

with

$$\Theta = -\frac{\frac{\partial B(\epsilon A z)}{\partial z}}{B(\epsilon A z)} = -C'(S).$$

It will satisfy the same PDE as $\hat{Q}^{(2)}$ does up to order $\mathcal{O}(\epsilon^2)$, i.e.

$$\hat{Q}^{(2)}(\tau, z, A) = e^{\epsilon^2\rho\nu A\Theta\tau}\hat{Q}^{(0)}(\tau, z, A)(1 + 2\epsilon\rho\nu z + \epsilon^2\nu^2 z^2 + \ldots).$$

Thus it gives:

$$Q^{(2)}(t, S_t, \alpha, T, S, A) = A^2 Q^{(0)}(t, S_t, \alpha, T, S)\left(1 + 2\epsilon\rho\nu z + \epsilon^2\nu^2 z^2 + \ldots\right) e^{\epsilon^2\rho\nu A\Theta(\tau - t)}.$$

Putting this in the integrated Fokker-Planck equation gives the PDE for Q:

$$\frac{\partial Q^{(0)}}{\partial T} \approx \frac{1}{2}\epsilon^2 A^2 \frac{\partial^2}{\partial S^2}\left[\left(1 + 2\epsilon\rho\nu z + \epsilon^2\nu^2 z^2\right) e^{\epsilon^2\rho\nu A\Theta(\tau - t)} C^2(S) Q^{(0)}\right].$$

It is argued Hagan et al. [30]that the choice

$$\Theta = \frac{C(S) - C(S_t)}{S - S_t},$$

gives better results than $\Theta = -C'(S)$. This is a first order Taylor expansion around S_t. This covers up a discontinuity at $S = 0$ in the definition of Θ for the SABR model case, i.e. $C(S) = S^\beta$. However it still satisfy

$$\lim_{S \to S_t} \Theta(S) = -C'(S_t).$$

Thus it gives a similar function for $S = S_t$. Setting $\epsilon = 1$ and $A = \alpha$ gives the resulting PDE.

B.1.2 Derivation of transformed PDE

The derived PDE by Hagan et al. [30] is given by:

$$\frac{\partial Q}{\partial T}(T,S) = \frac{\partial^2}{\partial S^2}\left(H(T,S)Q(T,S)\right),$$

with

$$H(T,S) = O^2(S)E(T,S).$$

The transformation is defined by the variable:

$$z(S) := \int_{S_0}^{S} \frac{1}{O(u)}\,\mathrm{d}u.$$

For convenience it is written $z := z(S)$ and $S := S(z)$. It is computed that

$$\begin{aligned}\frac{\partial}{\partial S} \equiv& \frac{\partial}{\partial z}\frac{\partial z}{\partial S} = \frac{1}{O(S)}\frac{\partial}{\partial z},\\ \frac{\partial^2}{\partial S^2} \equiv& \frac{1}{O(S)}\frac{\partial}{\partial z}\left\{\frac{1}{O(S)}\frac{\partial}{\partial z}\right\}.\end{aligned}$$

For ease of computation $O(S)$ is written as $O(z) := O(S(z))$ and $E(T,S)$ is written as $E(T,z) := E(T,S(z))$ in the new variables z and the new function θ is introduced:

$$\theta(T,z) := Q(T,S(z))O(z).$$

Putting this in the PDE results into:

$$\begin{aligned}&\frac{\partial}{\partial T}\left\{\frac{1}{O(z)}\theta(T,z)\right\} = \frac{\partial^2}{\partial S^2}\left\{O(z)E(T,z)\theta(T,z)\right\},\\ \Rightarrow&\frac{\partial\theta(T,z)}{\partial T} = \frac{\partial}{\partial z}\left\{\frac{\partial}{\partial S}\left\{O(z)E(T,z)\theta(T,z)\right\}\right\},\\ \Rightarrow&\frac{\partial\theta(T,z)}{\partial T} = \frac{\partial}{\partial z}\left\{\frac{1}{O(z)}\frac{\partial}{\partial z}\left\{O(z)E(T,z)\theta(T,z)\right\}\right\}.\end{aligned}$$

B.1.3 Derivation of the boundary conditions for the transformed PDE

The probabilities that accumulate the mass at the boundaries z^- and z^+ are respectively $\mathcal{P}^L(T)$ and $\mathcal{P}^R(T)$. In order that the total mass of the new probability density function integrates to one, it must hold that:

$$\begin{aligned}&\frac{\partial}{\partial T}\left(\mathcal{P}^L(T) + \int_{z^-}^{z^+}\theta(T,z)\,\mathrm{d}z + \mathcal{P}^L(T)\right) = 0,\\ \Rightarrow\ &\frac{\partial\mathcal{P}^L(T)}{\partial T} + \int_{z^-}^{z^+}\frac{\partial\theta(T,z)}{\partial T}\,\mathrm{d}z + \frac{\partial\mathcal{P}^L(T)}{\partial T} = 0,\\ \Rightarrow\ &\frac{\partial\mathcal{P}^L(T)}{\partial T} + \int_{z^-}^{z^+}\frac{\partial}{\partial z}\left\{\frac{1}{O(z)}\frac{\partial}{\partial z}\left\{O(z)E(T,z)\theta(T,z)\right\}\right\}\mathrm{d}z + \frac{\partial\mathcal{P}^L(T)}{\partial T} = 0,\\ \Rightarrow&\left(\frac{\partial\mathcal{P}^L(T)}{\partial T} - \frac{1}{O(z)}\frac{\partial}{\partial z}\left\{O(z)E(T,z)\theta(T,z)\right\}\Big|_{z=z^-}\right)\\ +&\left(\frac{\partial\mathcal{P}^R(T)}{\partial T} + \frac{1}{O(z)}\frac{\partial}{\partial z}\left\{O(z)E(T,z)\theta(T,z)\right\}\Big|_{z=z^+}\right) = 0.\end{aligned}$$

This gives the conditions for $\mathcal{P}^L$ and $\mathcal{P}^R$:

$$\frac{\partial \mathcal{P}^L(T)}{\partial T} = \frac{1}{O(z)}\frac{\partial}{\partial z}\left\{O(z)E(T,z)\theta(T,z)\right\}\Big|_{z=z^-}, \quad \frac{\partial \mathcal{P}^R(T)}{\partial T} = -\frac{1}{O(z)}\frac{\partial}{\partial z}\left\{O(z)E(T,z)\theta(T,z)\right\}\Big|_{z=z^+}.$$

In order for S_t to stay an martingale, it must hold:

$$\begin{aligned}
&\frac{\partial}{\partial T}\left(S_{\min}\mathcal{P}^L(T) + \int_{z^-}^{z^+} S(z)\theta(T,z)\,\mathrm{d}z + S_{\max}\mathcal{P}^L(T)\right) = 0,\\
&\Rightarrow\ S_{\min}\frac{\partial \mathcal{P}^L(T)}{\partial T} + \int_{z^-}^{z^+} S(z)\frac{\partial \theta(T,z)}{\partial T}\,\mathrm{d}z + S_{\max}\frac{\partial \mathcal{P}^L(T)}{\partial T} = 0,\\
&\Rightarrow\ S_{\min}\frac{\partial \mathcal{P}^L(T)}{\partial T} + \int_{z^-}^{z^+} S(z)\frac{\partial}{\partial z}\left\{\frac{1}{O(z)}\frac{\partial}{\partial z}\left\{O(z)E(T,z)\theta(T,z)\right\}\right\}\mathrm{d}z + S_{\max}\frac{\partial \mathcal{P}^L(T)}{\partial T} = 0,
\end{aligned}$$

by integration by parts:

$$\begin{aligned}
&\Rightarrow\ S_{\min}\frac{\partial \mathcal{P}^L(T)}{\partial T} + S(z)\frac{1}{O(z)}\frac{\partial}{\partial z}\left\{O(z)E(T,z)\theta(T,z)\right\}\Big|_{z=z^-}^{z=z^+}\\
&+\int_{z^-}^{z^+}\frac{\partial S(z)}{\partial z}\frac{1}{O(z)}\frac{\partial}{\partial z}\left\{O(z)E(T,z)\theta(T,z)\right\}\mathrm{d}z + S_{\max}\frac{\partial \mathcal{P}^L(T)}{\partial T} = 0.
\end{aligned}$$

Now note that

$$S_{\min}\frac{\partial \mathcal{P}^L(T)}{\partial T} + S(z)\frac{1}{O(z)}\frac{\partial}{\partial z}\left\{O(z)E(T,z)\theta(T,z)\right\}\Big|_{z=z^-}^{z=z^+} + S_{\max}\frac{\partial \mathcal{P}^L(T)}{\partial T} = 0,$$

due to the conditions of $\mathcal{P}^L$ and $\mathcal{P}^R$ and that it holds:

$$\frac{\mathrm{d}}{\mathrm{d}z}S(z) = \frac{\mathrm{d}}{\mathrm{d}z}\left(z^{-1}(S(z))\right) = \frac{1}{z'(S(z))} = O(z).$$

This gives:

$$\begin{aligned}
&\Rightarrow\ \int_{z^-}^{z^+}\frac{\partial S(z)}{\partial z}\frac{1}{O(z)}\frac{\partial}{\partial z}\left\{O(z)E(T,z)\theta(T,z)\right\}\mathrm{d}z = 0,\\
&\Rightarrow\ \int_{z^-}^{z^+}\frac{\partial}{\partial z}\left\{O(z)E(T,z)\theta(T,z)\right\}\mathrm{d}z = 0,\\
&\Rightarrow\ O(z)E(T,z)\theta(T,z)|_{z=z^-}^{z=z^+} = 0,
\end{aligned}$$

since $\frac{\partial S(z)}{\partial z} = O(z)$. This gives the boundary conditions

$$O(z)E(T,z)\theta(T,z)|_{z=z^-} = 0,\ \ O(z)E(T,z)\theta(T,z)|_{z=z^+} = 0.$$

B.2 Proof of Lemma 3.3

Three definitions and a theorem by Saad [35] are presented, which will be used to derive the proof of Lemma 3.3.

Definition B.1 (Irreducible Matrix)**.** The matrix A is called irreducible iff no permutation matrix P exists such that PAP^{T} is block upper triangular.

Definition B.2 (Irreducible Diagonal Dominant Matrix)**.** The matrix A is called irreducibly diagonal dominant iff A is irreducible and

$$|A_{ii}| \geq \sum_{j=1, j\neq i}^{n} |A_{ij}| \ \forall\ i = 1, \ldots, n$$

with strict inequality from at least one i.

Definition B.3 (M-Matrix)**.** The matrix A is an M-matrix iff it satisfies the following four properties

1. $A_{ii} > 0$ for $i = 1, \ldots, n$.
2. $A_{ij} \geq 0$ for $i \neq j$, $i, j = 1, \ldots, n$.
3. A is non-singular.
4. $A^{-1} \geq 0$.

Theorem B.4. *If the matrix A satisfies the following three properties*

1. *$A_{ii} > 0$ for $i = 1, \ldots, n$.*
2. *$A_{ij} \leq 0$ for $i \neq j$, $i, j = 1, \ldots, n$.*
3. *A is irreducibly diagonally dominant.*

Then A is a M-matrix.

Proof. A proof can be found in Saad [35]. □

Now the proof of Lemma 3.3 is given.

Proof. First it must be noted that for the Euler scheme the discretization leads to the matrix equation

$$\theta^n = M\theta^{n+1}, \tag{B.1}$$

where

$$M_{11} = 1 + \frac{\Delta t}{h}\left(\frac{\hat{O}_1\hat{E}_1(t_n)}{\hat{s}_2 - \hat{s}_1} + \frac{2\hat{O}_1\hat{E}_1(t_n)}{\hat{s}_1 - \hat{s}_0}\right),\ M_{jj} = 1 + \frac{\Delta t}{h}\left(\frac{\hat{O}_j}{\hat{s}_{j+1} - \hat{s}_j} + \frac{\hat{O}_j}{\hat{s}_j - \hat{s}_{j-1}}\right)\hat{E}_j(t_n),$$
$$M_{JJ} = 1 + \frac{\Delta t}{h}\left(\frac{2\hat{O}_J\hat{E}_J(t_n)}{\hat{s}_{J+1} - \hat{s}_J} + \frac{\hat{O}_J\hat{E}_J(t_n)}{\hat{s}_J - \hat{s}_{J-1}}\right),\ M_{j,j-1} = -\frac{\Delta t}{h}\left(\frac{\hat{O}_{j-1}}{\hat{s}_j - \hat{s}_{j-1}}\hat{E}_{j-1}(t_n)\right),$$
$$M_{j,j+1} = -\frac{\Delta t}{h}\left(\frac{\hat{O}_{j+1}}{\hat{s}_{j+1} - \hat{s}_j}\hat{E}_{j+1}(t_n)\right).$$

for $j = 1, \ldots, J$. All other indices of matrix M are zero. Now, note that due to the three diagonal structure of Matrix M, M is irreducible.

Furthermore, it is easy to verify that for $S > 0$, it holds that $E(T, S), O(S) > 0$, hence $M_{ii} > 0$ and $M_{ij} < 0$ for $i \neq j$. Due to condition 3.8, it follows that M is a irreducibly diagonally dominant matrix. The strict inequalities follow for row 1 and J.

Hence by Theorem B.4 it follows that M is a M-matrix. As a consequence it follows that $M^{-1} \geq 0$. Hence

$$\theta^{n+1} = M^{-1}\theta^n \geq 0$$

□

Appendix C

Derivations and proofs for Chapter 4

C.1 Derivation of the implied SDF and PDF for Hagan's formulas

In this section the first and second derivative of a call price with respect to the strike are computed. The survival density and probability density function can be computed using Lemma 2.19. All functions defined here are only used in this section and should not be confused with other functions. In the first two sections, general derivatives w.t.r. Hagan's Black and Bachelier formulas are derived respectively, followed by a third section where some general derivatives and limiting cases are computed.

C.1.1 Hagan's Black formula

The call price under Black's model is given by:

$$\mathrm{C}_{\mathrm{Black}}(t,T,K,\sigma) = S(t)F_{\mathcal{N}}(d_1) - KF_{\mathcal{N}}(d_2), \tag{C.1}$$

with

$$d_1 = \frac{\log\left(\frac{S(t)}{K}\right) + \frac{1}{2}\sigma^2(T-t)}{\sigma\sqrt{T-t}}, \quad d_2 = d_1 - \sigma\sqrt{T-t}.$$

where $F_{\mathcal{N}}(x)$ is the CDF of the standard normal distribution and $f_{\mathcal{N}}(x)$ is the PDF of the standard normal distribution. For convenience, $C_{\mathrm{Black}}(t,T,K,\sigma)$ is written by C and S_t by S. The implied Black volatilities for Hagan's Black formula are given by:

$$\sigma_B = I_1 \cdot (1 + I_2 \cdot T), \tag{C.2}$$

where

$$I_1 := I_1(\alpha,\beta,\rho,\nu,S,K) = \frac{\alpha z}{\chi\,(SK)^{\frac{1-\beta}{2}}\left(1 + \frac{(1-\beta)^2}{24}\log^2\left(\frac{S}{K}\right) + \frac{(1-\beta)^4}{1920}\log^4\left(\frac{S}{K}\right)\right)},$$

$$I_2 := I_2(\alpha,\beta,\rho,\nu,S,K) = \frac{(1-\beta)^2}{24}\frac{\alpha^2}{(SK)^{1-\beta}} + \frac{1}{4}\frac{\rho\beta\nu\alpha}{(SK)^{\frac{1-\beta}{2}}} + \frac{2-3\rho^2}{24}\nu^2,$$

$$z := z(\alpha,\beta,\nu) = \frac{\nu}{\alpha}\,(SK)^{\frac{1-\beta}{2}}\log\left(\frac{S}{K}\right),$$

$$\chi := \chi(z,\rho) = \log\left(\frac{\sqrt{1-2\rho z+z^2}+z-\rho}{1-\rho}\right).$$

For convenience, σ_B is written by σ and τ is introduced and defined by $\tau := T - t$.

First derivative

It can be derived that:

$$\frac{\partial C}{\partial K} = Sf_{\mathcal{N}}(d_1)\frac{\partial d_1}{\partial K} - Kf_{\mathcal{N}}(d_2)\frac{\partial d_2}{\partial K} - F_{\mathcal{N}}(d_2),$$

where

$$\begin{aligned}
\frac{d_1}{\partial K} &= \frac{\sigma\sqrt{T}\left(-K^{-1} + \sigma\frac{\partial\sigma}{\partial K}\tau\right) + \sqrt{\tau}\frac{\partial\sigma}{\partial K}\left(\log\left(\frac{S}{K}\right) + \frac{1}{2}\sigma^2\tau\right)}{\sigma^2\tau}, \\
\frac{\partial d_2}{\partial K} &= \frac{\partial d_1}{\partial K} - \frac{\partial\sigma}{\partial K}\sqrt{\tau}, \\
\frac{\partial\sigma}{\partial K} &= \frac{\partial I_1}{\partial K}(1 + I_2 T) + I_1\frac{\partial I_2}{\partial K}T.
\end{aligned}$$

Where

$$\begin{aligned}
\frac{\partial I_2}{\partial K} =& \frac{(1-\beta)^2}{24}\alpha^2 S^{\beta-1}(\beta-1)K^{\beta-2} + \frac{1}{4}\rho\beta\nu\alpha S^{\frac{\beta-1}{2}}\frac{\beta-1}{2}K^{\frac{\beta-3}{2}}, \\
\frac{\partial I_1}{\partial K} =& \alpha\frac{\partial}{\partial K}\left\{(SK)^{\frac{\beta-1}{2}}\right\}\left\{\frac{z}{\chi(z)\left(1 + \frac{(1-\beta)^2}{24}\log^2\left(\frac{S}{K}\right) + \frac{(1-\beta)^4}{1920}\log^4\left(\frac{S}{K}\right)\right)}\right\} \\
&+ \alpha(SK)^{\frac{\beta-1}{2}}\frac{\partial}{\partial K}\left\{\frac{z}{\chi(z)}\right\}\left\{\frac{1}{1 + \frac{(1-\beta)^2}{24}\log^2\left(\frac{S}{K}\right) + \frac{(1-\beta)^4}{1920}\log^4\left(\frac{S}{K}\right)}\right\} \\
&+ \alpha(SK)^{\frac{\beta-1}{2}}\frac{z}{\chi(z)}\frac{\partial}{\partial K}\left\{\frac{1}{1 + \frac{(1-\beta)^2}{24}\log^2\left(\frac{S}{K}\right) + \frac{(1-\beta)^4}{1920}\log^4\left(\frac{S}{K}\right)}\right\}, \\
\frac{\partial z}{\partial K} =& \frac{\nu}{\alpha}\left(\frac{1-\beta}{2}S^{\frac{1-\beta}{2}}K^{-\frac{\beta+1}{2}}\log\left(\frac{S}{K}\right) - K^{-1}(SK)^{\frac{1-\beta}{2}}\right).
\end{aligned}$$

Define[1]

$$g(K) := \left(1 + \frac{(1-\beta)^2}{24}\log^2\left(\frac{S}{K}\right) + \frac{(1-\beta)^4}{1920}\log^4\left(\frac{S}{K}\right)\right),$$

then

$$\begin{aligned}
g'(K) &= \frac{-(1-\beta)^2}{12}\log\left(\frac{S}{K}\right)K^{-1} - \frac{(1-\beta)^4}{480}\log^3\left(\frac{S}{K}\right)K^{-1}, \\
g''(K) &= \frac{(1-\beta)^2}{12}K^{-2}\left(1 + \log\left(\frac{S}{K}\right)\right) + \frac{(1-\beta)^4}{480}\log^2\left(\frac{S}{K}\right)K^{-2}\left(\log\left(\frac{S}{K}\right) + 3\right), \\
\frac{\partial}{\partial K}\left\{\frac{1}{g(K)}\right\} &= \frac{g'(K)}{g^2(K)}, \\
\frac{\partial^2}{\partial K^2}\left\{\frac{1}{g(K)}\right\} &= \frac{\partial}{\partial K}\left\{-\frac{g'(K)}{g^2(K)}\right\} = -\frac{g''(K)g^2(K) - 2g'(K)g^2(K)}{g^4(K)}.
\end{aligned}$$

[1]The derivatives of $\frac{z}{\chi(z)}$ will be provided in the general derivatives section, but it will involve the derivatives of z.

Second derivative

It can be derived

$$\begin{aligned}
\frac{\partial^2 C}{\partial K^2} =& S f_{\mathcal{N}}(d_1)\left(\frac{\partial^2 d_1}{\partial K^2} - d_1\left(\frac{\partial d_1}{\partial K}\right)^2\right) - 2 f_{\mathcal{N}}(d_2)\frac{\partial d_2}{\partial K} + K f_{\mathcal{N}}(d_2)\left(d_2\left(\frac{\partial d_2}{\partial K}\right)^2 - \frac{\partial^2 d_2}{\partial K^2}\right),\\
\frac{\partial^2 d_1}{\partial K^2} =& \frac{1}{\sigma^4\tau^2}\left(\left(K^{-2} + \left(\left(\frac{\partial \sigma}{\partial K}\right)^2 + \sigma\frac{\partial^2\sigma}{\partial K^2}\right)\tau\right)\sigma^3\tau^{\frac{3}{2}} - \left(\log\left(\frac{S}{K}\right) + \frac{1}{2}\sigma^2\tau\right)\sigma^2\tau\frac{\partial^2\sigma}{\partial K^2}\sqrt{\tau}\right.\\
& \left. -2\sigma^2\tau\left(\sigma\frac{\partial\sigma}{\partial K}\tau - K^{-1}\right)\sqrt{\tau}\frac{\partial\sigma}{\partial K} + 2\left(\log\left(\frac{S}{K}\right) + \frac{1}{2}\sigma^2\tau\right)\sigma\sqrt{\tau}\tau\left(\frac{\partial\sigma}{\partial K}\right)^2\right),\\
\frac{\partial^2 d_2}{\partial K^2} =& \frac{\partial^2 d_1}{\partial K^2} - \frac{\partial^2\sigma}{\partial K^2}\sqrt{\tau}.
\end{aligned}$$

Where

$$\begin{aligned}
\frac{\partial^2\sigma}{\partial K^2} =& \frac{\partial^2 I_1}{\partial K^2}(1 + I_2 T) + 2\frac{\partial I_1}{\partial K}\frac{\partial I_2}{\partial K}T + I_1\frac{\partial^2 I_2}{\partial K^2}T,\\
\frac{\partial^2 I_2}{\partial K^2} =& \frac{(1-\beta)^2}{24}\alpha^2 S^{\beta-1}(\beta-1)(\beta-2)K^{\beta-3} + \frac{1}{4}\rho\beta\nu\alpha S^{\frac{\beta-1}{2}}\frac{\beta-1}{2}\frac{\beta-3}{2}K^{\frac{\beta-5}{2}},\\
\frac{\partial^2 I_1}{\partial K^2} =& \alpha\frac{\partial^2}{\partial K^2}\left\{(SK)^{\frac{\beta-1}{2}}\right\}\left\{\frac{z}{\chi(z)g(K)}\right\} + \alpha(SK)^{\frac{\beta-1}{2}}\frac{\partial^2}{\partial K^2}\left\{\frac{z}{\chi(z)}\right\}\frac{1}{g(K)}\\
& + \alpha(SK)^{\frac{\beta-1}{2}}\frac{z}{\chi(z)}\frac{\partial^2}{\partial K^2}\left\{\frac{1}{g(K)}\right\} + 2\alpha\frac{\partial}{\partial K}\left\{(SK)^{\frac{\beta-1}{2}}\right\}\frac{\partial}{\partial K}\left\{\frac{z}{\chi(z)}\right\}\frac{1}{g(K)},\\
& + 2\alpha\frac{\partial}{\partial K}\left\{(SK)^{\frac{\beta-1}{2}}\right\}\frac{\partial}{\partial K}\left\{\frac{1}{g(K)}\right\}\frac{z}{\chi(z)} + 2\alpha\left\{(SK)^{\frac{\beta-1}{2}}\right\}\frac{\partial}{\partial K}\left\{\frac{z}{\chi(z)}\right\}\frac{\partial}{\partial K}\left\{\frac{1}{g(K)}\right\},
\end{aligned}$$

with

$$\begin{aligned}
\frac{\partial^2}{\partial K^2}\left\{(SK)^{\frac{\beta-1}{2}}\right\} =& S^{\frac{\beta-1}{2}}\frac{\beta-1}{2}\frac{\beta-3}{2}K^{\frac{\beta-5}{2}},\\
\frac{\partial^2}{\partial K^2}z =& \frac{\partial}{\partial K}\left\{\frac{\nu}{\alpha}\left(\frac{1-\beta}{2}S^{\frac{1-\beta}{2}}K^{-\frac{\beta+1}{2}}\log\left(\frac{S}{K}\right) - K^{-1}(SK)^{\frac{1-\beta}{2}}\right)\right\}\\
=& \frac{\nu}{\alpha}S^{\frac{1-\beta}{2}}\left(\frac{1+\beta}{2}K^{-\frac{3+\beta}{2}} - \frac{1-\beta}{2}K^{-\frac{\beta+3}{2}}\left(1 + \frac{\beta+1}{2}\log\left(\frac{S}{K}\right)\right)\right)\\
=& -\frac{\nu}{\alpha}S^{\frac{1-\beta}{2}}K^{-\frac{\beta+3}{2}}\left(\frac{1+\beta}{2}\left(\log\left(\frac{S}{K}\right)\frac{1-\beta}{2} - 1\right) - \frac{1-\beta}{2}\right).
\end{aligned}$$

C.1.2 Hagan's Bachelier formula

The call price under Bachelier's model is given by:

$$\mathrm{C}_{\mathrm{Bachelier}}(t,T,K,\sigma) = (S_t - K)F_{\mathcal{N}}(-d) + \sigma\sqrt{T-t}f_{\mathcal{N}}(d), \tag{C.3}$$

with

$$d = \frac{K - S_t}{\sigma\sqrt{T-t}}.$$

where $F_{\mathcal{N}}(x)$ is the CDF of the standard normal distribution and $f_{\mathcal{N}}(x)$ is the PDF of the standard normal distribution. For convenience, $C_{\mathrm{Black}}(t,T,K,\sigma)$ is written by C and S_t by S. The implied Bacheliers volatilities for Hagan's Bachelier formula are given by:

$$\sigma_N = I_1 \cdot (1 + I_2 \cdot T), \tag{C.4}$$

where

$$I_1 := I_1(\alpha,\beta,\rho,\nu,S,K) = \frac{\alpha(1-\beta)(S-K)}{S^{1-\beta}-K^{1-\beta}}\frac{\zeta}{\chi},$$
$$I_2 := I_2(\alpha,\beta,\rho,\nu,S,K) = \frac{\beta(\beta-2)\alpha^2}{24}(SK)^{\beta-1} + \frac{\alpha\beta\rho\nu}{4}(SK)^{\frac{\beta-1}{2}} + \frac{2-3\rho^2}{24}\nu^2,$$
$$\zeta := \zeta(\alpha,\beta,\nu,S,K) = \frac{\nu(S-K)}{\alpha(SK)^{\frac{\beta}{2}}},$$
$$\chi := \chi(z,\rho) = \log\left(\frac{\sqrt{1-2\rho\zeta+\zeta^2}+\zeta-\rho}{1-\rho}\right).$$

For convenience, σ_N is written by σ and τ is introduced and defined by $\tau := T-t$.

First derivative

It can be computed:

$$\frac{\partial C}{\partial K} = f_{\mathcal{N}}(d)\sqrt{\tau}\frac{\partial\sigma}{\partial K} - F_{\mathcal{N}}(-d), \text{ since } (K-S) = d\sigma\sqrt{\tau},$$

with

$$\frac{\partial\sigma}{\partial K} = \frac{\partial I_1}{\partial K}(1+I_2T) + I_1\frac{\partial I_2}{\partial K}T,$$

where[2]

$$\frac{\partial I_1}{\partial K} = \alpha(1-\beta)\left(\frac{\zeta}{\chi(\zeta)}\frac{\partial}{\partial K}\left\{\frac{S-K}{S^{1-\beta}-K^{1-\beta}}\right\} + \frac{S-K}{S^{1-\beta}-K^{1-\beta}}\frac{\partial}{\partial K}\left\{\frac{\zeta}{\chi(\zeta)}\right\}\right),$$
$$\frac{\partial}{\partial K}\left\{\frac{S-K}{S^{1-\beta}-K^{1-\beta}}\right\} = \frac{\beta K^{1-\beta}-S^{1-\beta}+(1-\beta)SK^{-\beta}}{(S^{1-\beta}-K^{1-\beta})^2},$$
$$\frac{\partial I_2}{\partial K} = \frac{\beta(\beta-2)\alpha^2}{24}S^{\beta-1}(\beta-1)K^{\beta-2} + \frac{1}{4}\rho\beta\nu\alpha S^{\frac{\beta-1}{2}}\frac{\beta-1}{2}K^{\frac{\beta-3}{2}},$$
$$\frac{\partial\zeta}{\partial K} = \frac{\nu}{\alpha}(KS)^{-\frac{\beta}{2}}\left(\frac{\beta}{2}-1-\frac{\beta}{2}SK^{-1}\right).$$

Second derivative

It can be computed:

$$\frac{\partial^2 C}{\partial K^2} = \sqrt{\tau}f_{\mathcal{N}}(d)\left\{\frac{\partial^2\sigma}{\partial K^2} + \sigma\left(\frac{\partial d}{\partial K}\right)^2\right\}, \text{ since } \frac{(K-S)}{\sqrt{\tau}} = d\sigma \Rightarrow \frac{1}{\sqrt{\tau}} = \sigma\frac{\partial d}{\partial K} + d\frac{\partial\sigma}{\partial K},$$
$$\frac{\partial^2\sigma}{\partial K^2} = \frac{\partial^2 I_1}{\partial K^2}(1+I_2T) + 2\frac{\partial I_1}{\partial K}\frac{\partial I_2}{\partial K}T + I_1\frac{\partial^2 I_2}{\partial K^2}T,$$
$$\frac{\partial d}{\partial K} = \frac{1+\sqrt{\tau}d\frac{\partial\sigma}{\partial K}}{\sigma\sqrt{\tau}}.$$

[2]The derivatives of $\frac{\zeta}{\chi(\zeta)}$ will be provided in the general derivatives section, but it will involve the derivatives of z.

Where

$$\begin{aligned}
\frac{\partial^2 I_1}{\partial K^2} &= \frac{\partial}{\partial K}\left\{\alpha(1-\beta)\left(\frac{\zeta}{\chi(\zeta)}\frac{\partial}{\partial K}\left\{\frac{S-K}{S^{1-\beta}-K^{1-\beta}}\right\}+\frac{S-K}{S^{1-\beta}-K^{1-\beta}}\frac{\partial}{\partial K}\left\{\frac{\zeta}{\chi(\zeta)}\right\}\right)\right\} \\
&= \alpha(1-\beta)\left(\frac{\zeta}{\chi(\zeta)}\frac{\partial^2}{\partial K^2}\left\{\frac{S-K}{S^{1-\beta}-K^{1-\beta}}\right\}+2\frac{\partial}{\partial K}\left\{\frac{S-K}{S^{1-\beta}-K^{1-\beta}}\right\}\frac{\partial}{\partial K}\left\{\frac{\zeta}{\chi(\zeta)}\right\}+\right. \\
&+ \left.\frac{S-K}{S^{1-\beta}-K^{1-\beta}}\frac{\partial^2}{\partial K^2}\left\{\frac{\zeta}{\chi(\zeta)}\right\}\right), \\
\frac{\partial I_2}{\partial K} &= \frac{\beta(\beta-2)\alpha^2}{24}S^{\beta-1}(\beta-1)(\beta-2)K^{\beta-3}+\frac{1}{4}\rho\beta\nu\alpha S^{\frac{\beta-1}{2}}\frac{\beta-1}{2}\frac{\beta-3}{2}K^{\frac{\beta-5}{2}}, \\
\frac{\partial^2\zeta}{\partial K^2} &= \frac{\nu\beta}{2\alpha}(KS)^{-\frac{\beta}{2}}\left(K^{-1}\left(1-\frac{\beta}{2}\right)+SK^{-2}\left(\frac{\beta}{2}+1\right)\right),
\end{aligned}$$

with

$$\begin{aligned}
\frac{\partial^2}{\partial K^2}\left\{\frac{S-K}{S^{1-\beta}-K^{1-\beta}}\right\} = \frac{1}{\left(S^{1-\beta}-K^{1-\beta}\right)^3}\left\{\left(\beta(1-\beta)K^{-\beta}-S\beta(1-\beta)K^{-(1+\beta)}\right)\left(S^{1-\beta}-K^{1-\beta}\right)\right. \\
\left.+\left(\beta K^{1-\beta}-S^{1-\beta}+(1-\beta)SK^{-\beta}\right)\left(2(1-\beta)K^{-\beta}\right)\right\}.
\end{aligned}$$

C.1.3 Limit cases and general derivatives

It can be noted that $\chi(z) \equiv \chi(\zeta)$. Thus only the derivatives of $\frac{z}{\chi(z)}$ and $\chi(z)$ are derived. Since all functions are dependent on one variable, let $fun^{'}$, $fun^{''}$ and $fun^{(n)}$ denote the first, second and nth derivative of a function fun. First, it is noted that

$$\lim_{K\to S} z = 0, \quad \lim_{K\to S}\chi(z) = 0.$$

Write $\chi(z) = \log(u(z)) - \log(1-\rho)$. Then:

$$\begin{aligned}
u(z) &= \sqrt{1-2\rho z+z^2}+z-\rho, & \lim_{K\to S} u(z) &= 1-\rho, \\
u^{'}(z) &= 1+\frac{z-\rho}{\sqrt{1-2\rho z+z^2}}, & \lim_{K\to S} u^{'}(z) &= 1-\rho, \\
u^{''}(z) &= \frac{1}{\sqrt{1-2\rho z+z^2}}-\frac{(z-\rho)^2}{(1-2\rho z+z^2)^{\frac{3}{2}}}, & \lim_{K\to S} u^{'''}(z) &= 1-\rho^2.
\end{aligned}$$

Then

$$\chi^{'}(z) = \frac{u^{'}(z)}{u(z)}, \quad \chi^{''}(z) = \frac{u^{''}(z)u(z)-\left(u^{'}(z)\right)^2}{u^2(z)}.$$

Then

$$\frac{\partial}{\partial K}\left\{\frac{z}{\chi(z)}\right\} = \frac{\chi(z)-\chi^{'}(z)z}{\chi^2(z)}\frac{\partial z}{\partial K},$$
$$\frac{\partial^2}{\partial K^2}\left\{\frac{z}{\chi(z)}\right\} = \frac{-\chi^{''}(z)z\chi^2(z)-2\chi(z)\chi^{'}(z)\left(\chi(z)-\chi^{'}(z)z\right)}{\chi^4(z)}\left(\frac{\partial z}{\partial K}\right)^2+\frac{\chi(z)-\chi^{'}(z)z}{\chi^2(z)}\frac{\partial^2 z}{\partial K^2},$$
$$\frac{\partial^2}{\partial K^2}\left\{\frac{z}{\chi(z)}\right\} = \frac{-\chi^{''}(z)z\chi^2(z)-2\chi(z)\chi^{'}(z)\left(\chi(z)-\chi^{'}(z)z\right)}{\chi^4(z)}\left(\frac{\partial z}{\partial K}\right)^2+\frac{\chi(z)-\chi^{'}(z)z}{\chi^2(z)}\frac{\partial^2 z}{\partial K^2}.$$

Now limits are derived for $K \to S$ are computed the functions above:

$$\lim_{K\to S}\frac{z}{\chi(z)} = 1, \quad \lim_{K\to S}\chi^{'}(z) = \lim_{K\to S}\frac{u^{'}(z)}{u(z)} = 1,$$
$$\lim_{K\to S}\chi^{''}(z) = \lim_{K\to S}\frac{u^{''}(z)u(z)-\left(u^{'}(z)\right)^2}{u^2(z)} = \frac{(1-\rho^2)(1-\rho)-(1-\rho)^2}{(1-\rho)^2} = \rho,$$
$$\lim_{K\to S}\frac{\chi(z)-\chi^{'}(z)z}{\chi^2(z)} = -\frac{\rho}{2} \text{ (by applying two times L'Hopital)},$$
$$\lim_{K\to S}\frac{-\chi^{''}(z)z\chi^2(z)-2\chi(z)\chi^{'}(z)\left(\chi(z)-\chi^{'}(z)z\right)}{\chi^4(z)} = \lim_{K\to S}-\left(\frac{z}{\chi}\right)^3\frac{z\chi^{''}\chi+2\chi^{'}(\chi-z\chi^{'})}{z^3}$$
$$= \frac{1}{2}\rho^2-\frac{1}{3}\chi^{(3)} \text{(by applying two times L'Hopital)}.$$

These limiting cases depend on the following calculations:

$$\chi^{(3)}(z) = \frac{\left(u^{(3)}u+u^{''}u^{'}-2u^{'}u^{''}\right)u^2-2uu^{'}\left(u^{''}(z)u(z)-\left(u^{'}(z)\right)^2\right)}{u^4} \to 3\rho^2-1 \text{ as } K\to S,$$
$$u^{(3)}(z) = -3\frac{z-\rho}{(1-2\rho z+z^2)^{\frac{3}{2}}}+\frac{3(z-\rho)^3}{(1-2\rho z+z^2)^{\frac{5}{2}}} \to 3\rho(1-\rho)(1+\rho) \text{ as } K\to S.$$

As a consequence

$$\lim_{K\to S}\frac{\partial^2}{\partial K^2}\left\{\frac{z}{\chi(z)}\right\} = \frac{1}{3}-\frac{1}{2}\rho^2.$$

Lastly, limiting cases of the derivatives of $\left((1-\beta)\frac{S-K}{S^{1-\beta}-K^{1-\beta}}\right)$ are computed:

$$\lim_{K\to S}\frac{\partial}{\partial K}\left((1-\beta)\frac{S-K}{S^{1-\beta}-K^{1-\beta}}\right)=\frac{\beta}{2}S^{\beta-1},$$
$$\lim_{K\to S}\frac{\partial^2}{\partial K^2}\left((1-\beta)\frac{S-K}{S^{1-\beta}-K^{1-\beta}}\right)=\frac{\beta}{6}(\beta-2)S^{\beta-2},$$
$$\begin{aligned}\frac{\partial}{\partial K}\left(\lim_{\beta\to 1}(1-\beta)\frac{S-K}{S^{1-\beta}-K^{1-\beta}}\right)&=\frac{\partial}{\partial K}\left(\frac{S-K}{\log(S)-\log(K)}\right)\\&=\frac{\log(K)-\log(S)+K^{-1}S-1}{(\log(S)-\log(K))^2},\\\frac{\partial^2}{\partial K^2}\left(\lim_{\beta\to 1}(1-\beta)\frac{S-K}{S^{1-\beta}-K^{1-\beta}}\right)&=\frac{\partial^2}{\partial K^2}\left(\frac{S-K}{\log(S)-\log(K)}\right)\\&=\frac{1}{(\log(S)-\log(K))^3}\left\{\left(K^{-1}-K^{-2}S\right)(\log(S)-\log(K))\right.\\&\quad\left.+2K^{-1}\left(\log(K)-\log(S)+K^{-1}S-1\right)\right\}.\end{aligned}$$

C.2 Proof of Lemma 4.16

Proof. For convenience at maturity the call price is written as $C(x)=(x-K)^+$, where K is the strike of the call option. There will be three cases distinguished: $\{x\le K,\ y\le K\}$, $\{x\ge K,\ y\le K\}$ and $\{x\ge K,\ y\ge K\}$. The case $\{x\le K,\ y\ge K\}$ is analogously to the case $\{x\ge K,\ y\le K\}$.

If $x\le K,\ y\le K$, then:

$$\begin{aligned}|C(x)-C(y)|&=|0-0|\\&\le|x-y|.\end{aligned}$$

If $x\ge K,\ y\le K$, then:

$$\begin{aligned}|C(x)-C(y)|&=|x-K|\\&=x-K\\&\le x-y\\&\le|x-y|.\end{aligned}$$

If $x\ge K,\ y\ge K$, then:

$$\begin{aligned}|C(x)-C(y)|&=|x-K-y+K|\\&=|x-y|.\end{aligned}$$

□

Bibliography

[1] Robert A. Adams. *Calculus, A Complete Course*. Pearson, sixth edition, 2003.

[2] Alkiviadis G. Akritas and Panagiotis S. Vigklas. Counting the number of real roots in an interval with vincents theorem. *Bull. Math. Soc. Sci. Math. Roumanie Tome*, pages 201–211, 2010.

[3] Michael Konikov Alexander Antonov and Michael Spector. Sabr spreads its wings. *Risk magazine*, July 2013.

[4] Jesper Andreasen and Brian Norsk Huge. Zabr – expansions for the masses. December 2011.

[5] Alexandre Antonov, Michael Konikov, David Rufino, and Michael Spector. Exact solution to cev model with uncorrelated stochastic volatility. *SSRN Electronic journal*, January 2014.

[6] Alexandre Antonov, Michael Konikov, and Michael Spector. The free boundary sabr: Natural extension to negative rates. *SSRN Electronic journal*, January 2015.

[7] Alexandre Antonov and Michael Spector. Advanced analytics for the sabr model. *SSRN Electronic journal*, March 2012.

[8] Philippe Balland and Quan Tran. Sabr goes normal. *Risk Magazine*, May 2013.

[9] Bruce Barlett. Hedging under sabr model. *WILMOTT magazine*, 2006.

[10] Bis. Bis quarterly review. Statistical Annex, 2015.

[11] Doust. No-arbitrage sabr. *Risk magazine*, January 2014.

[12] Andricopoulos et al. Advancing the universality of quadrature methods to any underlying process for option pricing. *Elsevier*, pages 600–612, December 2014.

[13] Monique Jeanblanc et al. *Mathematical Methods for Financial Markets*. Springer, 2009.

[14] Roger Lords et al. 50 shades of sabr model, 2014.

[15] Gary J. Kennedy Fabien Le Floch. Finite differrence techniques for arbitrage free sabr. *SSRN Electronic journal*, May 2014.

[16] J. Favard. Sur les polynomes de tchebicheff. *C.R. Acad. Sci, Paris*, 1935.

[17] Patrick. S. Hagan. Convexity conundrums: Pricing cms swaps, caps and floors. *WILMOTT magazine*, 2003.

[18] P. Henry-Labordère. *Analysis, Geometry and Modeling in Finance: Advanced Methods in Option Pricing*. Taylor and Francis Group, 2009.

[19] John C. Hull. *Risk Management and Financial Institutions*. Pearson, second edition, 2007.

[20] Othmane Islah. Solving sabr in exact form and unifying it with libor market model. *SSRN Electronic journal*, October 2009.

[21] Othmane Islah. Heun solutions to the sabr model. *SSRN Electronic journal*, January 2011.

[22] Kazuhiro Iwasawa. Analytic formula for the european normal black scholes formula. *http://www.math.nyu.edu/phd_students/iwasawa/normal.pdf*.

[23] Gianluca Iaccarino Jeroen A.S. Witteveen. Uncertainty propagation with monotonicity preserving robustness. *Conference Paper*, January 2014.

[24] Simon Johnson and Bereshad Nonas. Arbitrage-free construction of the swaption cube. *SSRN Electronic journal*, January 2009.

[25] Cornelis W Oosterlee Lech A Grzelak. An arbitrage-free hagan implied density via the stochastic collocation method. *SSRN Electronic journal*, November 2014.

[26] Maria Suarez-Taboada Cornelis W Oosterlee Lech A Grzelak, Jeroen Witteveen. The stochastic collocation monte carlo sampler: Highly efficient sampling from "expensive" distributions. *SSRN Electronic journal*, November 2014.

[27] Rendall J. Leveque. *Finite volume methods for hyperbolic problems.* Cambridge Texts in Applied Mathematics.

[28] Obloj. Fine-tune your smile: Correction to hagan et al. *arXiv*, January 2007.

[29] A. S. Lesniewski P. S. Hagan, D. Kumar and D. E. Woodward. Managing smile risk. *WILMOTT Magazine*, pages 84–108, September 2002.

[30] A. S. Lesniewski P. S. Hagan, D. Kumar and D. E. Woodward. Arbritrage free sabr. *Wilmott*, pages 60–75, January 2014.

[31] Hyukjae Park. Sabr symmetry. January 2014.

[32] Paulot. Asymptotic implied volatility at the second order with application to the sabr model. *SSRN Electronic journal*, June 2009.

[33] Leif B.G. Anderen & Vladimir V. Piterbarg. *Interest Rate Modeling, Volume I: Foundations and Vanilla Models*. Atlantic Financial Press, 2010.

[34] Marjon Ruijter and Cornelis W. Oosterlee. Numerical fourier method and second-order taylor scheme for backward sdes in finance. *SSRN Electronic journal*, September 2014.

[35] Yousef Saad. *Iterative Methods for Sparse Linear Systems*. PWS Publishing Companay, 1996.

[36] Matthew Dodgson Shalom Benaim and Dherminder Kainth. An arbitrage-free method for smile extrapolation. *http://www.quarchome.org/risktailspaper_v5.pdf*.

[37] S.E. Shreve. *Stochastic Calculus for Finance II: Continuous-Time Models*. Springer, 2000.

[38] J Michael Steele. *Stochastic Calculus and Financial Applications*. Springer, 2003.

[39] Stewart. *Afternotes on Numerical Analysis*. Siam, 1996.

[40] Jacques Charles Francois Sturm. Résolation des équations algébriques. *Bulletin des Sciences de Ferussac*, 1829.

[41] Nevana Šelić. An examination of the convexity adjustment technique in the pricing of constant maturity swaps, 2013.

[42] Zaza van der Have. Arbitrage-free methods to price european options under the sabr model. Master's thesis, TU Delft, 2015.